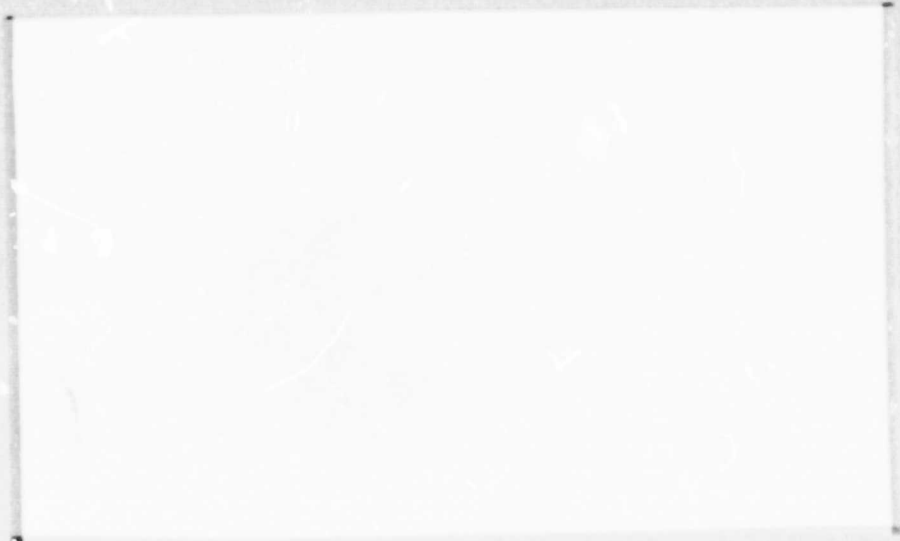


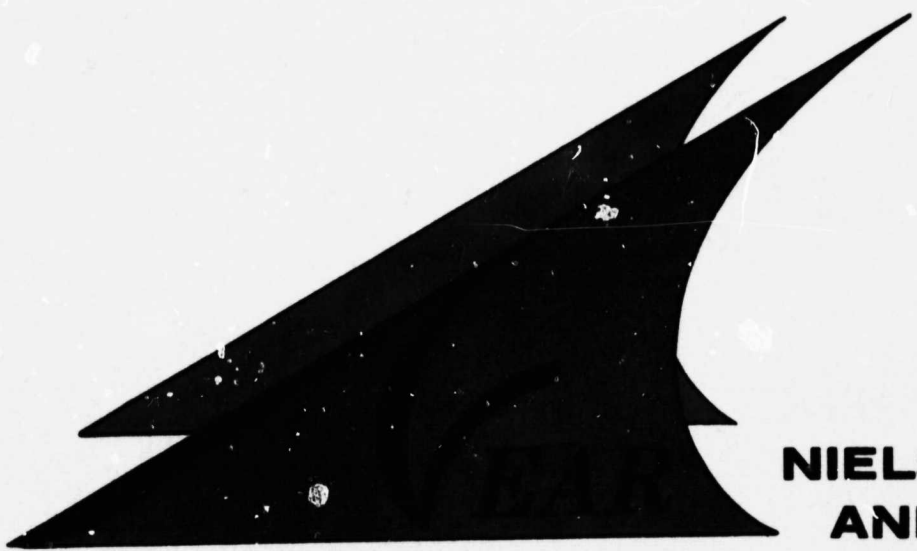
N O T I C E

THIS DOCUMENT HAS BEEN REPRODUCED FROM
MICROFICHE. ALTHOUGH IT IS RECOGNIZED THAT
CERTAIN PORTIONS ARE ILLEGIBLE, IT IS BEING RELEASED
IN THE INTEREST OF MAKING AVAILABLE AS MUCH
INFORMATION AS POSSIBLE

CR-152331
(T Gregory)



(NASA-CR-152331) CONTINUED DEVELOPMENT AND CORRELATION OF ANALYTICALLY BASED WEIGHT ESTIMATION CODES FOR WINGS AND FUSELAGES Contractor Technical Report, Jun. 1975 - May 1976 (Neilsen Engineering and Research, G3/05 N81-18044 Unclas 16241



**NIELSEN ENGINEERING
AND RESEARCH, INC.**

OFFICES: 510 CLYDE AVENUE / MOUNTAIN VIEW, CALIFORNIA 94043 / TELEPHONE (415) 968-9457

1 Report No. CR-152331		2 Government Accession No.		3 Recipient's Catalog No.	
4 Title and Subtitle CONTINUED DEVELOPMENT AND CORRELATION OF ANALYTICALLY BASED WEIGHT ESTIMATION CODES FOR WINGS AND FUSELAGES				5 Report Date March 1978	
7 Author(s) Joseph Mullen, Jr.				6 Performing Organization Code 325/C	
9 Performing Organization Name and Address Nielsen Engineering & Research, Inc. 510 Clyde Avenue Mountain View, California 94043				8 Performing Organization Report No. NEAR TR 161	
12 Sponsoring Agency Name and Address National Aeronautics and Space Administration Ames Research Center Moffett Field, California 94035				10 Work Unit No.	
				11 Contract or Grant No. NAS2-8558	
				13 Type of Report and Period Covered Contractor Technical Rept. June 1975 - May 1976	
15 Supplementary Notes None				14 Sponsoring Agency Code FAC	
16 Abstract <p>The implementation of the changes to the program for Wing Aeroelastic Design (WADES) recommended in part I of this work and the development of a program to estimate aircraft fuselage weights are described. The equations derived to implement the modified planform description, the stiffened panel skin representation, the trim loads calculation, and the flutter constraint approximation are presented. A comparison of the wing model with the actual F-5A weight material distributions and loads is given.</p> <p>The equations and program techniques used for the estimation of aircraft fuselage weights are described. These equations were incorporated as a computer code. The weight predictions of this program are compared with data from the C-141.</p>					
17 Key Words (Suggested by Author(s)) Structural Synthesis, Wings, Fuselages, Aeroelasticity, Approximation Concepts, Weight Estimation			18 Distribution Statement UNCLASSIFIED - Distribution Unlimited		
19 Security Classif. (of this report) UNCLASSIFIED		20 Security Classif. (of this page) UNCLASSIFIED		21 No. of Pages 138	22 Price*

CONTINUED DEVELOPMENT AND CORRELATION OF
ANALYTICALLY BASED WEIGHT ESTIMATION
CODES FOR WINGS AND FUSELAGES

by

Joseph Mullen, Jr.

NEAR TR 161

January 1980

Prepared under Contract No. NAS2-8558

for

NATIONAL AERONAUTICS AND SPACE ADMINISTRATION
Ames Research Center

by

NIELSEN ENGINEERING & RESEARCH, INC.
510 Clyde Avenue, Mountain View, CA 94043
Telephone (415) 968-9457

TABLE OF CONTENTS

<u>Section</u>	<u>Page</u>
SUMMARY	1
INTRODUCTION	2
SYMBOLS	4
SURVEY OF PROGRAM FOR THE ESTIMATION OF WING AND FUSELAGE WEIGHTS	6
Empirical Weight Estimation Programs	7
Semi-Empirical Weight Estimating Programs	11
Analytically Derived Weight Estimating Programs	13
Survey Summary	23
Recommendations of Survey	24
Modifications to Wing Design Code	26
Geometric Planform Definition	26
STIFFENED PANEL STRUCTURAL MODEL	28
STRUCTURAL DESIGN	29
Trim Loads Calculation	32
Critical Load Profile	34
SECONDARY WEIGHT EQUATIONS	37
Leading-Edge Structure	39
Trailing-Edge Structure	41
FLUTTER SENSITIVITY	43
Flutter Constraint Approximation	44
Comparison of WADES Estimates with the F-5A Wing	46

TABLE OF CONTENTS (concluded)

<u>Section</u>	<u>Page</u>
Structural Model of F-5A	46
Distribution of Material	48
Externally Applied Loads	50
Estimation of Fuselage Weights	51
Approach to Weight Estimation	54
FUSELAGE GEOMETRY DESCRIPTION	55
SECTION GEOMETRY	58
TORSIONAL GEOMETRY	66
STRUCTURAL GEOMETRY AND INERTIAS	69
Shell Cover Design Criteria	77
MINOR FRAME SIZING CRITERIA	79
SHELL BENDING CRITERIA	85
Miscellaneous and Secondary Structural Weight	95
Summary and Intermediate Output	96
Fuselage Module Sample Case	97
Conclusions and Recommendations	99
REFERENCES	101

LIST OF FIGURES

Figure

- 1 Aerodynamic planform descriptions
- 2 Structural planform descriptions
- 3 Geometric description of wing stiffened cover sheet model
- 4 Relative location of loads for trim flight
- 5 Equivalent reactions at wing-fuselage junction
- 6 FAR required maneuver and gust load factor envelopes
- 7 Typical design speed versus altitude envelope
- 8 Computed and Taylor series approximation of flutter dynamic pressure versus wing weight for variations in design variables
- 9 F-5A/B Planform layout and surface fit of skin thickness, $t(x,y)$
- 10 F-5A/B Cross-sectional area of structural material versus span
- 11 F-5A/B Moment of inertia, I_x , of structural material versus span
- 12 F-5 Limit spanwise wing loads, flight condition 123C-5
- 13 F-5 Limit spanwise wing loads, flight condition-dynamic landing, $\tau = 118$
- 14 AN-9102-D Detailed weight statement - Body Group, C141
- 15 Sears-Haack body with circular section
- 16 Double-lobe cross section geometry
- 17 Double-lobe structural sectors
- 18 Double-lobe closed torque box
- 19 Double-lobe torque box with lower cutout
- 20 Double-lobe torque box with upper cutout
- 21 Longerons and stringer structural geometry
- 22 Geometric model used in analysis of minor frames
- 23 Geometric model used in analysis of longitudinal members

LIST OF TABLES

Table

- I Summary of Empirical Weight Estimation Program Capabilities
- II Summary of Analytical Weight Estimation Program Capabilities
- III Comparison of Estimated and Actual Group Weights for the F-5A
- IV Comparison of Estimated and Actual C-141 Fuselage Group Weight Statements

CONTINUED DEVELOPMENT AND CORRELATION OF
ANALYTICALLY BASED WEIGHT ESTIMATION
CODES FOR WINGS AND FUSELAGES

By Joseph Mullen, Jr.
Nielsen Engineering & Research, Inc.

SUMMARY

The implementation of the changes to the program for Wing Aeroelastic Design (WADES) recommended in part I of this work and the development of a program to estimate aircraft fuselage weights are described. The equations derived to implement the modified planform description, the stiffened panel skin representation, the trim loads calculation, and the flutter constraint approximation are presented. A comparison of the wing model with the actual F-5A weight material distributions and loads is given.

The equations and program techniques used for the estimation of aircraft fuselage weights are described. These equations were incorporated as a computer code. The weight predictions of this program are compared with data from the C-141.

INTRODUCTION

Under the sponsorship of the National Research Council from 1972 to 1974, a program for the aeroelastic design of simplified conventional and multilayered composite wings for strength and flutter requirements (WADES) was written in order to study techniques in structural optimization. Under Contract No. NAS2-8558* from NASA/Ames Research Center, Nielsen Engineering & Research, Inc. was funded to incorporate this capability into ARC's aircraft synthesis program, ACSYNT. In the first phase of this contract detailed comparisons of the estimated weight, material distributions, and loads of the WADES program with those of the F-5A/B wing were made. As a result of that comparison certain program deficiencies were identified (ref. 1). In the second phase of this contract the changes recommended to correct those deficiencies were incorporated into the WADES program.

Part of the first phase of Contract NAS2-8558 was the integration of the wing aeroelastic design program as a module of the vehicle synthesis program, ACSYNT. In order to fully assess the potential of the advanced structural technology of this program on vehicle weights it was decided that both wing and body weights should be computed. The development of a program to predict fuselage weights was then undertaken as part of the second-phase work. A survey of current programs was made to take advantage of available technology. This is the final report summarizing the modifications to the WADES program and the derivation of the equations used in the prediction of the fuselage weight estimates.

The survey of computer codes was undertaken to compare the technology and adaptability of available computer programs for the estimation of wing and fuselage weights. A summary of the results of that survey is given here. As a result, some of the

* Technical Monitor: Dr. G. N. Vanderplaats.

methods employed by reference 2 have been adapted for use in this work. The purpose of this report is to explain the adaptation of those methods and the modifications are required to incorporate them into the current programs. Rederivation of much of the work in terms of geometric descriptors used by the ACSYNT program was required. The derived equations, the general flow of the programs, and the comparison of the computed results with actual aircraft data are given here.

SYMBOLS

C	Chord length
$d(\xi, \eta)$	Depth function describing the wing thickness over the planform
F_i	Discrete force or mass of i'th component
h	Altitude
i	Subscript or component location in an array
K	Weight coefficient
ΔK	Incremental weight coefficient
M	Mach number
M_x, M_y	Bending moments about x- and y-axes, respectively
N_z	Limit load factor
q	Dynamic pressure, or shear flow
R_1, R_2	Reaction forces at wing-body interface
R	Root chord
r	Local fuselage radius
S	Planform area
SPAN	Semi-span
$t(\xi, \eta)$	Thickness function describing skin cover gage over the planform
t/c	Thickness to chord ratio
V	Velocity
V_z	Shear force perpendicular to wing
W	Weight
W/S	Weight per unit area
x, y, z	Basic coordinates: x-streamwise, y-spanwise, z-transverse
x/c	Ratio of local x distance to chord
x_{LE}, x_{TE}	x/c locations from leading and trailing edges of structural planform
θ_1, θ_2	Leading and trailing edge sweep angles
μ	Poisson's ratio for material

SYMBOLS (Concluded)

ξ Nondimensionalized x-length; for wings $\xi = x/R$,
for fuselages $\xi = x/L_{fus}$

η Nondimensionalized y-length; $\eta = y/SPAN$

SURVEY OF PROGRAMS FOR THE ESTIMATION OF WING AND FUSELAGE WEIGHTS

A survey of weight estimating programs was undertaken in order to take advantage of prior technology and available computer codes in the development of a structural weight estimation for use with the ACSYNT program. This summary does not contain all the programs written to perform this task, but hopefully enough of the codes have been examined to formulate a representative approach to module development.

In the evaluation of the various programs, primary emphasis was placed upon their applicability to vehicles of interest to ACSYNT and their adaptability to vehicle synthesis. Where only the data base was of interest, the information was considered primarily for use by the WADES program. The scope of the codes examined was limited to those programs which predict the weights and structural responses of wing and fuselage structural components. The specific criteria employed included the following:

(a) The level of sophistication of the program was assessed to determine the complexity of the structural model and the computational speed of the program. This included a judgement of the program's potential use in either a Level I or Level II structural analysis or design in conjunction with the ACSYNT program. A Level I program in these contexts is a very fast executing program which generally provides a Group Weight Statement estimation of the component weight items based on the gross parameters of the aircraft. A Level II program requires longer execution times and generally is based on structural analysis and can provide weight estimation for Detail Weight Statement items. It usually has the analytical basis to assess new technology.

(b) Whether primary and/or secondary structural weights are estimated was determined.

(c) The technology level was assessed to determine the depth of the structural concepts used, the advanced design techniques used, and the ability of the program to consider multiple design criteria and advanced materials.

(d) The program's adaptability for use with the ACSYNT program was determined. This included an assessment of its potential for direct incorporation as a module of ACSYNT, its use as a data source (theoretical or empirical), its use as a stand-alone program to be employed vehicles under consideration. Its utility to ACSYNT was based initially on its adaptability to the WADES, SSAM, or SAD programs currently in use.

(e) The integration effort and data required from other modules to use the program were estimated.

The following programs were examined in the literature. They are partitioned according to types of analysis used to obtain the weight estimates: empirical, semi-empirical, or analytical.

Empirical Weight Estimation Programs

The most prevalent weight-estimating techniques used in preliminary vehicle synthesis are based on empirical data. Statistically correlated equations are derived to predict the weights of various components. The obvious pitfall is that the equations are only valid within the bounds of the original data. The use of such techniques is limited in value when considering new concepts that may lie outside the original data.

Three programs in this class were looked at closely. Each of these was being used in a vehicle synthesis program.

(1) WAVES Program - this is currently used in the ACSYNT program at Ames Research Center; maintained by Alice Barlow. It is a Level I program for conventional transport, fighter, and bomber aircraft types. The group weights of combined primary and secondary weights are computed. Little advanced technology data

were used in the derivation of the empirical coefficients. Advanced technology factors are available as user input.

(2) WAATS Program (ref. 3) - this is a Level I program including component weight equations for conventional transport and military aircraft including some component weight estimations for high-temperature (X-15) aircraft. Weight estimation includes both primary and secondary group weights. Advanced technology used in correlations includes some high-speed and high-temperature aircraft data. Programming features include a generalized form of the equations with coefficients input at execution time. The program or equations derived therein may be easily adapted to ACSYNT. Component correlations demonstrated no better agreement than WAVES equations. This program was originally written for use with ODIN at LRC and is also being used with EDIN at JSC.

(3) WTSIZ (refs. 4, 5 and 6) - this General Dynamics Level I program calculates the basic structural component weights of advanced fighter, bomber or cargo aircraft. Weight estimation includes both primary and secondary group weights. No explicit advanced technology factors were used in correlations with data. Programming features include an interactive mode in combination with performance and geometry modules for use in vehicle synthesis. Balance capability is also included. The program is primarily used in an interactive mode. It does contain the estimation of a number of subcomponent weights not available in the ACSYNT program.

Other statistical weight estimating methods and programs exist (refs. 7-14). Only the previous three were summarized with any depth, since the primary interest here is to examine semi-empirical and analytical approaches. Some other programs in use are:

HIPERAC - program used by Naval Air Development Center to study high-performance aircraft.

- VASCOMP - program used by Aeronautical Systems Branch at ARC for short-haul CTOL-V/STOL aircraft; developed by Boeing Vertol.
- HESCOMP - program used by Aeronautical Systems Branch at ARC to study rotary wing aircraft; developed by Boeing Vertol.
- GASP - program used by Aeronautical Systems Branch at ARC to study general aviation aircraft.
- EDIN - uses the mass- and volumetric-property programs SSP, VAMP, VASC, WAATS, CASPER, ESPER, and APSB.
- CASP - program used by Prototype Division of Air Force Flight Dynamics Laboratory for vehicle synthesis using WTSIZ routines.

TABLE I. - SUMMARY OF EMPIRICAL WEIGHT PROGRAM CAPABILITIES

Capability/Program	WAVES	WAATS	WTSIZ
LEVEL	I	I	I
Weight Types Computed			
Primary	x	x	x
Secondary	x	x	x
Subcomponent			x
Technology Level			
Conventional	x	x	x
Composites			
Thermal		x	
Input	x		x
Program Features			
Default Values	x		
Optional Input	x		x
Generalized Equations		x	
Vehicle Applicability			
Transports	x	x	x
Fighters	x	x	x
Bombers	x	x	x
General Aviation			
RPV's	x		
High-Speed Aircraft		x	
Missiles			
Cargo	x	x	x
ACSynt Compatibility			
Code	x	x	
Data Base	x	x	x
Stand-alone	x	x	x

Semi-Empirical Weight Estimating Programs

The second grouping of weight estimating methods examined is classified as semi-empirical. These techniques are analytically derived explicit or integral equations which size the structure or structural component to satisfy a single critical design criterion. The equations are then multiplied by a statistically obtained "non-optimum" factor to compute the actual structural weight. Because these equations typically try to predict weights of such complex structural components as wings and fuselages, there can be 20-30 percent error resulting from such "non-optimum" factors. The following semi-empirically derived weight estimating methods were examined:

(1) The wing and fuselage weight estimating equations by Shanley and Micks are given in reference 15 and 16. The explicit forms of the equations could be developed into Level I weight-estimating relationships. A numerically integrated form could be developed to handle geometric discontinuities within the guidelines of Level I. The weights computed are the primary structural weights, with the secondary weights calculated by the use of "non-optimum" factors or empirically based secondary component equations. The technology level used to derive these equations was derived from conventional metal construction. The analysis assumes certain optimal failure modes in deriving sizing criteria. Subsequent modification of these optimal relationships may be incorporated to provide limited capability for advanced technology. No direct program was currently available, though one could be assembled using the ACSYNT geometric descriptors. Minimal data from other modules would be required.

(2) Wing and body weights are computed as part of the TRANSYN program in reference 12 for transport-type aircraft. A similar derivation for elliptically shaped hypersonic configurations is found in reference 18. The transport wing weights are computed

using a multi-spar box beam sized on the basis of the critical instability modes in reference 19. The volume of material required for shear and bending is computed at each station and integrated spanwise. The structural model, however, incorrectly models shear flow in the wing. Torsion is included only in the carry-through structure, and only maximum symmetric pull-up loading is considered. Considerations of the detail of the structural model and relative computational speed suggest that this program is Level I. Secondary weights are computed by using a "non-optimum" factor. Advanced technology is limited to suitable modifications of critical instability modes. Design algorithms are limited to one-dimensional searches for point designs. The program follows a Shanley approach and does not provide sufficient improvement to merit direct incorporation.

The fuselage weight computation is an adaptation of Shanley's sizing procedure. Body sizing is based on maximum bending moment due to symmetric pull-up or dynamic landing loading conditions. This is also a Level I program. Secondary structural weights of attachments, bulkheads, etc. are estimated by a single "non-optimum" weight factor. No advanced technology has been incorporated. The only improvement over Mick's development is the inclusion of numerical integration along the body length, and consideration of the landing loads. No combined loading effects or area ruling effects are considered.

(3) A wing-box weight predicting method is proposed by Burt in references 20 and 21. His method basically follows the approach taken by Shanley of computing the volume of material needed for shear, bending, and torsional requirements. Burt's contribution was the consideration of several types of construction (skin-stringer-rib, honeycomb, corrugated core, etc.) in the weight equations. No program exists that could be readily adapted. It would be a Level I program. Only the primary structural weights are predicted analytically. The only advanced technology concepts

included in his derivations were the optional construction types. Most of these are mid-50's construction state-of-the-art. The associated data would be the only portion of the analysis with potential for adaptation as a structural weight estimation module of ACSYNT.

Analytically Derived Weight Estimating Programs

The third grouping of weight estimating programs examined is classified as analytical. These programs are generally derived to model the actual structural concept and analyze and design the structure to satisfy multiple loading conditions. Secondary structural component weights are usually included by either empirical or semi-empirical relationships. Analysis models fall into two categories: beam models and finite-element models. Design approaches include the use of point sizing, optimality criteria, and mathematical optimization and most of these programs use Level II category analyses and design. The following analytical weight-estimating programs were examined:

(1) The preliminary wing design program developed by Harold Switzky (Fairchild Republic Co.) is outlined in reference 22. This program is directed at the design of high-aspect-ratio box structures and uses a beam station analysis. Loads are generated by a vortex-lattice aerodynamic technique and scaled during the design to account for the changes in design weight. Effective skin thickness is based on a point design for the optimum skin/stringer combination using a Lagrangian multiplier method (LMM). A similar design approach is used to generate the optimum 0/+45/90 composite laminates. This is a Level II program, though it does not look long. Only primary structural components are computed. Secondary weights are computed semi-empirically or empirically. The report contains information on the variation of material properties with temperature and fatigue, which has been summarized in explicit form. The variety of construction types is representative

but limited to the available LMM derivations. A flutter design is included only as a lower bound to the stiffness via an optimality-criteria approach, though it considers only the first bending and torsional modes. The point design procedure used is relatively sophisticated but does not address the combined synthesis problem. The program could possibly be used in a stand-alone mode with ACSYNT but would best be used as a data base for a number of technology items. The required input data are unknown. No correlations with existing aircraft were given.

(2) The SWEEP program developed by North American Rockwell in reference 2 estimates complete vehicle weights. The fuselage and wing modules of interest here require up to 10 overlays and 109 subroutines. The wing and empennage weight section has preliminary design to satisfy strength and stiffness. A separate module is available for specifying a flutter design obtained via optimality criteria as the lower bound for the strength design. The wing program is generally restricted to high-aspect-ratio wings with torque-box structures. Loads are generated from a station analysis though allowance for flexibility iterations is made. The design procedures employ direct numerical search or interpolation to find a strength design or to obtain the best stringer or rib spacings. The program contains a comprehensive data base for several types of construction (i.e., stringer, corrugated sheet, composites, sandwich, etc.). The weights of secondary structural components such as flaps and ailerons are estimated from empirical data.

The fuselage module contains detailed estimations for internal and external geometry and loads for circular and a number of non-circular cross-sectional shapes applicable to both civil and military aircraft. Multilevel weight calculations are made for shell covers, major and minor frames, longerons, and bulkheads. In both modules weight correction factors for non-optimum weight are applied for a number of secondary weights. The program uses

multilevel types of analyses (input, rule-of-thumb, and detailed calculation) for secondary component weight estimation. Advanced structural technology includes some composite structures in the wing design. The use of optimality criteria in a companion flutter design program is the only apparent advanced numerical design technique. The portions of the code immediately usable by ACSYNT are the rule-of-thumb estimates of structural components and data associated with different construction types. Over two thousand inputs would have to be provided by ACSYNT to run the program as a direct module. Fuselage design takes between 10 and 60 seconds on a CDC 6600 computer.

(3) The TSO program outlined in reference 23 is used for the aeroelastic design of isotropic and multilayered composite wing skin panels. The structure is modeled as a trapezoidal equivalent flat plate, and stiffness and mass matrices are obtained by a Rayleigh-Ritz procedure. Optimization is carried out by sequential unconstrained minimization techniques (SUMT) with a penalty function. Material distributions are described by continuous functional distributions. The program uses Woodward-Carmichael steady aerodynamics and kernel-function unsteady aerodynamics. No buckling criteria or transverse shear (spars or ribs) are included in the design. This is a Level II program. No secondary weight estimates are made. In general the program provides less detailed weight information than previously discussed.

(4) The WIDOWAC (Wing Design Optimization with Aeroelastic Constraints) program outlined in references 24, 25, and 26 is currently being maintained at Langley Research Center for research studies in aeroelastic design. This is a Level II finite element structural program with symmetric shear web and membrane plate elements. It uses piston-theory supersonic aerodynamics and kernel-function subsonic aerodynamics. Optimization is by a SUMT search technique which uses approximate second derivatives in conjunction with Newton's method. Design-variable linking is used

to reduce the number of design variables. Run times typically require 1-5 minutes on the CDC 6600. Maximum stress, minimum gage, and flutter constraints are included in the design. No buckling or advanced material technology is included. No secondary structure weight estimation is included. WIDOWAC should best be used in a stand-alone mode with ACSYNT for comparative purposes where flutter is of concern since no compatible automatic data generation exists.

(5) The SWIFT program developed at Langley is outlined in reference 27. This is a Level II program for the minimum-weight design of wings for combined strength and flutter requirements. The program uses an equivalent plate structural analysis and piston-theory unsteady aerodynamics. No secondary structural weight is computed. Primary structural weight estimation is restricted to isotropic cover sheet material for a trapezoidal wing. No advanced structural concepts are used. This was a forerunner of the WADES program and has been superseded by enhanced versions.

(6) The SSAM program was adapted for use in the ODIN synthesis program and is outlined in reference 28. The program is applicable to the strength design of high-aspect-ratio swept wings. It uses the aeroelastic subsonic lifting-line theory developed by Gray and Schenk in reference 29. The box-beam structure is sized iteratively using a stress-ratio algorithm. Strength, buckling and minimum-gage constraints are included in the box structural model. No advanced materials such as composites are currently included. It may be used now as a stand-alone program with ACSYNT. Several non-optimum factors are included for the estimation of secondary structural weights. Automatic data generation would be required for use with ACSYNT directly. Execution times would be on the order of 1-2 seconds on a CDC 7600. The external loads are limited to the subsonic regime.

(7) The SAD program under development at Ames Research Center is a small intermediate-scale finite-element structural design program to support aerospace vehicle synthesis. This is a very efficient general structural design code for research in optimization. It contains stress, displacement, and frequency constraints. It has no plate buckling criteria, automatic data generation, or aerodynamic loads. Only primary structural weights are computed. No provisions for advanced structural concepts are currently incorporated. Superior advanced design concepts included are stress-ratio and feasible-directions numerical searches, inverse design space, Taylor-series constraint approximation, analytic gradients, design-variable linking, and multiple loading conditions. The only mode of operation with ACSYNT in the near future would be for stand-alone comparisons for variations in parameters. Configurations considered are limited only by generation of geometric and load data.

(8) The ACCESS program (refs. 30, 31, and 32) is a pilot program to study and demonstrate approximation-concept capabilities in the synthesis of general structures by means of the finite-element method of structural analysis. This is a very efficient Level II general purpose structural design code. It contains stress and displacement constraints. No plate buckling constraints, automatic data generation or aerodynamic loads are incorporated at this time. Only primary structural weight is computed. Flutter and composite materials are being incorporated. Advanced design concepts include NEWSUMT and feasible-directions numerical search techniques, design-variable linking, regionalization with respect to element configuration, inverse design variables, constraint deletion, Taylor-series constraint approximation, analytic gradient information, and multiple loading conditions. The only direct usefulness in vehicle synthesis would be the generation of trend information in a stand-alone mode. The design concepts may be of use in various program developments.

(9) The ORACLE program used by Boeing for the preliminary design of high-aspect-ratio wings is documented in reference 33. This program uses the finite-element flexibility model outlined in reference 29 and also used by the SSAM program. This version uses more structural detail than used by SSAM in the beam model to size the structural box. Non-optimum weight fractions and secondary weights are also computed from statistical methods. Approximately the same data generation for use with ACSYNT would be required for this program as for SSAM. Demonstrated correlations exist in the above reference.

(10) The APAS program was developed under Convair IRAD and is outlined in reference 34. The program can currently resize wing and fuselage components for strength requirements using a combination of beam and finite-element procedures. This is a Level II program primarily for transport aircraft. No documentation of comparisons with existing aircraft was accessible for the prediction of non-optimum structural weight or for secondary structural weights. A structural synthesis capability is available for a wide variety of structural concepts including composite sandwich construction. A mixed optimization method such as reported by Sobieszczanski and Loendorf (ref. 35) was the basis of the design philosophy. The Fiacco-McCormick method using the Fletcher-Powell-Davidon unconstrained minimization technique was used as the design algorithm. The effects of multiple design conditions and fatigue can be considered. The geometry and external loads are input rather than calculated internally. The program appears to be too large for direct incorporation in vehicle synthesis. Documentation would need further expansion to be of use as a source of information.

A comparison of various program features and capabilities is given in Table II. This includes an assessment of the applicability of the program, the advanced technology included in the design, and the advanced design techniques used in sizing the structure.

The table has been compiled from previously mentioned references and the information is dated. The programs examined do not represent the complete list of programs available in industry. These programs were examined in depth primarily because of their accessibility or the availability of documentation. In general, large-scale finite-element programs were excluded because of their computational expense in a vehicle synthesis environment.

TABLE II.- SUMMARY OF ANALYTICAL WEIGHT ESTIMATION PROGRAM CAPABILITIES											
Program	FAIRCHILD	SWEEP	TSO	WIDOWAC	SWIFT	MISSAM	SAD	ACCESS	ORACLE	APAS	NADES
ACSINT Level	II	II	II	II	II	II	II	II	II	II	II
Structural Model ¹	B	B	P	FE	P	B	FE	FE	B	B	P
Applicability											
Wings - High AR	x	x		x	x	x	x	x	x	x	
- Low AR			x	x	x		x	x			x
Fuselages - Transport		x					x	x		x	
- Fighter		x					x	x			
Arbitrary Shape		x					x	x			
Automatic Geometry Definition	x	x	x	x	x	x			x	x	x
Component Weight Estimation											
Primary	x	x							x	x	x
Secondary	x	x							x	x	x
Structural Technology											
Isotropic Materials			x	x	x	x	x	x	x	x	x
Orthotropic Materials	x	x				x		x	x	x	x
Composites	x	x	x					x		x	x
Thermal Analysis	x	x						x		x	
Fatigue	x	x							x	x	

¹B = beam model, P = plate model, FE = finite element representation

TABLE II.- Continued

SUMMARY OF ANALYTICAL WEIGHT ESTIMATION PROGRAM CAPABILITIES

Program	FAIRCHILD	SWEEP	TSO	WIDOWAC	SWIFT	SSAM	SAD	ACCESS	ORACLE	PAPAS	MADES
Capability											
ACSINT Level	II	II	II	II	II	II	II	II	II	II	II
Loads											
Constant Pressure					X						X
Piston Theory				X	X						X
Modified Strip Loading		X				X			X	X	X
F. E. Static Aerodynamics	X		X	X							
F. E. Unsteady Aerodynamics			X	X							
Discrete Loads	X	X				X	X	X	X	X	X
Discrete Masses	X	X	X	X		X	X	X	X	X	X
Aeroelasticity											
Flexible-Wing Loads		X	X	X		X			X	X	X
Flutter	X	X	X	X	X					X	X
Divergence			X								X
Reversal											
Control Feedback											
Structural Design Constraints											
Strength - Isotropic	X	X	X	X	X	X	X	X	X	X	X
- Orthotropic	X	X				X		X	X	X	X
- Composite	X	X	X					X		X	X
Buckling - Isotropic	X	X				X			X	X	X
- Orthotropic	X	X							X	X	X
- Composite	X	X								X	X
Interaction Curve	X	X				X			X	X	X
Displacement							X	X			X
Stiffness		X									X
Frequency							X				X
Flutter	X	X	X	X	X						X
Divergence			X								X
Minimum Gage	X	X	X	X	X	X	X	X	X	X	X
Design Algorithm/Technique											
Feasible Directions							X	X			X
SUMT			X	X	X			X		X	

TABLE II.- Concluded
SUMMARY OF ANALYTICAL WEIGHT ESTIMATION PROGRAM CAPABILITIES

Program	FAIRCHILD	SWEEP	TSO	WIDOWAC	SWIFT	SSAM	SAD	ACCESS	ORACLE	APAS	WADES
ACSYNT Level	II	II	II	II	II	II	II	II	II	II	II
Stress Ratio		x				x	x		x		x
Direct Search		x									
Integer Search		x							x	x	
Taylor-Series Expansion							x	x			
Inverse Design Space							x	x			
Lagrange Multiplier	x										
Optimality Criteria	x										

A number of other programs available in the literature were examined. Their references and a brief description of salient features are included here. Most were not given detailed consideration because of their large-scale or proprietary nature. The other programs examined were:

ASOP - This is a general large-scale finite-element program using a modified stress-ratio approach for strength and a numerical search for displacement constraints (refs. 36 and 37). A companion flutter and strength optimization program is described in reference 38.

SAVES - This program uses NASTRAN, Carmichael-Woodward aerodynamics, and stress resizing in an aeroelastic synthesis procedure for wings (ref. 39).

FADES - This is a fuselage design code using finite-element analysis and mixed optimization in which partitioning into substructures is performed for resizing (ref. 35).

OPTIM II - This is a general-purpose finite-element program for minimum weight structures subjected to static loading conditions. Optimization is based on optimality criteria. It contains no aerodynamic interface (refs. 40 and 41).

OPTSTATIC - This is a finite-element program for studying resizing statically loaded structures based on strain-energy-distribution optimality criteria (refs. 42 and 43).

OPTCOMPOSITE - This is a variation of the OPTSTATIC program adapted for the minimum-weight design of multilayered composites. (ref. 44).

NASTRAN - NASA-supported finite-element structural analysis program (ref. 45).

SNAP - This is a large-scale finite-element program.

ATLAS - This is a Boeing-produced large scale finite-element program for aircraft structures. It is a major aeroelastic analysis program with a strength resizing capability.

ASDP - This finite-element program is suitable for designing minimum-weight structures under static loading conditions. It uses a feasible-direction search technique (refs. 46 and 47).

WINGOPT - This is the original program from which the WADES program evolved. It also includes geometric parameters of the wing for designing for optimum configurations (ref. 48).

ECI-ICES-STRUDL/DYNAL - This a large-scale finite-element structural analysis program. It uses design-table look-up for minimum-weight strength sizing (ref. 49).

ARROW - This is a McDonnell-Douglas program for automated design of large aerospace structures subject to static loading. Optimization by both nonlinear programming and optimality criteria is being used together with the large finite-element code, FORMAT (ref. 50).

Survey Summary

The three classes of structural weight estimating programs examined were: I - Empirical weight-estimating procedures, II - Semi-empirically derived procedures, and III - Analytical design procedures. The detail and relative sophistication of the techniques increase in the order given.

The Class I weight estimating programs provide the most rapid estimating technique. They are often as accurate within the bounds of their data as the more complex methods. This is especially true when the estimation of secondary structure is involved. Only the WTSIZ program examined here provides subcomponent weight estimates.

The Class II weight-estimating equations are generally based on obtaining an equivalent volume of material to satisfy a given load distribution. This allows for a moderate amount of flexibility to compare technology used in sizing and to evaluate the sensitivity to major geometric variations but provides little consideration of changes in the critical loading or of effects of minor structural innovations. The statistical correlations required to compute secondary weights make these methods no more accurate than Class I equations.

The Class III techniques offer the full scope of analysis and design capabilities. These methods have still depended on the use of Class I estimates of secondary weights to be of use in vehicle synthesis. Of the programs examined, a wide variation in methods and technology exists. The industry-developed programs (1,2,6,9,10)* contain better technology and estimation of secondary weight.

These programs put considerable emphasis on detailed sizing of such structural components as stiffeners, ribs, rings, and

*Numbers refer to analytically based programs discussed in section 1.3.

bulkheads, and on the inclusions of all applicable constraints. This is consistent with the industry approach that the technology is more important than numerical methodology used to automate the design procedure. The research-oriented programs (Nos. 3,4,5,7, 8) have demonstrated the applicability and superiority of numerical design techniques but are currently capable of providing only trend information. In general, structural detail has been sacrificed in order to obtain computational efficiency.

Recommendations of Survey

The recommendations presented here are based in part on the evaluations of the programs described and in part on the intended use of the results in vehicle synthesis. The accuracy of the results is based on the requirements for first or second level analysis detail. The program requirements will be discussed in terms of the estimation of wing and fuselage weights.

Because of the optimization techniques used in vehicle synthesis many vehicle configurations must be examined rapidly. Explicit continuous functions such as those derived from statistical methods of weight estimation are best suited to vehicle design. The procedure recommended here is to generate analytically based explicit functions from second level type structural weight estimating programs. This procedure would entail computation of vehicle component weights by systematic variation of the vehicle design parameters about a nominal configuration. An explicit function developed from techniques as regression analysis would be derived for vehicle synthesis.

The general characteristics that must be possessed by structural wing weight estimating codes are that they model the requirements of the spectrum of configurations to be considered. For the transport and fighter aircraft expected to be examined the structural design code should be able to assess the influence

of wing flexibility on static loads and flutter; it should be able to model the skin as a stiffened metallic or composite plate and consider the effects of spar and rib spacing; and it should be able to estimate, at least by empirical methods, the secondary structural weights. The preferable technique for analyzing the flutter margin for design should incorporate a finite element stiffness approach. For most medium to high aspect ratio wings a beam finite element should suffice.

Of the second level programs considered the SWEEP program is the closest to being able to meet all the general requirements. The structural design for flutter and wing flexibility are normally performed separately from the strength sizing, which though not preferred, would be acceptable. The ORACLE program would be acceptable for subsonic strength design but is proprietary and lacks flutter and supersonic aerodynamic capabilities. Both programs have been correlated against wing weight estimates. Both programs would require consistent scaling of inputs to get proper sensitivity data. The WADES program with the stiffened plate skin and secondary weight equations should provide trend information for medium to low aspect ratio wings. The programs WIDOWAC, SAD, or ACCESS are still far from providing accurate total wing weight data, but they might be adapted to provide sensitivity information for unusual configurations. They are best for providing new design methodology that should be useful in the future.

The best compromise for a Level II structural design program for the estimation of fuselage weights is a modification of the SWEEP program to accept the geometry descriptors of the ACSYNT program. This should include a station analysis and design using a beam model. This model should be compatible with finite-element methods for later growth. The basic geometry within the program would not be significantly affected; only generation of certain parameters in terms of ACSYNT descriptors would then be necessary.

The secondary weight calculations would be used directly. To obtain vehicle sensitivities a consistent set of scaling relationships for the inputs will have to be generated.

Modifications to Wing Design Code

In the phase I work of this contract a number of limitations in the program modeling were identified which, when corrected, should improve the comparisons with actual aircraft. The recoding of the WADES program was undertaken in the second phase of this contract to incorporate the recommendations. The modifications incorporated and described here include: 1) expansion of the geometric planform definition to non-trapezoidal shapes, 2) incorporation of a stiffened panel structural model, 3) adaptation of a trim loads calculation reacting the wing-body interface loads at the fuselage junction, 4) estimation of secondary structural component weights, and 5) development of an approximate flutter constraint. The descriptions of the theoretical derivations and implementations of the modeling and design changes follows.

Geometric Planform Definition

As a result of the initial correlation studies, it was recommended to modify the definition of the aerodynamic and structural planforms to allow for a small number of planform discontinuities. This was considered necessary because in the comparisons with actual aircraft the estimation of the weight showed a strong correlation with the planform area used to define it. The use of a single trapezoidal wing segment was therefore inadequate for a reasonable weight estimate.

The original and the new planform description of the WADES wing model are shown in figures 1 and 2. In each case, both geometric descriptions are still acceptable inputs to the program. Figure 1 shows the two acceptable descriptions of the aerodynamic planform of the wing. The original description consisted of a

single trapezoidal region defined by the root chord, R , the semi-span, $SPAN$, and the leading- and trailing-edge angles, θ_1 and θ_2 . The new description consists of up to two adjacent trapezoidal regions. This allows for the presence of one major planform break in the wing. The presence of an overlapping fuselage of width from the centerline, $YFUS$, is also included. This also will be used in the definition of loads to specify the point at which the wing loads are transferred into fuselage. Only the portion of the wing outboard of the fuselage will be considered to carry aerodynamic loads. This alternate description is defined by the leading-edge coordinates XSA and YSA , the chord length, CSA , and t/c ratio, TC , at each of NSA stations ($NSA \leq 3$).

Figure 2 shows the two acceptable descriptions of the structural planform of the wing. The original planform description consisted of a single trapezoidal region whose leading and trailing edges were defined as a fixed percentage of the local chord. The new description consists of up to three adjacent trapezoidal regions. The breaks in the structural planform defined here do not have to correspond to the aerodynamic planform breaks. The spanwise location at each of i stations ($i \leq NSS$) is defined as a function of its fraction of span by $ETASS(i)$. Three values define the chordwise locations of the structural regions at each station. The first value, $XCSS(1,i)$, is the x/c location of the leading edge of the structural region at the station. The second, $XCSS(2,i)$, is the x/c location of the trailing edge inboard of that station. The third, $XCSS(3,i)$, is the x/c location of the trailing edge of the structure outboard of that station. This arrangement requires that the leading edge of the structure be continuous. However, the trailing-edge structure may be discontinuous. At the root and at the tip, $XCSS(2,i)$ equals $XCSS(3,i)$.

The computation of wing weight components was modified to reflect the changes in planform definitions. Primary structural

weights will be computed only for structural regions defined in figure 2. The calculation of secondary structural components (i.e., flaps, ailerons, and leading-edge slats) has been incorporated using empirical techniques. The details of the empirical equations that have been incorporated are given later in this report.

STIFFENED PANEL STRUCTURAL MODEL

Modifications to the WADES program during this period were directed towards implementing the proposed changes in the structural model to include the effects of stiffening and buckling of the wing covers. In order to implement the modeling of stiffeners an approximate "Z" stiffened plate description was developed. The variables used to describe this plate are discussed below.

The original description of the cover sheets of conventional wing structures used by the WADES program consisted of a single distributed function, $T(\xi, \eta)$. It was assumed that this was equivalent to the stiffened plate in total volume of material at the optimum design. It did not include its orthotropic effects on the wing stiffness. The initial description chosen to represent the skin-stiffener arrangement is shown in figure 3. The wing segment in figure 3 is partitioned into chordwise and spanwise panels. For the purposes of simplicity the ribs are assumed to be parallel to the x-axis, with a spacing in the spanwise direction of YRIB. This is typical of medium to low aspect ratios and sweeps. The structural reference angle, THET, has been included to define the principal axis along which the structure will be analyzed. This axis should be parallel to the primary direction of the load due to bending. Though some allowance for taper in the width of the stiffened panel is permitted, the internal loads will be estimated only parallel to the structural axes.

The panel cross-section in figure 3 shows the variables used to describe the skin and stringer dimensions. An integral "Z" stiffener is shown in this derivation, though the model is not restricted to that configuration. The isotropic skin thickness is again represented by $T(\xi, \eta)$. The variable describing the stiffener spacing is $B1$. The stiffener dimensions are the width of the web, $B2$, and the flange width, $B3$. For simplicity the flange and web thicknesses are both equal to $T2$. The thickness of the spar is shown to be $T3$ with a semi-height of D .

In order to facilitate the use of the variables in the design procedure each of these variables has been approximated by a function. This is necessary in order to incorporate them in the continuous function analysis approach used by the WADES program. The design variables are then the coefficients of the appropriate functions. This linking in design variables also reduces the total number of variables required. The stiffened plate is thus represented by the thickness function, $T(\xi, \eta)$, the stringer thickness, $T2(\eta)$, and stringer dimensions, $B2(\eta)$ and $B3(\eta)$. The stringer spacing, however, is represented by the inverse of the spacing, as $B11(\eta) = 1/B1$. This design variable was chosen in order to allow explicit integration in the weight equations. The stringer dimensions have initially been represented as functions of η only. This was an arbitrary simplification, and the dimensions may be expanded to functions of ξ and η if required. The code is being arranged so that any of the stringer variables may optionally be left in or left out of the design.

STRUCTURAL DESIGN

The variables used to describe and analyze the stiffened plate were described above and in figure 3. Their incorporation in the analysis and design is now described.

Where the inplane stiffness of the cover plates was described by the product of the modulus and the skin thickness, T , in the old model, it is now obtained as the superposition of the stiffness of the skin and that of the stringers. The stiffness is then written as

$$[E \cdot \bar{T}] = [E_{\text{skin}}]t + [R]^T [E_{\text{str}}] [R] (B_2 + 2 B_3) T^2 B_{11} \quad (1)$$

where $[R]$ is transformation rotating the modulus of the stringer along the structural axes.

The weight of the skin and stringers may be obtained as the sum of the weight of the skin, W_{skin} , and the weight of the stringers, W_{str} . They may be obtained by direct integration of the following equations:

$$W_{\text{skin}} = \int_A \rho t(\xi, \eta) dA \quad (2)$$

and

$$W_{\text{str}} = \int_A \rho (B_2 + 2 B_3) T^2 B_{11} dA \quad (3)$$

Here A is the structural planform over which the integration is carried out, and ρ is the material density. These weights are also used as the objective function during optimization.

The design procedure used to size the wing for strength can no longer be linearized as before. The procedure used now will be similar to that used to size the composite design. Instead of the von Mises' stress being held constant during a sizing cycle, the component edge loading will be held stationary. This technique still allows for changes in load path between skin and stringers during the optimization sequence. Thus, the addition of the buckling imposes a new nonlinearity in the constraints.

The strength constraints on the wing design that will be considered are the von Mises' stress resultant in the skin, the

panel buckling of the skin panels, the buckling of the stringers, and the minimum gage requirements on both. The panel buckling will be in the form of a standard interaction formula for combined shear and compressive buckling of a rectangular panel. Local buckling of the panel will be calculated assuming the lower bound buckling coefficients for panels of infinite aspect ratio. The strength design must satisfy the following inequalities:

Von Mises' stress:

$$\sigma_{VM} \leq S_{max_c} \quad (4)$$

Buckling interaction:

$$1 \geq R_c + R_s^2 = \frac{f_c}{F_{max}} + \left(\frac{f_s}{F_{scr}} \right)^2 \quad (5)$$

Here f_c is the compressive stress along the structural axis and f_s is the shear stress. The buckling allowables are obtained as averages of the tensile and compressive allowables. This is used to average the difference in gages of the upper and lower skins. The longitudinal and shear allowables may then be written as

$$F_{max} = 1/2 \left[S_{max_t} + \min \left(\frac{4\pi^2 E_r (T/Bl)^2}{12(1 - \mu^2)}, S_{max_c} \right) \right] \quad (6)$$

and

$$F_{scr} = \min \left(\frac{5.62\pi^2 E_r (T/Bl)^2}{12(1 - \mu^2)}, \tau_{max} \right) \quad (7)$$

where E_r is the reduced modulus of the material, and S_{max_c} , S_{max_t} , and τ_{max} are the ultimate compressive, tensile and shear allowables, respectively.

Similarly, the stringers are sized by their allowable buckling stresses. No shear effects are included in the sizing of

the stringers. The allowable stress for the web is written as

$$F_{web} = 1/2 \left[S_{max_t} + \min \left(S_{max_c}, \frac{4\pi^2 E_r (T2/B2)^2}{12(1 - \mu^2)} \right) \right]$$

and the allowable for the stringer flange is written as

$$F_{flange} = 1/2 \left[S_{max_t} + \min \left(S_{max_c}, \frac{0.426\pi^2 E_r (T2/B3)^2}{12(1 - \mu^2)} \right) \right]$$

Trim Load Calculation

In the previous version of WADES, the externally applied loads were calculated from one of three methods: piston theory, constant pressure wing loading, or modified strip loading. The appropriate method was selected at program load time and was limited to that method for the remainder of execution. The present program version was modified to incorporate two types of load calculations - modified strip loading and either piston theory or constant pressure wing loading. It is intended that these two methods would represent subsonic and supersonic aerodynamic loads. The choice of the method is specified by the user through the analysis option control parameter, IANAL(2,IFLT). The choice of piston theory or constant pressure wing loading routines is controlled at program load time. Only one of the methods may be loaded during a given run.

Longitudinal trim of the aircraft was incorporated into the loads estimation in order to assess the weight penalty due to center of gravity travel. The center of gravity location is specified as the fraction of the mean aerodynamic chord forward of aerodynamic center (PMAC). The equivalent tail load (P_T) and gross lift (GLR) required to trim the aircraft are then computed. Figure 4 shows the relative location of the aircraft center of gravity at the stress gross weight (SGW), the mean aerodynamic chord (C_{MAC}) and the tail load. The gross lift required and the

tail load are computed from the following summation of forces and moments:

$$GLR - N_Z \cdot SGW + P_T + \Sigma F_i = 0$$

$$GLR \cdot X_{MAC} - N_Z \cdot SGW (X_{MAC} - PMAC C_{MAC}) + P_T X_{HT} + \Sigma F_i X_i = 0$$

Then the gross lift required becomes:

$$GLR = \frac{N_Z \cdot SGW (X_{MAC} - PMAC \cdot C_{MAC} - X_{HT}) - \Sigma F_i X_i + X_{HT} \Sigma F_i}{X_{MAC} - X_{HT}} \quad (10)$$

and the tail load required for trim is:

$$P_T = -GLR + N_Z \cdot SGW - \Sigma F_i \quad (11)$$

The reaction of tail and fuselage loads into the wing is incorporated as an equivalent force couple at the wing-body junction. That is, the total force and moment of the body and tail loads are resolved into two forces at the leading and trailing edges of the structural planform. Figure 5 depicts the relative locations of the two equivalent reactions between the wing and fuselage taken from figure 4 at the y-location of the wing-fuselage junction (Y_{FUS}). The reactions are then included in the structural analysis as concentrated forces. The reaction forces are computed from the summation for forces and moments as follows:

$$R_1 = \frac{-N_Z \cdot W_{BODY} (X_B - X_{R2}) + P_T (X_{HT} - X_{R2})}{2 (X_{R1} - X_{R2})} \quad (12)$$

$$R_2 = \frac{1}{2} [-N_Z \cdot W_{BODY} + P_T - R_1] \quad (13)$$

The calculated load distribution on the wing varies slightly between the modified strip loading and the constant pressure or piston theory loads. In the first, the input values of the location and length of the mean aerodynamic chord are used only as a first guess. The values are subsequently recalculated and the updated values used in later calculations. In the second, the trim conditions are dependent on the input values of X_{MAC} and C_{MAC} .

Critical Load Profile

The identification and specification of the critical loading conditions to be used to size the primary structural elements of the structure form a necessary part of determining the design loads. Here it is intended only to provide guidelines to assist in that selection of flight conditions.

The basic strength requirements must satisfy FAR Part 25 for civil aircraft and MIL-A-008860A or its equivalent for military aircraft. In general the strength requirements must be met for every combination of velocity and load factor within the maneuvering and gust envelopes in figure 6. Typically, the maximum level speed (V_C) and the design dive speed (V_D) are the critical gust conditions and their determination is the primary concern. Figure 7 is a plot of a typical structural design airspeed profile versus altitude. Typically the dive speed or dive Mach limit (M_D) can be specified in terms of V_C or the equivalent cruise Mach limit (M_C), so that only V_C or M_C must be determined.

Once the speed profile of the mission is determined the three remaining parameters to be specified are the maximum maneuvering load factor (n_z), the maximum gust load factor (n_g), and the structural gross weight (SGW). In lieu of special requirements suggested values for the limit maneuver load factors from MIL-A-8861 are as follows:

limit maneuver load factor - n_z

Vehicle Class	subsonic	supersonic	negative	flaps
Fighter, Attack	8.0	6.5	-3.0	4.0
Bomber I	4.0	4.0	-2.0	2.5
Bomber II	3.0	3.0	-1.0	2.0
Cargo Assault	3.0	3.0	-1.0	2.0
Cargo Transport	2.5	2.5	-1.0	2.0

The limit gust load factor may be calculated either from a theoretical gust profile or from the appropriate FAR or MIL empirical equation. The FAR-25 equation for the estimation of the gust load factor coded in the WADES program is as follows:

$$n_z = 1 + \frac{K_g U_{de} V_a}{498 (W/S)} \quad (14)$$

where

$$K_g = \frac{0.88 \rho_g}{5.3 + \rho_g} = \text{gust alleviation factor} \quad (15)$$

$$\rho_g = \frac{2(W/S)}{\rho \bar{C}_a g} = \text{airplane mass ratio}; \quad (16)$$

U_{de} = derived gust velocities (fps);

ρ = density of air (slugs/cu.ft.);

W/S = wing loading (psf);

\bar{C} = mean geometric chord (ft.);

g = acceleration due to gravity (ft./sec.);

V = airplane equivalent speed (knots);

a = slope of the airplane normal force coefficient curve C_{N_A} per radian if the loads are applied to the wings and horizontal tail surfaces simultaneously in a rational method.

The derived gust velocity, U_{de} , is also specified by FAR-25 to be computed from the following:

{	<u>rough-air gust at V_e</u>	
	66 fps	$0 \leq h \leq 20000$
	$\left[66 - \frac{h-20000}{30000} 28 \right]$ fps	$20000 < h \leq 50000$
	<u>gust at V_c</u>	
	50 fps	$0 \leq h \leq 20000$
	$\left[50 - \frac{h-20000}{30000} 25 \right]$ fps	$20000 < h \leq 50000$
<u>gust at V_D</u>		
25 fps	$0 \leq h \leq 20000$	
$\left[25 + \frac{h-20000}{30000} 12.5 \right]$ fps	$20000 < h \leq 50000$ (17)	

The structural gross weight used in the estimation of the critical maneuver loading condition is the weight which produces the maximum stresses in the wing or produces the maximum stresses in the wing or produces the maximum load on the fuselage. The cases which should be checked for this condition include:

- 1) For fuel carried in the wing, the maximum vehicle weight with only the fuel reserves left in the wing.
- 2) The maximum vehicle weight with zero fuel in the wings.

3) The maximum weight at which the maximum maneuver load factor may first be achieved as specified by the mission profile.

The additional loading conditions, which may be critical in the flight and ground handling envelope, are as follows:

1) The maximum load factor in the extended flaps conditions during takeoff.

2) The maximum aileron roll condition with flaps retracted and extended during takeoff.

3) The lg trimmed landing impact condition.

4) The maximum braking roll condition.

SECONDARY WEIGHT EQUATIONS

In order to estimate the weight of leading- and trailing-edge devices, ailerons and fixed secondary structure, a set of empirical equations was included in the WADES program. References 2 and 22 were examined for possible equations. Because of the additional detail and documentation included, the equations of reference 2 were added to the WADES program. The use of these equations does require some additional user input. Appropriate values are calculated from the WADES geometry description wherever possible. The calculated program values may optionally be over-written by the user where specific secondary structural unit weights are known.

The approach taken in the SWEEP program (ref. 2) was to estimate each major leading- and trailing-edge component with statistical equations based on component geometry parameters and/or vehicle design criteria. The basic equations for control surface devices are modified so that the unit weights can be adjusted through specific types of data in the input. The form of the equations has been derived using a general equation form. The weight estimation equation can be expressed in general form as:

$$w/s = K_0 [K_1 + \Sigma \Delta K] [(w/s)_0] \quad (18)$$

where

- w/s = estimated unit weight
- K_0 = general weight coefficient to be used by the user, 1.0 unless changed
- K_1 = basic statistical equation correlation factor, different for all components
- $\Sigma \Delta K$ = derived unit weight modification factors
- $(w/s)_0$ = basic statistical unit weight (function of vehicle environment and geometry)

For all devices, provisions are made in the input data set and analysis logic to allow the user to specify desired unit weights, in lieu of the program derived data.

The basic statistical unit weight, $(w/s)_0$, is derived for each component in one of the following three forms:

$$w/s = C_1 (C_2 X_1 + C_3) \quad (19)$$

$$w/s = C_4 (X_2)^{C_5} + C_6 (X_3)^{C_7} \quad (20)$$

$$w/s = C_8 (X_4)^{C_9} \quad (21)$$

where the C_{1-9} are equation constants, and the X_{1-4} are estimation parameters based on vehicle criteria and component geometry.

The unit weight modification factor $\Sigma \Delta K$ consists of three terms:

$$\Sigma \Delta K = \Delta K_2 \left[\frac{(t/c)_{\text{ref}}}{(t/c)_i} \right]^{0.25} + \Delta K_3 + \Delta K_4 \left[N^{0.125} \dots 1.0 \right] \quad (22)$$

where

ΔK_2 = basic incremental factor for thickness ratio
 ΔK_3 = basic incremental factor for available volume
 ΔK_4 = basic incremental factor for number of actuators

$(t/c)_{ref} = 0.10$, constant

$(t/c)_i$ = aerodynamic thickness ratio at midspan of each segment panel

N = number of actuators per segment panel

Term 1 of equation (18) is included in the fixed structure equations.

Leading-Edge Structure

The leading-edge structure is assumed to include all structures forward of the front spar and between the reference lines defined by the y -coordinate of the wing-fuselage junction and the outboard tip of the structure. Four leading-edge unit weight equations for various types of devices have been included and are optionally available through the program parameter, ISEC(1). The optional unit weight equations are:

ISEC(1) = 0, user inputs (w/s) .

ISEC(1) = 1, fixed leading-edge structure:

$$(w/s)_o = 0.00077 \left[\frac{0.8 Q_{max} S_{le}}{C_{ave}} \right] + 0.83 \quad (23)$$

$$(w/s)_w = K_w \left\{ 1.50 + 0.10 \left[\frac{0.10}{(t/c)_{ave}} \right]^{0.25} \right\} (w/s)_o \quad (24)$$

where

Q_{max} = maximum dynamic pressure, generally determined at V_L , sea level

S_{le} = exposed theoretical leading-edge planform area

C_{ave} = average chord determined by dividing exposed area by exposed leading-edge span measured along front spar

$(t/c)_{ave}$ = aerodynamic thickness ratio at exposed leading-edge midspan

ISEC(1) = 2, leading-edge slats:

$$(w/s)_o = \left[0.551 \left(\frac{N_{zult} DGW}{S_w} \right)^{0.32} + 1.0 \left(\frac{0.8Q_{max} S_{pnl}}{b_{pnl}} \right)^{0.25} \right] \quad (25)$$

$$(w/s)_{sl} = K_{sl} \left\{ 1.0 + 0.10 \left[\frac{0.10}{(t/c)_{ave}} \right]^{0.25} + 0.01 + 1.0 \left[N^{0.125} - 1.0 \right] \right\} (w/s)_o \quad (26)$$

ISEC(1) = 3, leading-edge Kruger flaps:

$$(w/s)_o = \left[0.413 \left(\frac{N_{zult} DGW}{S_w} \right)^{0.32} + 0.667 \left(\frac{0.8Q_{max} S_{pnl}}{b_{pnl}} \right)^{0.25} \right] \quad (27)$$

$$(w/s)_{kr} = K_{kr} \left\{ 1.0 + 0.10 \left[\frac{0.10}{(t/c)_{ave}} \right]^{0.25} + 0.01 + 0.75 \left[N^{0.125} - 1.0 \right] \right\} (w/s)_o \quad (28)$$

ISEC(1) = 4, droop leading edge:

$$(w/s)_o = \left[0.00077 \left(\frac{0.8Q_{max} S_{pnl}}{C_{ave}} \right) + 0.83 \right] + \left[0.33 \left(\frac{0.8Q_{max} S_{pnl}}{b_{pnl}} \right)^{0.25} \right] \quad (29)$$

$$(w/s)_{dn} = K_{dn} \left\{ 1.725 + 0.10 \left[\frac{0.10}{(t/c)_{ave}} \right]^{0.25} + 0.01 + 0.50 \left[N^{0.125} - 1.0 \right] \right\} (w/s)_o \quad (30)$$

where

- N_{zult} = ultimate positive load factor
- DWG = basic flight design gross weight
- S_w = gross wing planform area
- S_{pnl} = planform area for each device segment
- b_{pnl} = device segment span measured along forward device control line
- C_{ave} = average device segment chord

Trailing-Edge Structure

Trailing-edge structure unit weights may be computed for three different types of devices: flaps, ailerons, and fixed trailing-edge structure. The effects of multisegment flap devices are included in the correlation coefficient, K_{type} . All trailing-edge structural planform not specified as either flap or aileron is considered to be fixed trailing edge. The calculation of the appropriate device is controlled by the option parameter, ISEC. The following unit weight equations have been incorporated.

Trailing-edge flaps - ISEC(2) = 0, user inputs (w/s),
 ISEC(2) > 0,

$$(w/s)_o = 0.69 \left[\frac{14.4 Q_{max} \left(\frac{S_f}{b_f} \right)^2}{100 (t/c)_{ave}} \right]^{0.25} \quad (31)$$

$$(w/s)_f = K_f \left\{ K_{type_i} + 0.10 \left[\frac{0.10}{(t/c)_{ave}} \right]^{0.25} + 0.01 + 1.5 \left[N^{0.125} - 1 \right] \right\} (w/s)_o \quad [i = ISEC(2)] \quad (32)$$

Fixed trailing-edge structure (secondary structure) - the basic statistical equation correlation factor, K_1 in the general equation 18, is adjusted for fixed trailing structures by a coefficient that is sensitive to the maximum design dynamic pressure. The correction factor ΔK_q is determined as:

$$\Delta K_q = C_a \left[\left(\frac{Q_{max}}{Q_o} \right)^{C_b} - 1 \right] \quad (33)$$

Here C_a and C_b are constants, currently assigned values of 1.0 and 0.70 for wing and 0.75 and 0.70 for horizontal and vertical tail surfaces, and

Q_o = reference dynamic pressure, 950 psf
 Q_{max} = maximum dynamic pressure, psf

ISEC(3) = 0, user inputs (w/s),
 ISEC(3) = 1,

$$(w/s)_o = 0.0165 \left[\frac{0.35 Q_{max} S_{te}}{b_{te}} \right] + 1.45 \quad (34)$$

$$(w/s)_w = K_w \left\{ 1.0 + \Delta K_q + 0.10 \left[\frac{0.10}{(t/c)_{ave}} \right]^{0.25} \right\} (w/s)_o \quad (35)$$

Ailerons - ISEC(4) = 0, user inputs (w/s)
 ISEC(4) = 1,

$$(w/s)_o = \left\{ 0.01825 \left[\frac{0.35 Q_{\max} S_a}{b_a} \right] + 1.55 + 0.50 \left[0.35 (Q_{\max})^{0.25} \right] \right\} \quad (36)$$

$$(w/s)_a = K_a \left\{ 1.0 + 0.10 \left[\frac{0.10}{(t/c)_{\text{ave}}} \right]^{0.25} + 0.01 \right. \\ \left. + 0.10 \left[N^{0.125} - 1 \right] \right\} (w/s)_o \quad (37)$$

The K_{type} factor in equation 32 is selected from a table of factors based on the type of flap specified. The following table values for K_{type} along with the indicator control word values.

FLAP-TYPE INDICATOR AND CORRELATION COEFFICIENTS

Flap Type	Indicator Value ISEC (2)	Correlation Coefficient K_{type}
Simple	1	1.000
Single-slotted	2	1.250
Double-slotted	3	1.500
Triple-slotted	4	1.750

The flap segment area, S_f , found in equation (31), is the sum of all chordwise panel areas. Thus, for triple-slotted flaps, actual planform areas are computed for each of the three chordwise panels. S_f is then the sum.

FLUTTER SENSITIVITY

In the original version of the WADES program that was integrated with ACSYNT the design loop that performed simultaneous

strength and flutter optimization was left out due to core limitations. In order to get flutter back into the synthesis loop, it is anticipated that an approximation concept flutter constraint can be derived. In order to test its feasibility for use in the WADES program a sensitivity run was attempted to compare a flutter approximation with actual flutter computations. In this example an initial strength design was first obtained and then each design variable was perturbed about that design point. The flutter speed was evaluated for each perturbed design variable. The computed flutter point was then compared with a Taylor series approximation of the flutter dynamic pressure obtained by finite difference. Figure 8 is a plot of two such sensitivity runs for two of the ten design variables used in the example. The flutter dynamic pressure and its Taylor series approximation are plotted versus wing weight. Because the design variables are coefficients of a polynomial function the perturbed variables were selected so as to obtain a unit change in the wing weight. The range of given variable changes spans about a 25% change in the total wing weight.

Flutter Constraint Approximation

A constraint based on the sensitivity information discussed in section 2.8 was incorporated in the WADES program. The basic procedure used was: (1) analyze initial structure; (2) generate the gradients of the flutter speed by finite difference; (3) express the flutter dynamic pressure, q_f , and Mach number, M_f , as Taylor series expansions in terms of the design variables, x_i ; and (4) include the series in the following constraints on the flutter dynamic pressure and Mach number in the strength design iteration:

Minimum flutter dynamic pressure:

$$g_k = 1 - \frac{q_{fo_k} + \sum_{i=1}^{NDV} \frac{\partial q_{fk}}{\partial x_i} (x_i - x_{o_i})}{QFMIN} \leq 0 \quad (38)$$

Minimum flutter dynamic pressure:

$$g_k = 1 - \frac{M_{fo_k} + \sum_{i=1}^{NDV} \frac{\partial M_{fk}}{\partial x_i} (x_i - x_{o_i})}{FMMIN} \leq 0 \quad (39)$$

k=1, NOFC

where

QFMIN = minimum allowable flutter dynamic pressure

FMMIN = minimum allowable flutter Mach number

()_o = initial value of parameter

After the structure is resized, the wing weight is checked for convergence and the design procedure is either restarted or terminated if no change was observed during the last iteration. The gradient calculation may be computed every iteration or may be updated periodically in order to reduce computational effort. The origin, about which the Taylor series is computed, is updated during every iteration.

A preliminary example of this procedure for flutter design was executed using the combined strength and flutter wing design problem of Stroud. Ten cycles of the strength design were performed to obtain an initial material distribution that satisfied the strength constraints but violated the flutter Mach number requirement by 10 percent. Two iterations of combined flutter and strength optimization were performed. The reanalysis of the designs using an approximate flutter constraint after each

iteration showed that the actual flutter Mach numbers were within 0.4 percent of the estimated values.

The user sheets and descriptions were also updated to reflect the new program variables. The program descriptions were expanded to include the new planform definitions, buckling, and secondary weight calculations. A few new variables will be required to execute this program version and will be noted in the documentation. The changes in old variable descriptions or definitions will also be noted.

Comparison of WADES Estimates with the F-5A Wing

In phase I of this contract a number of areas for improvement were identified and changes recommended. The previous section described their integration into the WADES program. The computer code was used to recompute the estimates of the F-5A wing weights performed in phase I. The comparisons of the material distributions, estimated component weights, and spanwise loading distribution computed by the WADES program follow. The results shown here reflect the modifications described in the previous section. A comparison with previous estimates is not given here but may be obtained from reference 1.

Structural Model of F-5A

A re-correlation of the F-5A weight calculations was performed. The input data were modified to reflect the changes in required inputs. The changes were made primarily to reflect the program changes in planform description of the aerodynamic and structural models, in the calculations of loads for trimmed flight, and in the addition of the calculation of secondary structural component weights. The use of the multiregion planform descriptions of the various portions of the wing is described.

Figure 9 is a pictorial representation of the geometry of the mathematical model used by the WADES program to analyze the

F-5A wing. The regions outlined in the interior of the wing planform show the use of the new structural planform description. The three segment structural planform follows the carry-thru, intermediate and outboard panels used in the F-5A as primary load carrying structure. The leading edge and trailing edge flaps and the ailerons are indicated where secondary structural component weights have been computed for these devices. The actual dimensions of these devices have been used in the empirical weight calculations. The remaining planform is designated as secondary structure, and a unit weight estimated as a fixed trailing edge structure. The planform area used in the estimation of aerodynamic loads is that area outboard of the wing-body intersection. Structurally, only that planform area is considered to carry aerodynamic loads. No weights are computed for the planform area interior to the vehicle fuselage except for the wing carry-through structure.

Within the structural planform in figure 9 is a contour plot of the functional representation of the F-5A skin thickness distribution generated from the upper surface of the wing cover. This is the functional representation, $t(\xi, \eta)$, used by the WADES program to analyze the F-5A. A least-squares functional fit of the material distribution over the surface of the wing in reference 51 was computed for both the skin thickness, $t(\xi, \eta)$, and the equivalent thickness, $\bar{t}(\xi, \eta)$, in order to compare the analysis results predicted by the WADES program. The equivalent thickness was computed by distributing the additional spar cap material as wing covering in order to assess the inclusion of the bending effectiveness of the spars. These functional approximations of the skin thickness are used to check the accuracy of the analysis model and as initial values to the design procedure. Subsequent designs are compared with these to assess their validity.

Distribution of Material

Four cases were used to check the estimation of the structural material distributions by the WADES program. The first two analyze the F-5A wing using the thickness functions obtained from the surface fits of the skin covering, $t(\xi, \eta)$, and the equivalent thickness, $\bar{t}(\xi, \eta)$. Only the static analysis was performed for these cases. The third and fourth cases used the first two material distributions as initial functions and redesigned the material distributions to satisfy the constraints defined by the program for sizing only the skin thickness, $t(\xi, \eta)$, and for sizing the skin thickness with equivalent spar caps. The spar caps were approximated by including a stringer of minimum gage. The material gates were resized to satisfy the buckling, strength, and minimum gage requirements for the stresses generated by the WADES program. The estimated of these four examples were then compared to data obtained from the F-5A.

Figure 10 is a plot of the cross-sectional area of structural material versus span for the F-5A and the four WADES check cases. The F-5A structural areas were those used in reference 52 to determine the margins of safety for the wing stress analysis. The cross-sectional areas estimated by the WADES program were obtained by integrating the skin thickness parallel to the structural reference axis along the 35 percent chord. The discontinuities in the material distributions are due to discrete changes in the planform describing the structure. The estimates by the WADES program are generally within 15 percent of the actual distributions. In the first two cases, the functional distributions obtained from surface fits are below F-5A net areas over most of the span. The low values indicate that a certain amount of additional material that contributes to the bending strength is not included in the equation fits. The structural areas estimated by the sizing algorithm are mixed both high and low in various segments of the wing. Some material is missed in the

skin resizing cycle at wing stations outboard of WS 100 due to insufficient loading conditions. This region is sized by minimum gage and external store separation criteria. The low area value at the root for the redesign of $t(\xi, \eta)$ is part due to clamped boundary condition and due to the over-estimation of the depth of the carry-through structure by the depth function.

Figure 11 is a plot of the estimated moment of inertia, I_x , of structural material versus span for the F-5A and the four WADES check cases. The F-5A structural areas were effective moments of inertia used in the wing stress analysis in reference 52. The moments of inertia estimated by the WADES program were obtained by integrating the product of the skin thickness and the square of the wing depth parallel to the structural reference axis. The inertias generally follow the trends displayed by the areas. The excessive inertias through the carry-through structure are primarily the result of an over-estimation of the depth of the structure at the root. The depth function was derived to approximate the theoretical t/c at the root, rather than the constant section carry-through structure.

Table III compares the weights predicted by the WADES program for each of the four check cases to the values obtained from the F-5A wing group weight statement. Of the six component items in the table estimated by the WADES program the center and outboard section weights are computed from structural analysis. The secondary structural weights, ailerons, and flaps are estimated from empirical techniques. For the purposes of generating weight correlation factors the center and outboard sections and the secondary structure are combined as one parameter for the basic structural weight. At the bottom of the table are the ratios of actual to computed groups. The first is the ratio of the net weights. The second is the ratio of the sum of the center, outboard, and secondary structure weights. The third is the ratio of the sum of the aileron and leading and trailing edge flap weights.

Of the sample cases in the table, the functional fit of the skin thickness, t , underestimated the net weight, the available structural area, and the moment of inertia. The functional fit of the effective skin thickness, \bar{t} , and the thickness distribution from the redesign of t gave the most consistent comparison with F-5A areas and inertias and their predicted weights were within one percent. The use of the stringers in the redesign procedure to represent spar caps predicted the best weight, but over-estimated the structural areas and inertias. The average ratio of actual to computed total weight of the four check cases was 1.23. As a group the aileron and flap weights were within nine percent of the actual values.

TABLE III
Comparison of Estimated and Actual
Group Weights for the F-5A

Wing Component	F-5A	Skin function fit		Redesign	
		t	\bar{t}	t	\bar{t}
1. Center Section-Basic Structure	122.3	159.7	170.6	157.3	182.3
2. Outer Section-Basic Structure	716.6	360.8	411.1	415.3	446.2
3. Secondary Structure	36.6	119.6	119.6	119.6	119.6
4. Ailerons	35.7	38.3	38.3	38.3	38.3
5. Flaps - Trailing Edge	61.2	51.4	51.4	51.4	51.4
6. - Leading Edge	69.9	63.6	63.6	63.6	63.6
Total	1041.7	793.4	854.5	845.7	901.4
(W_{act}/W_{comp})	1.00	1.31	1.22	1.23	1.16
$(W_{act}/W_{comp})_{1+2+3}$	1.00	1.37	1.25	1.27	1.17
$(W_{act}/W_{comp})_{4+5+6}$	1.00	1.09	1.09	1.09	1.09

Externally Applied Loads

Two modifications previously described have significant impact on the agreement of the estimated externally applied loads

with F-5A shear and moment distributions. The inclusion of the tail load required for trimmed flight increases the total lift on the wing, and the reaction of the resulting body weight at the wing-fuselage junction pushes the shear and moment distributions outboard. Figures 12 and 13 are plots of the limit spanwise wing loads versus span for the F-5A and the loads estimated by the WADES program. Figure 12 shows the shear and moment distributions for flight condition 123C-5, one of the maximum symmetric loadings which designs the F-5A. Figure 13 shows the loading distributions for the dynamic landing condition, 358B $\tau = 118$.

The F-5A was structurally sized by three flight conditions in these check cases. The maximum symmetric load factor flight conditions, 104 and 123C-5, and the dynamic landing case, 358, were modeled as the critical loading cases in WADES. The resulting analysis and design indicated that the maximum symmetric load factor conditions sized the WADES design. The loads predicted by the WADES program for condition 123C-5, in figure 12 were within 5-10 percent of actual values for the shear, V_z , and bending moment, M_x , over the entire span. The torsional moment, M_y , was about 20 percent low at the root. However, no pitching moment was input into the aerodynamic computations. The dynamic landing case shows fair correlation at the root but varies considerably over the span. The Northrop loads were generated from the dynamics of the landing profile; the WADES loads were estimated as a static equivalent load at impact simulating the force required to absorb the kinetic energy due to the aircraft sink rate.

Estimation of Fuselage Weights

Development of an analytically based computer code for the estimation of aircraft fuselage weights was identified as the second contract item. The derivation of this code was originally

intended to be developed with the geometry descriptors of the ACSYNT program and to be called directly as a module of ACSYNT. The development of a fuselage design code was intended to provide a means of assessing analytically the effects of advanced technology in aircraft design. Part of the survey of available computer codes given earlier in this report was directed towards assessing aircraft fuselage design programs to satisfy these requirements.

Three factors were considered in establishing the approach taken in the development of the fuselage code: the recommendations of the computer code survey, the requirements of the ACSYNT program, and the development of other codes for structural design to complement the ACSYNT program.

The original recommendations of the survey of available computer codes were directed towards assessing the programs' potential for rapid estimates of structural weight or Level I weights estimation. In these terms the survey suggests that a combination of the procedures outlined by Shanley (ref. 15) and methods employed by the SWEEP program (ref. 2) should be adapted. The basic structural components would be estimated analytically with a great number of secondary structural component weights adapted from the SWEEP program. This approach generally restricts itself to a station analysis of the fuselage.

The vehicle synthesis and optimization procedures used in the ACSYNT program have evolved using empirically based equations. Because the user typically does not have the expertise to generate all inputs alone it has been decided that the more detailed structural design programs would not be executed from within the synthesis loop. The more detailed structural designs would be made outside of the vehicle synthesis loop either to calibrate a point design or to generate analytical data which may be used to modify the statistically derived equations.

During this contract period, a program for aircraft structural synthesis (PASS) was developed by Erwin Johnson under the sponsorship of the National Research Council. This beam finite-element program has initially been written to analyze the aeroelastic effects of wing flutter and redesign. It is being developed with the full vehicle analysis capability as a goal.

The approach taken in developing this fuselage design code incorporated each of these items. Rather than restrict the analytical procedures to simplistic approaches, the more detailed structural analysis techniques (Level II) employed in the SWEEP program were adapted for the estimation of basic fuselage shell weights. The program structure was then written to accept the shear, bending moments and external loads from the PASS program, or as direct input. It is anticipated that this approach will provide more detail and potential in which to assess advanced technology. This should satisfy the third function of providing analytically derived data which may then be used to check point designs or modify existing statistical equations.

In developing the computer code, certain portions of the fuselage design code were extracted directly from the SWEEP program. The modifications made to the original code were to improve the readability of the code and to incorporate the geometric descriptions used by the ACSYNT program. In certain instances failure criteria, such as sizing the fuselage for acoustic fatigue, have been deleted because of lack of input from the ACSYNT program. Their deletion from the code will be marked for future reference.

The details of theoretical background behind the development of the computer are described here. The basic flow of the program and the equations used to size the primary structure are also outlined. An example case for the C-141 follows.

Approach to Weight Estimation

The basic approach taken in computing fuselage weights will be to compute the items listed in figure 14. The weights predicted here are categorized as basic or secondary structure according to the definitions of MIL-STD-1374 and are listed by line items on form AN-9102-D. This is the basic military standard form of weights classification. The civil transport aircraft weight reporting format essentially follows this form with minor modifications for special items.

All items in this weight statement are computed either by direct analysis or by empirical equations. Most analytical equations used to predict component weights with the exception of the sizing of the major frames have been excerpted from reference 2. The major frames computations have been left out until such time as integrated approach is implemented which incorporates the interaction between fuselage, wing, tail, and landing gear loads. They will be accounted for by the use of empirical equations.

Of the items listed under BASIC STRUCTURE the weights of bulkheads, minor frames, covering, stiffeners, and longerons are computed analytically by estimating the required material distribution at up to twenty synthesis cuts. The remaining items and all SECONDARY STRUCTURE items are computed individually from empirical equations. Three methods are available for computing most secondary structural weights. They may be input, estimated from rule-of-thumb weights, or calculated from geometric information for fighters, transports, and bombers. Most calculated weights are estimated based on a unit weight of the items.

Weight of the primary structure is estimated by computing the required material gages at each synthesis cut. An outline of procedure used to generate these estimates follows:

1. Input geometry and loading conditions.

For each synthesis cut:

2. Determine maximum loading condition and material properties.
3. For a given stringer and minor frame spacing compute unit weight of minor frames, cover panels, and longerons or stringers.
4. Increment the stringer or minor frame spacing if desired to search for minimum weight spacing. Return to (3) until minimum unit weight is obtained.
5. Compute minimum weight pressure bulkheads if required.

At completion of synthesis cuts:

6. Summarize primary structural weights and apply non-optimum weight factors.
7. Compute secondary structural weights.
8. Print summary.

FUSELAGE GEOMETRY DESCRIPTION

All geometric dimensions used in the analytical equations are obtained from the description of the external geometry. The basic technique of inputting the geometric shape employs the use of a restricted set of automatic geometry descriptors (AGD's) to describe the basic shell size and shape. The descriptors derived here are restricted to circular and double-lobed circular shapes. Reference 2, which may also be implemented, employs a basic rounded-rectangle as the primary AGD.

The external geometry is defined according to the control option, IGM. For $IGM = 1$, the fuselage is defined according to the ACSYNT program vehicle synthesis AGD to have a circular cross section and a Sears-Haack area distribution. For $IGM > 1$, the particular AGD description of the local cross section is input

at up to ten body stations. Of these geometry cuts, the first and last define the nose and tail. Intermediate cuts may currently be defined at up to eight stations. Sharp geometric changes, such as occur forward and aft of duct inlets, are described by double cuts immediately forward and aft of the shape transition. The standard body axis system with the x-axis positive out the tail and the z-axis positive up is used to define the vehicle coordinate system.

Structural sizing is performed at up to 19 synthesis cuts (XO). These cuts are located at NC stations along the longitudinal axis of the vehicle between the nose and the tail. These locations do not have to correspond to the locations defining the external geometry. However, they must be used to define the boundaries of such structural features as cutouts, bulkheads, and locations of particular interest to the user. Shell dimensions at these synthesis cuts are obtained by linear interpolation between AGD descriptions of the external geometry. A description of the parameters that make up the circular and double-lobe circular AGD's follows. For a description of the rounded-rectangle see reference 2.

In the discussions that follows, the term "cut" refers to a synthesis cut at which the various structural details such as cross-sectional geometry, loads, and material gages are evaluated. Similarly, the term "segment" refers to vehicle properties computed between two synthesis cuts. The following section describes the geometric properties and equations derived for the Sears-Haack body input (IGM = 1) and the circular and double-lobe circular shapes (IGM = 2).

The Sears-Haack body is assumed to be circular in shape and is partitioned into three sections: a nose, a constant section body, and a tail. The input parameters (IGM = 1) defining the body radius and length at any cut are: the body length (BODL),

the body diameter (BDMAX) and the nose (FRN) and tail (FRAB) fineness ratios. Figure 15 is a picture of the Sears-Haack body and circular cross section. The radius of the cross section at any station is defined by:

$$r = \frac{\text{BDMAX}}{2} \left[\frac{\xi(1 - \xi)}{2} \right]^{3/4}, \quad \text{for } 0 \leq \frac{x}{\text{BDMAX}} \leq \text{FRN} \quad (40)$$

where: $\xi = \frac{x}{2 \text{FRN BDMAX}}$

$$r = \frac{\text{BDMAX}}{2}, \quad \text{for } \text{FRN} < \frac{x}{\text{BDMAX}} < 1 - \text{FRAB} \quad (41)$$

$$r = \frac{\text{BDMAX}}{2} \left[\frac{\xi(1 - \xi)}{2} \right]^{3/4}, \quad \text{for } 1 - \text{FRAB} \leq \frac{x}{\text{BDMAX}} \leq 1 \quad (42)$$

where: $\xi = \frac{\text{BODL} - x}{2 \text{FRAB BDMAX}}$

The floor location in this description has been specified at a uniform height above the bottom of the cross section of maximum diameter. It is input as the ratio (ZFLRU) of the floor height to maximum body (BDMAX) diameter. The locations of synthesis cuts (XO) are input as the distance from the tip of the nose. All remaining section properties are either input for the synthesis cut location or are interpolated using the description of the body radius.

The input parameters that define the double-lobe circular cross section in figure 16 (IGM = 2) are the scaling factors (RFLB and SCALEB), the perimeter correction factor (PERI), the

nondimensional values of the upper lobe radius (A1), the lower lobe radius (A2), the vertical offset of the centers of the upper radius (E1), and the lower radius (E2). These values are nondimensionalized according to the scaling factors

$$A1 = R1 \left(\frac{SCALEB}{RFLB} \right) \quad (43)$$

The input cross sections are defined at up to NGM (less than or equal to ten) stations (XI). The location of the floor (ZFLR) is either input as the ratio of floor height above the bottom to the local body diameter for circular sections or computed as the height at the intersection between the upper and lower lobes for noncircular sections. The perimeter may be adjusted by multiplying by the correction factor, PERI. The locations of synthesis cuts (XO) are input with respect to the user defined vehicle reference axes. The double-lobe cross sectional description reduces identically to the circular section for either $E1 = E2$ or for $A2 = 0$. In the latter case, $A2$ is set equal to $A1$ and $E2$ is equal to $E1$.

SECTION GEOMETRY

The structural sizing techniques in this program follow the methods employed in reference 3. For structural sizing the cross section is partitioned into four shell sectors representing the upper, lower, and two sides. For the purpose of simplicity, the shell sectors are assumed to be symmetric about the centerline of the aircraft. The section quantities estimated for the structural geometry in routine FSECTN are: the radii of the sector (R_{CU} , R_{CL} , and R_{CS}) and the sector arc lengths BU, BL, and BS) for the upper, lower and two sides, the total perimeters (PER), the area of the cross section (ARCS), the maximum section depth (DF), the maximum section width (WF), the ratio of the floor height to section depth (DKHT), and the width of the floor at

the section (W_{FLR}). Figure 17 shows the relationships among these various geometric quantities for the double-lobed section.

For program efficiency the upper and lower lobes are described internally by the angles from the vertical to the deck intersection. The upper lobe is defined by the arc swept out by ALPU measured clockwise from the positive centerline. The lower lobe is defined by the angle ALPL measured counterclockwise from the negative centerline. The structural sectors are similarly defined by the angles θ_u and θ_l . They are limited to 45° of the upper and lower lobe angles. If the section is circular the sectors are still defined by the location of the floor. If no floor exists, the upper lobe is defined by $ALPU = 3\pi/4$ and the lower lobe is set to $ALPL = \pi/4$. The equations used to generate these parameters follow.

The following quantities are defined for the double-lobed cross section. The maximum section depth is:

$$DF = R_{CU} + R_{CL} + EU - EL \quad (44)$$

The deck height to section depth ratio is:

$$DKHT = \frac{R_{CL} - R_{CU} \cos \beta + EU - EL}{DF} \quad (45)$$

where:

$$\cos \beta = \frac{[(EU - EL)^2 + R_{CU}^2 - R_{CL}^2]}{2 R_{CU} (EU - EL)} \quad (46)$$

The floor width is:

$$WFLR = 2\sqrt{R_{CL}^2 - (DKHT \cdot DF - R_{CL})^2} \quad (47)$$

The angle of the upper lobe arc measured from the positive centerline is:

$$ALPU = \frac{\pi}{2} + \sin^{-1} \left[\frac{EU - EL - R_{CL} + DKHT \cdot DF}{R_{CU}} \right] \quad (48)$$

The angle of the lower lobe arc measured from the negative centerline is:

$$ALPL = \frac{\pi}{2} - \sin^{-1} \left[\frac{R_{CL} - DKHT \cdot DF}{R_{CL}} \right] \quad (49)$$

The maximum section width is:

$$WF = \max \begin{cases} R_{CU} \cdot \sin \left[\min \left(ALPU, \frac{\pi}{2} \right) \right] \\ R_{CL} \cdot \sin \left[\min \left(ALPL, \frac{\pi}{2} \right) \right] \end{cases} \quad (50)$$

If the section is circular and no floor exists the geometric properties may then be defined as:

$$DF = 2 \cdot R_{CU} \quad (51)$$

$$DKHT = 0. \quad (52)$$

$$WFLR = 0. \quad (53)$$

$$ALPU = \frac{3\pi}{4} \quad (54)$$

$$ALPL = \frac{\pi}{4} \quad (55)$$

$$WF = 2 \cdot R_{CU} \quad (56)$$

The section sectors used in synthesis are similarly defined by the angles θ_u and θ_l measured from the centerline to the boundary. These sectors partition the perimeter into three regions according to the types of loading they will be carrying. The upper and lower sectors are designed for fuselage bending loads and stiffness while the two side sectors provide shear

strength and lateral stiffness. The angle θ_u is measured from the positive centerline to the sector boundary. The angle θ_l is measured from the negative centerline to the sector boundary. The angles θ_u and θ_l are defined as:

$$\theta_u = \min (ALPU, \frac{\pi}{4}), \text{ and} \quad (57)$$

$$\theta_l = \min (ALPL, \frac{\pi}{4}) \quad (58)$$

The choice of upper bound of $\pi/4$ is arbitrary. For circular sections this partitions the perimeter into four equal sectors.

The fuselage perimeter (PER) and sector arc lengths (BU, BL, BS) are then defined as:

$$PER = 2(R_{CU} \cdot ALPU + R_{CL} \cdot ALPL) \cdot KC \quad (59)$$

$$BU = 2 \cdot R_{CU} \cdot \theta_u \quad (60)$$

$$BL = 2 \cdot R_{CL} \cdot \theta_l \quad (61)$$

$$BS = \frac{1}{2}(PER - BU - BL) \quad (62)$$

The radius of curvature of the side is approximated from the weighted average of radii of upper and lower sector multiplied by their fraction of the side sector perimeter. This is used to provide a measure of effective radius when estimating the curvature corrections in various sizing criteria. The equation for the effective side radius is:

$$R_{CS} = \left[\frac{R_{CU}^2 (ALPU - \theta_u) + R_{CL}^2 (ALPL - \theta_l)}{BS} \right] \quad (63)$$

The centroid of the cross section is approximated as the centroid of a shell perimeter of unit thickness. The lateral

centroid is assumed to lie on the centerline. The vertical centroid which defines the neutral surface is:

$$Z_0 = \frac{2 R_{CU} (EU \cdot ALPU + R_{CU} \cdot \sin ALPU) + 2 R_{CL} (EL \cdot ALPL - R_{CL} \cdot \sin ALPL)}{PER} \quad (64)$$

The location of the center of curvature for the upper and lower lobes relative to the vertical centroid is:

$$Z_U = EU - Z_0 \quad (65)$$

$$Z_L = EL - Z_0 \quad (66)$$

The cross sectional area is:

$$ARCS = R_{CU}^2 \cdot ALPU + R_{CL}^2 \cdot ALPL + \frac{1}{2} W_{FLR} (EU - EL) \quad (67)$$

Segment geometry is defined for four types of segments: the nose, the tail, the normal segment, and the sharp transition-al segment. The four segment properties defined in routine FSECTN are the length (DELX), the surface area (SF), the internal volume (VOL), and the center of mass of the volume (XBAR). The segment properties of the nose are:

$$DELX = XO_1 - XI_1 \quad (68)$$

$$XBAR = XO_1 - DELX_1 \frac{(2r_1 + r_2)}{3(r_1 + r_2)} \quad (69)$$

$$SF = \pi (r_1 + r_2) \cdot \sqrt{DELX^2 + (r_1 - r_2)^2} \quad (70)$$

$$VOL = \frac{\pi}{3} DELX (r_2^2 + r_2 r_1 + r_1^2) \quad (71)$$

where:

$$r_1 = \text{radius at nose} \quad (72)$$

$$r_2 = \frac{\text{PER}_1}{2\pi} \quad (73)$$

The segment length at the tail is:

$$\text{DELX} = \text{XI}_{\text{NGM}} - \text{XO}_{\text{NC}} \quad (74)$$

The equations for XBAR, SF, and VOL at the tail are the same as for the nose with the exceptions that:

$$r_1 = \frac{\text{PER}_{\text{NC}}}{2\pi}, \text{ and} \quad (75)$$

$$r_2 = \text{radius at tail} \quad (76)$$

The properties for intermediate segments are:

$$\text{DELX}_j = \text{XO}_j - \text{XO}_{j-1} \quad (77)$$

$$\text{XBAR}_j = \frac{1}{2} (\text{XO}_j + \text{XO}_{j-1}) \quad (78)$$

$$\text{SF}_j = \pi(r_1 + r_2) \sqrt{\text{DELX}^2 + (r_2 - r_1)^2} \quad (79)$$

$$\text{VOL}_j = \frac{\text{DELX}_j}{3} \left(\text{ARCS}_j + \text{ARCS}_{j-1} + \sqrt{\text{ARCS}_j \cdot \text{ARCS}_{j-1}} \right) \quad (80)$$

where:

$$r_1 = \frac{\text{PER}_{j-1}}{2\pi} \quad (81)$$

and

$$r_2 = \frac{PER_j}{2\pi} \quad (82)$$

If the segment is a sharp transition ($DELX \leq 2$ inches) the surface area and volume are approximated by:

$$SF_j = PER_j DELX_j \quad (83)$$

$$VOL_j = DELX_j ARCS_j \quad (84)$$

The unit inertias for the fuselage and its contents are generated in routine INERT. The unit inertias of a segment are the inertia per unit weight of the fuselage shell and its contents about its centroid. The inertia is computed assuming the segment is a solid cylinder with the average properties of its ends. The unit inertia is estimated by dividing the local volume inertia for a solid cylinder of average dimensions by its cross sectional area. The pitch (UIY), roll (UIX) and yaw (UIZ) unit inertias are calculated by assuming:

1. The weight of the fuselage and its contents are uniformly distributed within the volume of the segment.
2. The center of mass is at the centroid of the segment.

The inertias per pound of weight for the double-lobed circular shape are defined for the normal geometry transition from the following:

$$\alpha_u = \frac{1}{2} (ALPU_j + ALPU_{j-1}) \quad (85)$$

$$\alpha_L = \frac{1}{2} (ALPL_j + ALPL_{j-1}) \quad (86)$$

$$r'_u = \frac{1}{2} (R_{CU_j} + R_{CU_{j-1}}) \quad (87)$$

$$r'_l = \frac{1}{2} (R_{CLj} + R_{CLj-1}) \quad (88)$$

$$z'_u = \frac{1}{2} (z_{Uj} + z_{Uj-1}) \quad (89)$$

$$z'_l = \frac{1}{2} (z_{Lj} + z_{Lj-1}) \quad (90)$$

$$W_j = \frac{1}{2} (W_{FLRj} + W_{FLRj-1}) \quad (91)$$

$$A_j = r'_u{}^2 \alpha_u + r'_l{}^2 \alpha_l + \frac{1}{2} W_j (z'_u - z'_l) \quad (92)$$

$$\begin{aligned} UIY_j = & \left\{ 2r'_u{}^2 \left[\left(\frac{1}{2} z'_u{}^2 + \frac{1}{8} r'_u{}^2 \right) \alpha_u + \frac{2}{3} r'_u z'_u \sin \alpha_u \right. \right. \\ & + \left. \frac{1}{16} r'_u \sin 2\alpha_u \right] + 2r'_l{}^2 \left[\left(\frac{1}{2} z'_l{}^2 + \frac{1}{8} r'_l{}^2 \right) \alpha_l \right. \\ & \left. \left. + \frac{2}{3} r'_l z'_l \sin \alpha_l + \frac{1}{16} r'_l \sin 2\alpha_l \right] \right\} \frac{1}{A_j} + \frac{DELX_j^2}{12} \quad (93) \end{aligned}$$

$$UIZ_j = \left[\frac{1}{4} r'_u{}^4 \left(\alpha_u - \frac{1}{2} \sin 2\alpha_u \right) + \frac{1}{4} r'_l{}^4 \left(\alpha_l - \frac{1}{2} \sin 2\alpha_l \right) \right] \frac{1}{A_j} + \frac{DELX_j^2}{12} \quad (94)$$

$$UIX_j = UIY_j + UIZ_j - \frac{DELX_j^2}{6} \quad (95)$$

For sharp transition segments the unit inertias are based on the properties at the aft end of the segment.

For the nose and tail segments, the equivalent section radius is used to calculate the inertia. The nose segment inertia is defined as follows:

$$UIX_1 = \frac{3(r_1^5 - r_1^5)}{10(r_1^3 - r_1^3)}, \text{ and} \quad (96)$$

$$UIY_1 = UIZ_1 = \frac{UIX_1}{2} + \frac{27}{80} (XO_1 - XBAR_1)^2 \quad (97)$$

The inertia of the fuselage is computed by summing the segment inertias about the aircraft center of gravity.

TORSIONAL GEOMETRY

The internal geometric arrangement is required in order to determine the thickness to satisfy any torsional rigidity (GJ) requirements at a given synthesis cut. Evaluation of the torsional capability of the shell is based on the presence of a closed torque cell. The presence of an open torque cell is considered structurally inefficient, and will not be considered in these calculations. The values calculated here are also used in the evaluation of pressure bulkheads.

The thickness required to satisfy a given torsional rigidity is derived from the torsional constant for thin-walled closed sections of general shape. The torsional constant, J, is defined as follows:

$$J = \frac{4A^2}{\int \frac{ds}{t}} \quad (98)$$

The thickness required is estimated for a uniform thickness (TGJ) around the perimeter of the torque cell as:

$$TGJ = \frac{(GJ)_{reqd} \text{ PER}}{4A^2 G} \quad (99)$$

where:

A = enclosed cross-section area

B = panel shear modulus

PER = peripheral length of enclosed torque cell

The only geometric parameters required in the evaluation of the required thickness are the enclosed torque cell peripheral length (PER) and cross sectional area (A). Since the presence of cutouts is assessed, the internal geometry must be capable of establishing a consistent torque cell. The primary internal partition that may be used to define the cell configuration is the horizontal deck. The presence of a cutout defines the orientation of the torque cell, upper or lower. The horizontal deck, then, is the structural member that establishes the closed torque cell shape. All decks and upper and lower cutouts are bounded by synthesis cuts. Therefore, at any synthesis cut, there may be two different conditions defining the structure forward and aft of the cut and two corresponding required thickness values. These differences are evaluated by calculating torque cell data on both sides of each cut.

Certain geometric combinations are not compatible with the assumption of a single closed section. The program approach for these arrangements is as follows:

1. Should decks exist without any cutouts, the external section geometry is used to define the torque cell. The influence of the deck upon torsional stiffness will be ignored.
2. Should cutouts exist without any decks, the external section geometry is used to define the torque cell, and the loss of torsional stiffness due to cutouts will be ignored.
3. Should both upper and lower panel cutouts exist in the presence of a deck, the section above the deck is used to define the torque cell, and the loss of torsional stiffness due to the upper panel cutout will be ignored.

Figure 18 depicts the different internal arrangements and the corresponding geometric variables immediately forward of a cut. Variables in the calculations are:

ACRS	Total shell cross-section area at cut
PER	Shell external perimeter at cut
ANTF, ANTA	Torque cell cross-section area immediately forward and aft of the cut, respectively
PERF, PERA	Torque cell peripheral length immediately forward and aft of the cut
PRDF, PRDA	Deck peripheral length immediately forward and aft of the cut
DEPF, DEPA	Depth of the torque cell immediately forward and aft of the cut
WIDF, WIDA	Width of cell between two walls (beaming distance) immediately forward and aft of the cut

For the presence of a pressure bulkhead at a synthesis cut, the above variables define the geometry of the pressurized compartment. In these instances the width, depth, perimeter, and area describe the dimensions of the bulkhead.

In addition to the basic closed cross section, two arrangements that incorporate cutouts in the upper and lower covers are defined. The equations defining the structural geometry of the torque box for a cutout in the lower sector shown in figure 19 are:

$$\text{PERF} = 2R_{\text{CU}} \cdot \text{ALPU} + W_{\text{FLR}} \quad (100)$$

$$\text{DEPF} = \text{DF}(1 - \text{DKHT}) \quad (101)$$

$$\text{WIDF} = \begin{cases} 2 \cdot R_{\text{CU}} & , \text{ if } \text{ALPU} \geq 90^\circ \\ 2 \cdot R_{\text{CU}} \cdot \sin \text{ALPU} & , \text{ if } \text{ALPU} < 90^\circ \end{cases} \quad (102)$$

$$\text{ANTF} = \text{ALPU} \cdot R_{\text{CU}}^2 - \frac{1}{2} W_{\text{FLR}} (R_{\text{CU}} - \text{DEPF}) \quad (103)$$

$$\text{PRDF} = W_{\text{FLR}} \quad (104)$$

Similarly, the equations defining the structural geometry of the torque box for a cutout in the upper sector shown in figure 20 are:

$$\text{PERF} = 2R_{\text{CU}} \cdot \text{ALPL} + W_{\text{FLR}} \quad (105)$$

$$\text{DEPF} = \text{DF} \cdot \text{DKHT} \quad (106)$$

$$\text{WIDF} = \begin{cases} 2R_{\text{CL}} \cdot \sin \text{ALPL} & , \text{ if } \text{ALPL} < 90^\circ \\ 2R_{\text{CL}} & , \text{ if } \text{ALPL} \geq 90^\circ \end{cases} \quad (107)$$

$$\text{ANTF} = \text{ALPL} \cdot R_{\text{CL}} - \frac{1}{2} W_{\text{FLR}} (R_{\text{CL}} - \text{DEPF}) \quad (108)$$

$$\text{PRDF} = W_{\text{FLR}} \quad (109)$$

The minimum material thickness required to satisfy the torsional stiffness requirements (GJRD) may then be written for the forward segment as:

$$T_{\text{GJF}} = \frac{\text{GJRD} \cdot \text{PERF}}{4\text{ANTF}^2 \cdot G} \quad (110)$$

The properties for the aft segment are defined in the same manner.

STRUCTURAL GEOMETRY AND INERTIAS

Determining the precise internal loads distribution is not within the scope of this program. The maximum bending and shear stresses in the cross section are estimated from an equivalent beam analogy. If certain assumptions are made, the internal load distribution can be approximated solely on the basis of structural geometry. The primary assumptions are first that the centroid of the material area moment lies at the centroid of the unit cover; second, that all sizing elements within a sector are the same; and third, that the bending contribution of the skin

in a postbuckled state is negligible compared to the contributions from the longerons or stringers.

From beam theory, the maximum shear flow occurs along the axis of the centroid and can be expressed as:

$$q = \frac{VQ}{I} \quad (111)$$

where:

V = vertical shear at the synthesis cut

q = shear flow in pounds per inch

Q = area moment of the axial elements in one quadrant

I = total area moment of inertia of all the bending elements

Similarly, the shell bending stress at any vertical coordinate relative to the centroidal axis is:

$$\sigma = \frac{M(Z - Z_0)}{I} \quad (112)$$

where:

M = bending moment at the synthesis cut

Z = vertical coordinate of the member

I = total area moment of inertia

Z₀ = vertical location of the area centroid

The maximum positive and negative stresses occur for the corresponding external distances from the centroid.

The area moment, Q, is defined as the summation of the axial elements in the upper quadrant:

$$Q = \int Z da = A_{LU} \int Z + A_{LS} \int Z + A_{IT} \int Z + T_{CU} \int Z da + T_{CS} \int Z da \quad (113)$$

where:

A_{LU} = area of each upper longeron or stringer

A_{LS} = area of each side stringer

A_{IT} = area of each secondary longitudinal member

T_{CU} = thickness of upper sector cover

T_{CS} = thickness of side sector cover

ds = incremental panel length

$\sum Z$ = summation of vertical coordinates of elements

The area moment of inertia is:

$$I = \int Z^2 dA = A_{LU} \sum Z^2 + A_{LS} \sum Z^2 + A_{IT} \sum Z^2 + A_{LL} \sum Z^2 + T_{CU} \int Z^2 ds + T_{CS} \int Z^2 ds + T_{CL} \int Z^2 ds \quad (114)$$

where:

A_{LL} = area of each lower longeron or stringer

T_{CL} = thickness of lower sector cover

The approach taken in this program is to compute the area moments and inertias for a unit thickness or area of the contributing elements in each sector. This contribution is a function only of the arrangement of the bending elements: covers, longerons, and stringers. The initial approximation to the maximum shear is based on the geometry.

The arrangement of structural members for the double-lobed circular sector is shown in figure 21. Two optional structural arrangements are depicted for longeron and stringer construction. Longeron construction is characterized by four primary longitudinal members at the boundaries of the sectors which sustain the bending load. Stringer construction, on the other hand, is characterized by longitudinal stiffeners at an even spacing,

BSTR, around the perimeter of the shell. The unit inertias for each sizing member in each sector are calculated in subroutine ILONG1. For the purposes of consistent notation the symbol I_Y will refer to vertical inertia about an axis parallel to the y-axis. Likewise, I_Z will refer to the lateral inertia about the z-axis.

The equations used to calculate the unit vertical bending inertias about ZO for the upper, lower, and side sectors are:

$$\left(\frac{I_Y}{T_{CU}}\right) = 2R_{CU} \left[\left(Z_U^2 + \frac{1}{2} R_{CU}^2 \right) \theta_u + 2Z_U \cdot R_{CU} \sin \theta_u + \frac{1}{4} R_{CU}^2 \sin 2 \theta_u \right] \quad (115)$$

$$\left(\frac{I_Y}{T_{CL}}\right) = 2R_{CL} \left[\left(Z_L^2 + \frac{1}{2} R_{CL}^2 \right) \theta_\ell + 2Z_L \cdot R_{CL} \sin \theta_\ell + \frac{1}{4} R_{CL}^2 \sin 2 \theta_\ell \right] \quad (116)$$

$$\begin{aligned} \left(\frac{I_Y}{T_{CS}}\right) &= 2R_{CU} \left[\left(Z_U^2 + \frac{1}{2} R_{CU}^2 \right) ALPU + 2Z_U \cdot R_{CU} \sin ALPU + \frac{1}{4} R_{CU}^2 \sin 2ALPU \right] \\ &+ 2R_{CL} \left[\left(Z_L^2 + \frac{1}{2} R_{CL}^2 \right) ALPL + 2Z_L \cdot R_{CL} \sin ALPL + \frac{1}{4} R_{CL}^2 \sin 2ALPL \right] \\ &- \left(\frac{I_Y}{T_{CU}}\right) - \left(\frac{I_Y}{T_{CL}}\right) \end{aligned} \quad (117)$$

The equations used to calculate the unit lateral bending inertias about the centerline for the upper, lower, and side sectors are:

$$\left(\frac{I_Z}{T_{CU}}\right) = R_{CU}^3 \left(\theta_u - \frac{1}{2} \sin 2 \theta_u \right) \quad (118)$$

$$\left(\frac{I_Z}{T_{CL}}\right) = R_{CL}^3 \left(\theta_\ell - \frac{1}{2} \sin 2 \theta_\ell \right) \quad (119)$$

$$\begin{aligned} \left(\frac{I_Z}{T_{CS}}\right) &= R_{CU}^3 \left(ALPU - \frac{1}{2} \sin 2 \cdot ALPU \right) - \left(\frac{I_Z}{T_{CU}}\right) \\ &+ R_{CL}^3 \left(ALPL - \frac{1}{2} \sin 2 \cdot ALPL \right) - \left(\frac{I_Z}{T_{CL}}\right) \end{aligned} \quad (120)$$

The distance of the extreme fibers of the upper and lower covers from the neutral axis are defined for vertical bending as follows:

$$Z_{\max} = Z_U + R_{CU} \quad , \quad \text{and}$$

$$Z_{\min} = Z_L - R_{CL}$$

In the presence of cutouts, a cutout longeron is positioned along each side of the hole to carry the bending load around the removed structure. The cutout longerons are assumed symmetric about the vertical centerline and computed wherever the effective cutout widths R_{TU} and R_{TL} for the upper and lower sectors are nonzero. The unit inertias of these longitudinal members are proportional to the square of their distances from the neutral axes. The horizontal and vertical distances of the upper cutout longeron (Y_{CU} , Z_{CU}) are defined as:

$$Y_{CU} = R_{CU} \cdot \sin \theta \quad , \quad \text{and} \quad (121)$$

$$Z_{CU} = Z_U + R_{CU} \cos \theta \quad (122)$$

where $\theta = 1/2 (R_{TU}/R_{CU})$ is the angular location of the longerons measured from the vertical centerline. The horizontal and vertical distances from the neutral axes for the lower cutout longeron (Y_{CL} , Z_{CL}) are defined as:

$$Y_{CL} = R_{CL} \cdot \sin \theta \quad (123)$$

$$Z_{CL} = Z_L - R_{CL} \cos \theta \quad (124)$$

where $\theta = 1/2 (R_{TL}/R_{CL})$ is measured from the negative centerline.

The unit inertias for longitudinal stiffening elements are computed for two structural arrangements: stringers and longeron construction. The stringer unit inertias are estimated assuming the stringer spacing, B_{STR} , is sufficiently small in comparison to the perimeter that the effective unit inertias can be distributed as an equivalent thickness. The unit inertias of the stringers may then be written in terms of the unit inertias of the cover as:

Upper, Lower and Side Vertical unit inertias -

$$\left(\frac{I_Y}{A_{LU}} \right) = \frac{\left(\frac{I_Y}{T_{CU}} \right)}{B_{STR}} \quad (125)$$

$$\left(\frac{I_Y}{A_{LL}} \right) = \frac{\left(\frac{I_Y}{T_{CL}} \right)}{B_{STR}} \quad (126)$$

$$\left(\frac{I_Y}{A_{LS}} \right) = \frac{\left(\frac{I_Y}{T_{CS}} \right)}{B_{STR}} \quad (127)$$

Upper, Lower and Side Lateral unit inertia -

$$\left(\frac{I_Z}{A_{LU}} \right) = \frac{\left(\frac{I_Z}{T_{CU}} \right)}{B_{STR}} \quad (128)$$

$$\left(\frac{I_Z}{A_{LL}}\right) = \frac{\left(\frac{I_Z}{T_{CL}}\right)}{B_{STR}} \quad (129)$$

$$\left(\frac{I_Z}{A_{LS}}\right) = \frac{\left(\frac{I_Z}{T_{CS}}\right)}{B_{STR}} \quad (130)$$

The maximum shear stress due to bending is computed from the maximum shear flow at the neutral axis. The area moment, Q , used to calculate the shear flow may be estimated from the geometry of only one quadrant of the shell. The equations for the vertical and lateral unit area moments for the upper lobe stringers in figure 21 are:

$$\left(\frac{Q}{A_{LU}}\right)_V = R_{CU} \frac{(Z_U \cdot \theta + R_{CU} \sin \theta)}{B_{STR}} \quad (131)$$

$$\left(\frac{Q}{A_{LU}}\right)_L = R_{CU}^2 \frac{(1 - \cos \theta)}{B_{STR}} \quad (132)$$

where θ is the angle from the centerline to the intersection of the neutral axis, ZO , with the upper lobe. If θ is greater than $ALPU$, the lower lobe geometry is used.

The unit inertias for longeron construction are approximated for primary and secondary longerons as:

$$\left(\frac{I_Y}{A_{LU}}\right) = \sum z^2 = \frac{N_{LNG}}{2} z_{LNG}^2 \quad (133)$$

where

$$z_{LNG} = z_U + R_{CU} \cos \theta_{LNG} \quad (134)$$

$$\left(\frac{I_Y}{A_{LL}}\right) = \frac{N_{LNG}}{2} (z_L - R_{CU} \cos \theta_{LNG})^2 \quad (135)$$

$$\left(\frac{I_Y}{A_{IT}}\right) = N_{SEC} \left(\frac{z_{LNG}}{2}\right)^2 \quad (136)$$

where θ_{LNG} is the angular location of the primary longerons measured from the sector centerline. The vertical location may optionally be located by the ratio of the vertical height to total fuselage depth. N_{LNG} and N_{SEC} are the numbers of primary and (if requested) secondary longerons. Secondary longerons are located at half the height of primary longerons. Similarly the unit lateral inertias are:

$$\left. \begin{aligned} \left(\frac{I_Z}{A_{LU}}\right) &= \sum y^2 = \frac{N_{LNG}}{2} (R_{CU} \sin \theta_{LNG})^2 \\ \left(\frac{I_Z}{A_{LL}}\right) &= \frac{N_{LNG}}{2} (R_{CL} \sin \theta_{LNG})^2 \\ \left(\frac{I_Z}{A_{IT}}\right) &= N_{SEC} \frac{1}{2} [(R_{CU} \sin \theta_{SEC})^2] \end{aligned} \right\} \quad (137)$$

Only the primary longerons are assumed to contribute to the shear flow. The equations for the vertical and lateral unit area moments for the upper lobe longerons are defined as follows:

$$\left. \begin{aligned} \left(\frac{Q}{A_{LU}}\right)_V &= z_{LNG} \\ \left(\frac{Q}{A_{LU}}\right)_L &= R_{CU} \sin \theta_{LNG} \end{aligned} \right\} \quad (138)$$

The properties of the internal and structural geometry for the rounded rectangular shaped cross section are given in reference 2.

Shell Cover Design Criteria

During the sizing of a given shell segment a number of assumptions are made to simplify the analysis. For the synthesis of shell structures in bending the circumference of the segment is assumed to be partitioned into four quadrants: two sides, and upper and lower sectors. All bending loads are assumed to be carried by the upper and lower sectors, while the sides are assumed to carry all shear loads. The contribution of the longitudinal members within all sectors is included when determining the net bending moment carried by the section, and when determining the maximum shear stress along the sides. Frames are sized to provide shell stability, and stringers are sized to carry both bending load and provide buckling stability. The basic covers are also checked for pressure integrity. The sizing criteria examined are broken into four types: shear criteria, bending criteria, stability criteria, and pressure design criteria. The following constraints will be used to size the fuselage cover elements:

Cover Element Sizing Criteria -

$$(1) \quad \text{Minimum gage} \quad - \quad T_C \geq T_{C_{min}} \quad (139)$$

$$(2) \text{ Ultimate shear stress} \quad - T_C \geq \frac{q}{F_{su} \cdot C_R} \quad (140)$$

$$(3) \text{ Shear buckling} \quad - f_s \leq F_{scr} \quad (141)$$

$$(4) \text{ Postbuckling} \quad - f_s \leq F_{s_{allow}}$$

$$= F_{scr} + \sin \alpha \cos \alpha (C_R F_{tu} - F_{scr})$$

$$\alpha = 45^\circ \quad (142)$$

$$(5) \text{ Cabin pressure} \quad - T_C \geq \frac{PR_C}{\sigma} \text{ (M.S.)}$$

(M.S. = 2.0 manned
= 1.5 unmanned) (143)

$$(6) \text{ Diaphragm pressure} \quad - T_C \geq \frac{1.3769 b p^{2.484} E_C^{1.984}}{\sigma^{4.467}} \text{ (M.S.)}$$

$$T_L \geq \frac{1.646 b p^{0.897} E_C^{0.394}}{\sigma^{1.288}} \text{ (M.S.)}$$

(144)

$$(7) \text{ Local panel flutter (M>1)} \quad - T_C \geq T_F$$

$$T_L \geq T_F$$

$$T_F = \phi_B L \left(\frac{q_f}{F(M) \cdot E_C} \right)^{1/3} C_{BNDRY} \quad (145)$$

$$\phi_B = 0.5551841 - 0.1686944 \left(\frac{L}{W} \right) + 0.02169992 \left(\frac{L}{W} \right)^2 + 0.00096394 \left(\frac{L}{W} \right)^3 \quad (146)$$

where

- f_s - sector shear stress = q/T_C
- T_L - panel thickness at landings
- q - maximum shear flow at neutral axis; $q = V_z Q/I_y$
- F_{su} - ultimate shear stress
- F_{scr} - critical buckling stress
- F_{tu} - ultimate tensile stress
- R_C - radius of curvature of shell sector
- σ - material allowable stress
- p - shell limit pressure, psi
- q_f - cover flutter critical Mach number
- $F(M)$ - Mach number correction obtained from reference 2, Vol VII, figure 14.
- C_{BNDRY} - boundary layer correction

Only the side sector cover panels are sized for the maximum shear stress. Therefore, only the side panel thicknesses are checked against the ultimate shear stress, shear buckling, and postbuckling requirements.

MINOR FRAME SIZING CRITERIA

During the synthesis of a given shell cut, minor frame or ring design is carried out at fixed frame spacings (SFRM) and the total shell weight determined. A search is then made for the spacing which predicts the least weight. Figure 22 is a drawing of the assumed geometric model used in the analysis of the minor frames. Several simplifying assumptions have been made in the geometry to minimize the number of design variables. The frame depth (FD) and cap width (BFCM) are input by the user or from default values. Only the ring thickness (t_r) is sized.

The geometric properties of the ring may then be written for the area, area moment of inertia, and radius of gyration as:

Ring area:

$$A_r = t_r \left(4 \text{ BFCM} + \frac{FD}{2} \right) \quad (147)$$

Ring moment of inertia:

$$I_{xx} = t_r \left(\text{BFCM} FD^2 + \frac{2}{3} \text{ BFCM}^3 - \text{BFCM}^2 FD + \frac{FD^2}{24} \right) \quad (148)$$

Radius of gyration:

$$\rho_r = \sqrt{\frac{I_{xx}}{A_r}} \quad (149)$$

The equations used to size the ring thickness are explained in reference 2. A summary of the equations and constraints used in subroutine MINFR is given here. The constraints used to design the ring thickness are:

1. Minimum gage requirement (TFCM):

$$t_r \geq \text{TFCM} \quad (150)$$

2. Shanley's general shell stability requirement:

$$t_r \geq \frac{M_{\max} \left(\frac{\text{PER}}{\pi} \right)^2 \text{CF}}{E_r \text{SFRM} \left(\frac{I_{xx}}{t_r} \right)} \quad (151)$$

where

M_{\max} = magnitude of maximum bending moment

$\frac{\text{PER}}{\pi}$ = effective body diameter at the synthesis cut

CF = Shanley's coefficient to prevent general shell instability (= 1/16000)

E_r = ring modulus of elasticity

SFRM = minor frame spacing

$\frac{I_{xx}}{t_r}$ = moment of inertia per unit thickness

3. Forced crippling requirement for shear panels: This constraint is checked when the cover shear panel is considered to be postbuckled ($f_s \geq F_{scr}$). The forced crippling requirement is obtained iteratively between satisfaction of equilibrium of the net loads carried by stringers, rings, and skins and the compatibility of stresses and strains. This is contingent upon estimating the diagonal tension angle, α , at which the load is effectively carried through the skin.

The diagonal tension factor for curved plates is:

$$K = \tanh \left(0.5 + 300 \frac{TC \cdot RLD}{R_{CS}} \right) \log_{10} \left(\frac{f_s}{F_{scr}} \right) \quad (152)$$

where

T_C = cover thickness

R_{CS} = shell radius of shear panel

$RLD = \max \left(\frac{SFRM}{BPAN}, \frac{BPAN}{SFRM}, 2 \right)$

$BPAN = \frac{\text{stringer}}{\text{longeron spacing}}$

Where stringer and longeron equation differences occur, the two will be presented side by side. The initial estimate for diagonal tension angle is:

<u>Stringer</u>	<u>Longeron</u>
$A = \frac{\frac{BPAN}{R_{CS}} \sqrt{\frac{E_C}{f_s}}}{\sqrt{1 + \frac{T_C \cdot E_C}{2} \left(\frac{BPAN}{A_s E_s} + \frac{SFRM}{A_r E_r} \right)}}$	$A = 0 \quad (153)$

Since the stringer/longeron area is not yet known, an initial estimate of the required area to satisfy minimum area, ASTRM, and/or maximum bending load is made.

<u>Stringer</u>	<u>Longeron</u>
$A_s \geq ASTRM$	$A_s \geq ASTRM \quad (154)$

$$A_s \geq \frac{M_{\max} \frac{D}{2}}{\left[\left(\frac{I}{A_s} \right)_u + \left(\frac{I}{A_s} \right)_l \right] F_{cy}} \quad (155)$$

Then

$$\alpha_{PDT} = \frac{\frac{\pi}{4} + 0.1443 A}{1 + 0.175622 A + 0.013411 A^2} \quad (156)$$

And

$$\alpha \approx \alpha_{PDT} K^{0.25} \quad (157)$$

The load in the stringers is distributed evenly between stringers. The load in the longerons is carried only between the upper and lower longerons. The maximum average stress may then be written for each as:

$$f_{ST} = \frac{f_s K \cot \alpha}{\left[\frac{A_s}{BPAN T_{CS}} + 0.5(1-K) \frac{E_c}{E_s} \right]}, \quad f_{ST} = \frac{f_s K \cot \alpha}{\left[\frac{2 A_s}{BPAN T_{CS}} + 0.5(1-K) \frac{E_c}{E_s} \right]} \quad (158)$$

The maximum induced stress in the ring versus the maximum average stress is defined in terms of the panel aspect ratio as

$$\frac{f_{RG \text{ MAX}}}{f_{RG}} = \begin{cases} 1.0 & , \text{ if } \frac{SFRM}{BPAN} > 1.2 \\ 1.0 + 0.78(1-K) - 0.65 \frac{SFRM}{BPAN} (1-K) & , \text{ if } \frac{SFRM}{BPAN} \leq 1.2 \end{cases} \quad (159)$$

The allowable ring stress is

$$f_{RG \text{ allow}} = A K^{2/3} \left(\frac{t_r}{TC} \right)^{1/3} G \quad (160)$$

where

$$A = \begin{cases} (0.18695 + 0.00075238 R_{CS}) \left(\frac{E_r}{E_c} \right)^{1/9} & , 0 < R_{CS} < 151.586 \\ 0.30100 \left(\frac{E_r}{E_c} \right)^{1/9} & , R_{CS} \geq 151.586 \end{cases} \quad (161)$$

and

$$G = \frac{F_{CY}}{5.88} \sqrt{\frac{F_{CY}}{E_r} + 0.002} \quad (162)$$

The solution for α and t_r is iterative. The following calculations for α are carried out three times to obtain an approximate value.

Strain in cover:

$$\epsilon_c = \frac{f_s}{E_c} \frac{2K}{\sin 2\alpha} + \sin 2\alpha (1 - K)(1 + \mu) \quad (163)$$

Strain in ring:

$$\epsilon_r = \frac{f_{RG}}{E_r} \quad (164)$$

Strain in stiffener:

$$\epsilon_s = \frac{f_{ST}}{E_s} \quad (165)$$

the value of α is computed from:

$$\tan^2 \alpha = \frac{\text{Stringer}}{\epsilon_c - \epsilon_r + \frac{1}{24} \left(\frac{BPAN}{R_{CS}} \right)^2}, \quad \tan^2 \alpha = \frac{\text{Longeron}}{\epsilon_c - \epsilon_r + \frac{1}{8} \left(\frac{SFRM}{R_{CS}} \right)^2 \tan^2 \alpha} \quad (166)$$

and

$$\alpha = \tan^{-1} \alpha$$

The iteration on the calculation of α , either returns to equation 163 or terminates after three cycles.

The ring thickness required is computed from the following quartic equation:

$$t_r (t_r X_b + X_c)^3 - X_a = 0 \quad (167)$$

Newton's method is used to solve for the ring thickness. If t_r is greater than the value estimated for stability and minimum

gage, the procedure starting with the α iteration is repeated a second time to update α . The coefficients X_a , X_b , and X_c are:

$$X_a = \left[\left(\frac{f_s \tan \alpha}{AG} \right) \left(\frac{f_{RG \text{ MAX}}}{f_{RG}} \right) \right]^3 T_C K \quad (168)$$

$$X_b = \frac{\left(4 \text{ BFCM} + \frac{FD}{2} \right)}{\left[1 + \left(\frac{FD}{2\rho_r} \right)^2 \right] \text{SFRM } T_C} \quad (169)$$

$$X_c = 0.5(1 - K) \left(\frac{E_c}{E_r} \right) \quad (170)$$

where

E_s = stringer/longeron modulus of elasticity

E_c = cover modulus of elasticity

F_{cy} = ring compressive yield strength

$\left(\frac{I_y}{A} \right)_{u,\ell}$ = moment of inertia contributions per area of upper and lower longeron or stringers

D = total body depth at cut

SHELL BENDING CRITERIA

The longitudinal material required to resist bending is determined from the sum of the components that may carry bending loads. The covers are first sized to satisfy pressure requirements. The bending contributions of the cover material are then determined for tensile and compressive sides. On the tensile side, the entire cover is considered effective. On the compressive side, reductions are made for the effective width of the skin carrying moment. The difference between the total moment required and the moment carried by the cover is used to size the

longerons or stringers. The contribution of the side covers to resist bending loads is neglected. The presence of cutouts is predicted by elimination of cross sectional material where indicated, and by material addition in other areas. Only the maximum up-bending and down-bending loading conditions are used to size the material. In addition, bending stiffness (EI_y and EI_z) requirements are checked.

Figure 23 is a sketch of the geometric configuration of the assumed model of the longitudinal member used in evaluation of the forced crippling strength of the shell. Several simplifying assumptions have been made in the geometric proportions to reduce the number of variables. Stiffener (longeron) geometry is set up with flange width equal to web height, HSTR. The stringer flange to height ratio, RSTRH, and web height have programmed default values which may be overridden by user input. The area, first moment, and the moment of inertia of the stiffener are:

Area for forced crippling:

$$AFC = t_s HSTR(3 + RSTRH) \quad (171)$$

First moment and centroid:

$$\left. \begin{aligned} AFCY &= t_s HSTR^2 (0.5 + RSTRH) \\ e &= HSTR \left(\frac{0.5 + RSTRH}{3 + RSTRH} \right) \end{aligned} \right\} \quad (172)$$

Moment of inertia:

$$I_{xx} = t_s HSTR \left[2e^2 + \frac{HSTR^2}{12} + \left(\frac{HSTR}{2} - e \right)^2 + RSTRH (HSTR - e)^2 \right] \quad (173)$$

The equations used to size the stiffener thickness, t_s , and the area of primary longerons, $A_{LU,LS,LL}$, secondary longerons, A_{IT} , and cutout longerons, $ALC_{u,l}$, are explained in reference 2. A summary of the equations and constraints used in subroutine FBEND is given here. The constraints and equations used to size the stiffener thickness and longeron areas are:

1. Minimum area:

$$A_{LU,LS,LL} \geq ASTRM \quad (173)$$

2. Thickness to resist forced crippling: During the synthesis of minor frames an approximation to the stiffener area based on minimum area and strengths requirements was made. The diagonal tension angle, α , was determined for forced crippling in the ring. The longitudinal stiffener is now sized to resist the forced crippling using the geometry of figure 21 and the α computed in MINFR.

The average stress is defined in equation 160 for stringers and longeron construction. Sizing to the allowable stress for the stiffener proceeds as in equation 169.

The maximum induced stress is then

$$f_{STmax} = \frac{K f_s}{\tan \alpha [t_s X_B + X_C]} \left(\frac{FST}{FST_{max}} \right) \quad (174)$$

where

$$\frac{f_{STmax}}{FST} = 1 + (1 - K) \left[0.78 - 0.65 \frac{BPAN}{SFRM} \right] \quad (175)$$

The maximum load carried by the stiffeners is

$$P_{max} = f_{STmax} A_s \quad (176)$$

3. Maximum down bending carried by upper longitudinal members: The nominal maximum allowable stresses for the longitudinal members and covers are established as:

$$\text{Longeron: } F_{\max} = 0.9 F_{cy} \quad (177)$$

$$\text{Cover: } SC_{\max} = 0.76 F_{tu} \quad (178)$$

If different materials are used

$$F_{\max} = \min \left(F_{\max}, SC_{\max} \frac{E_{\ell}}{E_c} \right) \quad (179)$$

and

$$SC_{\max} = \min \left(SC_{\max}, F_{\max} \frac{E_c}{E_{\ell}} \right) \quad (180)$$

Initial stiffener area estimates are

<u>Stringers</u>	<u>Longerons</u>	
$A_{LU} = \text{ASTRM}$	$A_{LU} = \text{AFC}$	}
$A_{LS} = \text{AFC}$	$A_{LS} = 0$	
$A_{LL} = \text{ASTRM}$	$A_{LL} = \text{AFC}$	
	$A_{IT} = \text{ASTRM}$	

(181)

Initial cutout longerons are:

$$ALC_u = \begin{cases} 0 & , \text{ if } RTU = 0 \\ \text{ASTRM}, & \text{ if } RTU > 0 \end{cases} \quad (182)$$

$$ALC_{\ell} = \begin{cases} 0 & , \text{ if } RTL = 0 \\ \text{ASTRM}, & \text{ if } RTL > 0 \end{cases} \quad (183)$$

where RTU and RTL are the apparent width of the section out from the shell.

The down bending moment carried by upper cover, side and intermediate longitudinal members is:

$$M_{AV} = T_{CU} \left(\frac{SC_{max}}{Z_{max}} \right) \left(\frac{I_Y}{t} \right)_u \left(1 - \frac{RTU}{BU} \right) + \frac{1}{2} \left(\frac{F_{max}}{Z_{max}} \right) \left[AL_s \left(\frac{I_Y}{AL} \right)_s + AIT \left(\frac{I_Y}{AIT} \right) \right] \quad (184)$$

where Z_{max} is the distance to the upper cover extreme fiber. If $2M_{AV}$ is less than the required moment, the difference in the moments, ΔM_u , is used to size the longitudinal area

$$A_{LU} \geq \frac{\Delta M_u Z_{max}}{F_{max} \left(\frac{I_Y}{AL} \right)_u} \quad (185)$$

If stringer construction is used, an additional cutout longeron on each side is inserted to carry the bending loads which should have been reacted by stringers. The area is sized as:

$$ALC_u \geq \frac{\Delta M_u \left(\frac{RTU}{BU} \right) Z_{max}}{2F_{max} Z_{CU}^2} \quad (186)$$

where Z_{CU} is the vertical distance from the neutral axis to the extreme fiber of upper sector.

4. The down bending moment carried by the lower sector in compression is similar to the tensile side, except only a portion of the cover material is considered to be effective in

carrying load. The critical buckling stress for thin walled curved sectors is:

$$F_{CCR} = \left[9 \left(\frac{T_{Cl}}{R_{Cl}} \right)^{5/3} + 0.16 \left(\frac{T_C}{SFRM} \right)^{4/3} + \frac{4\pi^2}{12(1 - \mu^2)} \left(\frac{T_C l}{WPAN} \right)^2 \right] E \quad (187)$$

where

$$WPAN = \begin{cases} BL & \text{for longerons} \\ B_{STR} & \text{for stringers} \end{cases}$$

$$B_{STR} = \text{stringer spacing}$$

if F_{CCR} is greater than the SC_{max} the center cover is effective. If not, an effective width of the cover is computed.

$$W_{eff} = 1.7 T_{Cl} \sqrt{\frac{E_c}{F_{CCR}}} \quad (188)$$

The moment carried by the effective cover is

$$M_C = (W_{eff} T_{Cl}) \left(\frac{SC_{max}}{Z_{min}} \right) \left(\frac{I_y}{AL} \right)_l W_{AV} \quad (189)$$

where

$$W_{AV} = \begin{cases} BL & \text{for longerons} \\ BL-RTL & \text{for stringers} \end{cases}$$

Z_{min} = vertical distance to extreme fiber of lower sector

If $SC_{\max} \leq F_{ccr}$,

$$M_C = (T_{C\ell}) \left(\frac{SC_{\max}}{Z_{\max}} \right) \left(\frac{I_Y}{t} \right)_{\ell} \left(\frac{BL-RTL}{BL} \right) \quad (190)$$

The total moment carried by the cover, side stiffeners, and secondary longerons is:

$$M_{AV} = M_C + \frac{1}{2} \frac{F_{\max}}{Z_{\min}} \left[A_{LS} \left(\frac{I_Y}{AL} \right)_S + A_{IT} \left(\frac{I_Y}{A_{IT}} \right) \right] \quad (191)$$

The difference between the available moment and the applied moment, M_{ext} , for the lower cover is:

$$\Delta M_{\ell} = \frac{M_{ext}}{2} - M_{AV} \quad (192)$$

If ΔM_{ℓ} is greater than zero, the longitudinal areas sized are:

Stringers

$$APL = \frac{\Delta M_{\ell} Z_{\min}}{F_{\max} \left(\frac{I_Y}{AL} \right)_{\ell}}$$

$$A_{LL} \geq APL$$

Longerons

$$APL = \frac{\Delta M_{\ell} Z_{\min}}{F_{\max} \left(\frac{I_Y}{AL} \right)_{\ell}} \quad (193)$$

$$A_{LL} \geq APL \quad (194)$$

Cutout Longerons

$$ALC = \frac{\Delta M_{\ell}}{2} \frac{RTL}{BL} \frac{Z_{\min}}{F_{\max} Z_{CL}^2}$$

Combined Loading

$$A_{LL} \geq \frac{(F_{\max}) (BST) (APL) + P_{\max}}{(0.9) (F_{cy})}$$

(195)

The procedure is then repeated for the maximum up-bending case.

C-2

5. The upper longitudinal members and cover are checked for up-bending assuming all members are in compression.

6. The lower longitudinal members are checked for up-bending assuming all members are in tension.

7. Vertical stiffness requirement (EI_y): The total vertical bending stiffness available (EIVA) is determined from the sum of the components. Because the structure is sized for the postbuckled configuration, only those members contributing to the shell strength are considered.

$$EIVA_O = E_c \left(\frac{I_y}{t} \right)_u T_{CU} \left(1 - \frac{RTU}{BU} \right) + E_L \left[\left(\frac{I_y}{A_{IT}} \right) A_{IT} + \left(\frac{I_y}{A_s} \right) A_{LS} + ALC_u^2 ZCU^2 + ALC_\ell^2 ZCL^2 \right] \quad (196)$$

Longitudinal member stiffness.

<u>Stringer</u>	<u>Longeron</u>
$EIVA = EIVA_O + \left[\left(\frac{I_y}{A} \right)_u A_{LU} \left(1 - \frac{RTU}{BU} \right) + \left(\frac{I_y}{A} \right)_\ell A_{LL} \left(1 - \frac{RTL}{BL} \right) \right] E_L$	$EIVA = EIVA_O + \left[\left(\frac{I_y}{A} \right)_u A_{LU} + \left(\frac{I_y}{A} \right)_\ell A_{LL} \right] E_L \quad (197)$

If the available stiffness is less than the required stiffness (EIVT), the difference is used to size the following areas:

$$\Delta EI = EIVT - EIVA \quad (198)$$

<u>Stringers</u>	<u>Longerons</u>	}
$ALC_u = ALC_u + \frac{\Delta EI}{4E_L ZCU^2}, \text{ if } RTU > 0$	$A_{LU} = A_{LU} + \frac{\Delta EI}{2E_L \left(\frac{I}{A}\right)_u}$	
$AL_u = AL_u + \frac{\Delta EI}{2E_L \left(\frac{I}{A}\right)_u}, \text{ if } RTU \leq 0$		
	(199)	

<u>Stringer</u>	<u>Longeron</u>	}
$ALC_\ell = ALC_\ell + \frac{\Delta EI}{4E_L ZCL^2}, \text{ if } RTL > 0$	$A_{LL} = A_{LL} + \frac{\Delta EI}{2E_L \left(\frac{I}{A}\right)_\ell}$	
$A_{LL} = A_{LL} + \frac{\Delta EI}{2E_L \left(\frac{I}{A}\right)_\ell}, \text{ if } RTL \leq 0$		
	(200)	

8. Side bending stiffness requirement (EI_z): The total side bending stiffness available (EISA) is determined from the sum of the components.

$$EISA_O = \frac{1}{2} E_C \left(\frac{I_z}{t}\right)_S TC_S + E_L \left[\left(\frac{I_z}{A_{IT}}\right) A_{IT} + 2ALC_u YCU^2 + 2ALC_\ell YCL^2\right] \quad (201)$$

<u>Stringer</u>	<u>Longeron</u>
$EISA = EISA_O + \left(\frac{I}{A}\right)_u A_{LU} \left(1 - \frac{RTU}{BU}\right)$ $+ \left(\frac{I}{A}\right)_\ell A_{LL} \left(1 - \frac{RTU}{BU}\right)$ $+ \left(\frac{I}{A}\right)_s A_{LS} E_L$	$EISA = EISA_O + \left(\frac{I}{A}\right)_u A_{LU}$ $+ \left(\frac{I}{A}\right)_\ell A_{LL} E_L$
	(202)

If the available side stiffness is less than the required stiffness (EISD), the difference is used to size the following areas:

$$\Delta EI = EISD - EIVA \quad (203)$$

The members resized are:

<u>Stringer</u>	<u>Longeron</u>
$A_{LS} = A_{LS} + \frac{\Delta EI}{E_L \left(\frac{I}{A}\right)_s}$	$A_{LU} = A_{LU} + \frac{\Delta EI}{2E_L \left(\frac{I}{A}\right)_u}$
	$A_{LL} = A_{LL} + \frac{\Delta EI}{2E_L \left(\frac{I}{A}\right)_\ell}$
	} (204)

The unit weight of longitudinal members is determined as follows for the two construction types:

Stringers

Longerons

$$\begin{aligned} \text{TOT}_s &= \left[A_{LU} \frac{BU}{B_{STR}} \left(1 - \frac{W_{cut_u}}{BU} \right) \right. \\ &+ A_{LL} \frac{BU}{B_{STR}} \left(1 - \frac{W_{cut_\ell}}{BL} \right) \\ &+ 2A_{LS} \frac{BS}{B_{STR}} \\ &+ N_{sec} A_{IT} + 2ALC_u \\ &\left. + 2ALC_\ell \right] \rho_L \end{aligned} \quad \begin{aligned} \text{TOT}_s &= \left[\frac{1}{2} N_{st} A_{LU} + \frac{1}{2} N_{st} A_{LU} \right. \\ &+ N_{sec} A_{IT} + 2ALC_u \\ &\left. + 2ALC_\ell \right] \rho_L \end{aligned} \quad (205)$$

where

$W_{cut_{u,\ell}}$ = widths of upper and lower cutouts

B_{STR} = stringer spacing

N_{sec} = number of secondary stringers

N_{st} = number of longerons

Miscellaneous and Secondary Structural Weight

The estimation of a number of miscellaneous items under the heading Basic Structure (see figure 14) are computed from statistical methods. The joints, splices and fasteners are computed as a fraction of cover and longitudinal member weight. Longitudinal partition weight is estimated as a fraction of cover and minor frame weight. Flooring and supports items are estimated on a unit weight basis for the type of floor used and its width and surface area. The engine drag beam and the

fitting weights are computed empirically to estimate the attachment weight penalty for a buried-engine concept and for the attachments for the wing, horizontal tail, vertical tail, nacelles, and other fuselage mounted components.

Secondary structural items for which statistical weights are computed are generally separated into secondary structural items such as canopies, windshields, window, and radomes, and into doors, panels, and other access structure. Three methods of weight prediction are available for most of these items: a rule-of-thumb estimate, a statistical calculation based on additional component definition, and direct input by the user. The program is arranged on input into three variable groups according to calculation requirements. The weight indicator and the component CG are required to decide whether to calculate the item and its location. If a calculative technique is used, a second group of additional required variables must be input. The third group of variables may optionally be input in lieu of variables in the second group when available.

The equations used to estimate the secondary structural components are defined in reference 2. At least one coefficient in each of the statistical equations may also be redefined by the user on input. These coefficients are stored in the program array, EQN, and are initialized by the program input routine. Subsequent input variables may be used to override the default values.

Summary and Intermediate Output

A summary output of both the computed results and intermediate program values is available. Six print variables currently control the output of all print with the exception of certain error messages. These suppress or print the input and output summaries and control the printing of the intermediate calculations from geometry descriptions, and the synthesis of the

covers, the bending material, and the minor rings. The intermediate print is available for most parameters used in the synthesis loop at each out. These consist primarily of temporary variables that are not saved for the final summary print.

The summary print contains the basic geometric descriptors, material gages, and weights computed during the fuselage synthesis. The basic shell cut geometry and segment properties used in the structural design of the bending and torsional stiffnesses are given. The shell material gages required to satisfy panel flutter, torsion, minimum gage, and strength requirements in the skins and landings as well as the required stiffener and longeron areas including the effects of cutouts are output for each cut. The estimated weight for each segment for each of the skin, frames, and longitudinal members is given. A basic AN-9102-D weight statement and accompanying balance statement as given in figure 14 is used to summarize the weight prediction.

Optional output also includes a print of the inputs generated for the PASS program and plots of the basic configuration and material distribution.

Fuselage Module Sample Case

A sample test case of the C-141A transport aircraft was run as check of the program's accuracy. The computer run was for a metallic design with stringer construction. A fixed spacing on stringers and minor frames was used, and only the optimum search for bulkhead weight was exercised. The input data were derived from the demonstration case in reference 2. Since no external loads calculation exists within the program, a number of shear and bending moment distributions were excerpted from the demonstration case output. The detailed weight statement and balance summary are shown in figure 14.

The ratio of the C-141A fuselage weight computed to the weight computed here in reference 2 is 1.05. The ratio of the actual C141A fuselage to the weight computed in figure 14 is 1.15. The computed weights include the weight index factors for the cover, longerons, frames and bulkheads suggested in reference 2 to estimate non-optimum weight increments. About eighty percent of the individual components estimated agreed exactly with the computations in reference 2. Since major portions of the code were adapted directly, the close correlation was expected.

The major source of differences in estimated structural weight was the lack of sufficient loading input. A total of sixteen loading conditions were used in the demonstration problem. Of these only two occurred in the summary output in complete enough form to be used as input in this check case. In general, the new geometry descriptors were within a percent of the rounded-rectangle representation. The other source of differences was the estimation of the major frames. An empirical relation was used in lieu of detailed frame calculations. Though the individual frame weights varied significantly, the net weight of frames and bulkheads agreed within 3 percent.

A detailed comparison of each line item in the AN-9102-D weight statement was not possible due to the unavailability of the C-141A data. A comparison of data from AN-9103-D data is given in the following table. The weights are broken down according to the summaries of the items on each of the three pages in the detailed weight statement. The comparison of the C-141A group data with the results computed by the present program and those presented in reference 2 are given in Table IV.

As group items the estimation of secondary structural components does appear to be satisfactory. The estimation of the basic structure still requires additional correlation to establish weight index factors, and the proper generation of the load spectrum.

TABLE IV

Comparison of Estimated and Actual C-141A
Fuselage Group Weight Statements

Item / Source	C-141A	SWEEP	Fuselage Code
Body Group (total)	29,342	26,679	25,462
Fuselage or Hull-Basic Structure	21,438	18,859	17,909
Secondary Structure-Fuselage of Hull	1,060	1,138	1,049
-Doors, Panels & Misc.	6,844	6,680	6,503

Conclusions and Recommendations

The objectives of this work were the improvement of the deficiencies in the WADES program for wing design identified in reference 1 and the development of a program for the estimation of fuselage weights. The enhancements were incorporated into the wing design code and comparisons of the results for the F-5A were made. A program for the estimation of aircraft fuselage weights was written which adapted the descriptors used in the ACSYNT program and the methods employed in reference 2. A check case for the C-141 was executed and the estimated weights compared.

The wing design code (shown in both the estimation of the material and the load distributions improvement due to the incorporated enhancements). The extended geometric representation of the wing carry-through structural loads and the inclusion of trim significantly improved the load distributions. The inclusion of the empirical calculation of secondary structural component weights and the extended planform definition lowered the ratio of computed to structural weight from 1.9 to 1.2 for the F-5A. The distributions of structural area and inertia improved slightly. The best comparisons were with the surface fit of \bar{t} , and the redesign of only $t(\xi, \eta)$. The closest weight estimation, however, occurred when redesigning with spar caps.

The strength design procedure proved to be sensitive to the influence of spar or stringer spacing, but the use of the free coefficients associated with the sizing of the stringers in the synthesis process was inconclusive without the additional constraints on rib spacing and global panel buckling. A more general set of constraints including core and rib design would be required to compute these properly. The inclusion of the approximate flutter constraint was very efficient after the initial derivative evaluation. The convergence for the combined flutter and strength design appeared limited only by the convergence of the internal load distribution.

The generation of a computer code for the estimation of aircraft fuselage component weights was accomplished. The estimated weights for the check case of the C-141 were within sixteen percent of the actual weight. This weight discrepancy is due in part to inadequate definition of the load profile. No external load calculations were incorporated in the program initially. All shear and moment distributions were read in directly in lieu of procedure which would generate loads on a full aircraft configuration. The coupling of this program to an external aerodynamic loads estimating routine is the recommended extension for improved usability of the program. The program was structural initially so that this additional feature could be readily incorporated.

REFERENCES

1. Mullen, Joseph: Integration of a Code for Aeroelastic Design of Conventional and Composite Wings into ACSYNT, An Aircraft Synthesis Program, NASA CR-137805, May, 1976.
2. Hiyana, R.: A Structural Weight Estimation Program (SWEEP) for Aircraft. ASD/XR 74-10, vol. VII, June, 1974.
3. Glatt, C. R.: WAATS - A Computer Program for Weights Analysis of Advanced Transportation Systems. NASA CR-2420, Sept., 1974.
4. Oman, B. H., Pederson, S. E., Karll, N. P., and Reed, T. F.: Computer Program to Perform Aircraft Design Synthesis. AFFDL-TR-74-35, vols. I and II., April, 1974.
5. Reed, T. F.: WTSIZ - Interactive Graphics Program for Aircraft Weight Sizing. Convair Aerospace Report GDC-ERR-1644, December, 1971.
6. Caddell, W. E.: Generalized Weight Estimating Methods for Aircraft Structures and Equipment. Convair Aerospace Report GEC-ERR-ZW-039, 1960.
7. Sanders, Karl L.: Initial Gross Weight and Size Estimation, Emphasizing Fighter Aircraft. SAWE Tech. Paper 760, May, 1969.
8. Aircraft Predesign Weight Estimation Handbook. Ryan Report No. 29244-2, Vol. I.
9. Anderson, Joseph L.: Operational Weight Estimation of Commercial Jet Transport Aircraft. Paper No. 946, presented at 31st Annual Conference of Society of Aeronautical Weight Engineers, Inc., Atlanta, Georgia, May 22-25, 1972.

REFERENCES (continued)

10. Ripley, E. L.: A Method of Fuselage Structure Weight Prediction. Royal Aircraft Establishment, Report No. Structures 93, November, 1950.
11. Solvey, J.: The Estimation of Wing Weight. Aircraft Engineering, May, 1951.
12. Wood, K. D.: Preliminary Design Weight Estimation. Reproduced from Boeing Report in Airplane Design, Johnson Publishing Co., 1963.
13. Carreyette, J. F.: Aircraft Wing Weight Estimation. Aircraft Engineering, January, 1950.
14. Rosenthal, L. W.: The Weight Aspect in Aircraft Design. J. Roy. Aeron. Soc., March, 1950, pp. 187-210.
15. Shanley, F. R.: Weight-Strength Analysis of Aircraft Structures. Second ed., Dover Publications, Inc., 1960.
16. Micks, W. R.: Structural Weight Analysis - Fuselage and Shell Structures. Project Rand Report R-172, Jan., 1950.
17. Ardema, M. D. and Williams, L. J.: Transonic Transport Study - Structures and Aerodynamics. NASA TM X-62, 157, May, 1972.
18. Ardema, M. D.: Structural Weight Analysis of Hypersonic Aircraft. NASA TM D-6692, March, 1972.
19. Crawford, R. F. and Burns, A. B.: Minimum Weight Potentials for Stiffened Plates and Shells. AIAA Jour., vol. 1, no. 4, April, 1963, pp. 879-886.
20. Burt, M. E.: Weight Prediction for Wings of Box Construction. Royal Aircraft Establishment, Report No. Structures 186, August, 1955.

REFERENCES (continued)

21. Burt, M. E.: Structural Weight Estimation for Novel Configurations. Royal Aircraft Establishment, Report No. Structures 270, December, 1961.
22. Switzky, H.: Preliminary Design of Wings. AFFDL-TR-74-20, vols. I thru IV, March, 1974.
23. McCullers, L. A. and Lynch, R. W.: Dynamic Characteristics of Advanced Filamentary Composite Structures. Vol. II - Aeroelastic Synthesis Procedure Development. AFFDL-TR-73-111, September, 1974.
24. Haftka, Raphael T.: Automated Procedure for Design of Wing Structures to Satisfy Strength and Flutter Requirements. NASA TN D-7264, 1973.
25. Haftka, R. T.: Parametric Constraints with Application to Optimization for Flutter Using a Continuous Flutter Constraints. AIAA Jour., vol. 13, no. 4, April, 1975, pp. 471-475.
26. Haftka, R. T. and Starnes, J. H., Jr.: WIDOWAC (Wing Design Optimization with Aeroelastic Constraints). Program Manual. NASA TM X-3071, 1974.
27. Stroud, W. J., Dexter, C. B., and Stein, M.: Automated Preliminary Design of Simplified Wing Structures to Satisfy Strength and Flutter Requirements. NASA TN D-6534, December, 1971.
28. Hague, D. S. and Glatt, C. R.: Optimal Design Integration of Military Flight Vehicles - ODIN/MFV. AFFDL-TR-72-132, December, 1972.
29. Gray, W. L. and Schenk, K. M.: A Method for Calculating the Subsonic Steady-State Loading on an Airplane with a Wing of Arbitrary Planform and Stiffness. NACA TN-3030, December, 1953.

REFERENCES (continued)

30. Schmit, L. A., Jr. and Miura, H.: A New Structural Analysis/Synthesis Capability - ACCESS 1. AIAA Paper No. 75-703, presented at the AIAA/ASME/SAE 16th Structures, Structural Dynamics, and Materials Conference, Denver, Colorado, May 27-29, 1975.
31. Schmit, L. A., Jr.: Use of Mathematical Programming Methods for Structural Optimization. Abstract of Lecture for AGARD Lecture Series No. 70, October, 1974.
32. Schmit, L. A., Jr. and Miura, H.: Approximation Concepts for Efficient Structural Synthesis, NASA CR-2552, March 1976, NASA Langley.
33. Rogers, J. T.: ORACLE - A Program for Preliminary Structural Design of High-Aspect-Ratio Wings. Boeing Company Report D6-41475, March, 1974.
34. Kruse, G. S. and Peterson, L. M.: Automated Structural Sizing Techniques for Aircraft and Aerospace Vehicle Structures. General Dynamics/Convair Report GDCA-ERR-1748, December, 1972.
35. Sobieszczanski, J. and Loendorf, D.: A Mixed Optimization Method for Automated Design of Fuselage Structures. AIAA Paper No. 72-330, presented at the 13th AIAA/ASME/SAE, Structures, Structural Dynamics and Materials Conference, San Antonio, Texas, April, 1972.
36. Dwyer, W. J., Emerton, R. K., and Ojalvo, I. V.: An Automated Procedure for the Optimization of Practical Aerospace Structures. Vol. I - Theoretical Development and Users Information. AFFDL-TR-70-118, March, 1971.

REFERENCES (continued)

37. Lansing, W., Dwyer, W., Emerton, R., and Ranalli, E.: Application of Fully Stresses Design Procedures to Wing and Empennage Structures. Jour. of Aircraft, vol. 8, no. 9, September, 1971, pp. 683-688.
38. Wilkinson, K., Markowitz, J., Lerner, E., Chipman, R., George, D: An Automated Procedure for Flutter and Strength Analysis and Optimization of Aerospace Vehicles, Volume I - Theory and Application. AFFDL-TR-75-137, December, 1975.
39. Giles, G. L., Blackburn, C. L., and Dixon, S. C.: Automated Procedures for Sizing Aerospace Vehicle Structures. Jour. of Aircraft, vol. 9, no. 12, December 1972, pp. 812-819.
40. Gellatly, R. A., Dupree, M. D., and Berke, L.: OPTIM II - A MAGIC Compatible Large-Scale Automated Minimum Weight Design Program, vols. I and II. AFFDL-TR-74-97, July, 1974.
41. Gellatly, R. A. and Berke, L.: Optimal Structural Design ATTDL-TR-70-165, April, 1971.
42. Venkayya, V. B., Khot, N. S., and Reddy, V. S.: Energy Distribution in an Optimum Structural Design. AFFDL-TR-68-156, 1968.
43. Venkayya, V. B.: Design of Optimum Structures. An International Journal, Computers and Structures, vol. 1, no. 1/2, August, 1971, pp. 265-309.
44. Khot, N. S., Venkayya, V., Johnson, C. D., and Tishler, V. A.: Application of Optimality Criterion to Fiber-Reinforced Composites. AFFDL-TR-73-6, 1973.
45. MacNeal, R. H.: The NASTRAN Theoretical Manual (Level 15). NASA SP-221(01), April, 1972.

REFERENCES (concluded)

46. Karnes, R. N., Tocher, J. L., and Twigg, D. W.: Automated Analysis and Design of General Engineering Structures. Boeing Document D6-24387, 1970.
47. Tocher, J. L. and Karnes, R. N.: The Impact of Automated Structural Optimization on Actual Design. ASME/AIAA Structures and Materials Conference, Anaheim, California, April 19-21, 1971.
48. Miura, H.: An Optimal Configuration Design of Lifting-Surface Type Structures under Dynamic Constraints, Ph.D. Thesis, Division of Solid Mechanics, Structures and Mechanical Design, Case Western Reserve University, Cleveland, Ohio, Report No. 48, October, 1971.
49. User's Manual ECI-ICES-STRU DL/DYNAL. McDonnell-Douglas Automation Co., St. Louis, Missouri.
50. Dodd, A. J.: Specification for a Static Structural Optimization Capacity. Douglas Aircraft Division IRAD Report MDC-J5442, 1972.
51. Anderson, G. O. and Betz, V. L.: F-5A/B Wing Stress Analysis. Northrop Norair Report NOR-62-94, January, 1964.
52. Anderson, G. O. and Betz, V. L.: F-5A/B Wing Section Properties, Shear Flow, and Bending STress Distribution. Vol. I, Revision "A", January, 1965, vol. II Revision "B", April, 1965. Northrop Norair Report NOR-62-92, September, 1963.
53. Northrop Corporation, Norair Division: F-5A/B Wing Design Loads. Report NOR 62-89, September, 1974.

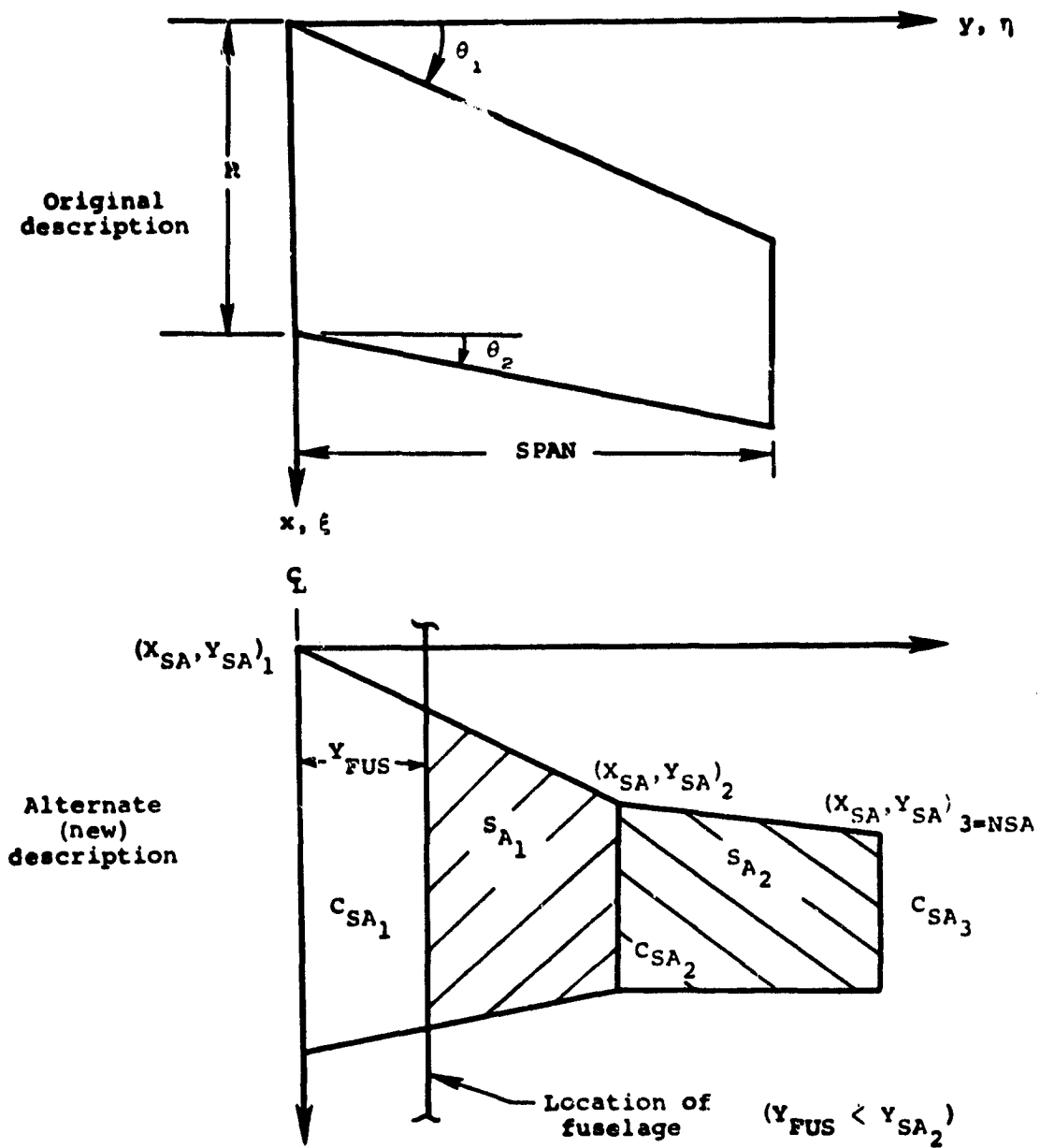


Figure 1.- Aerodynamic planform descriptions.

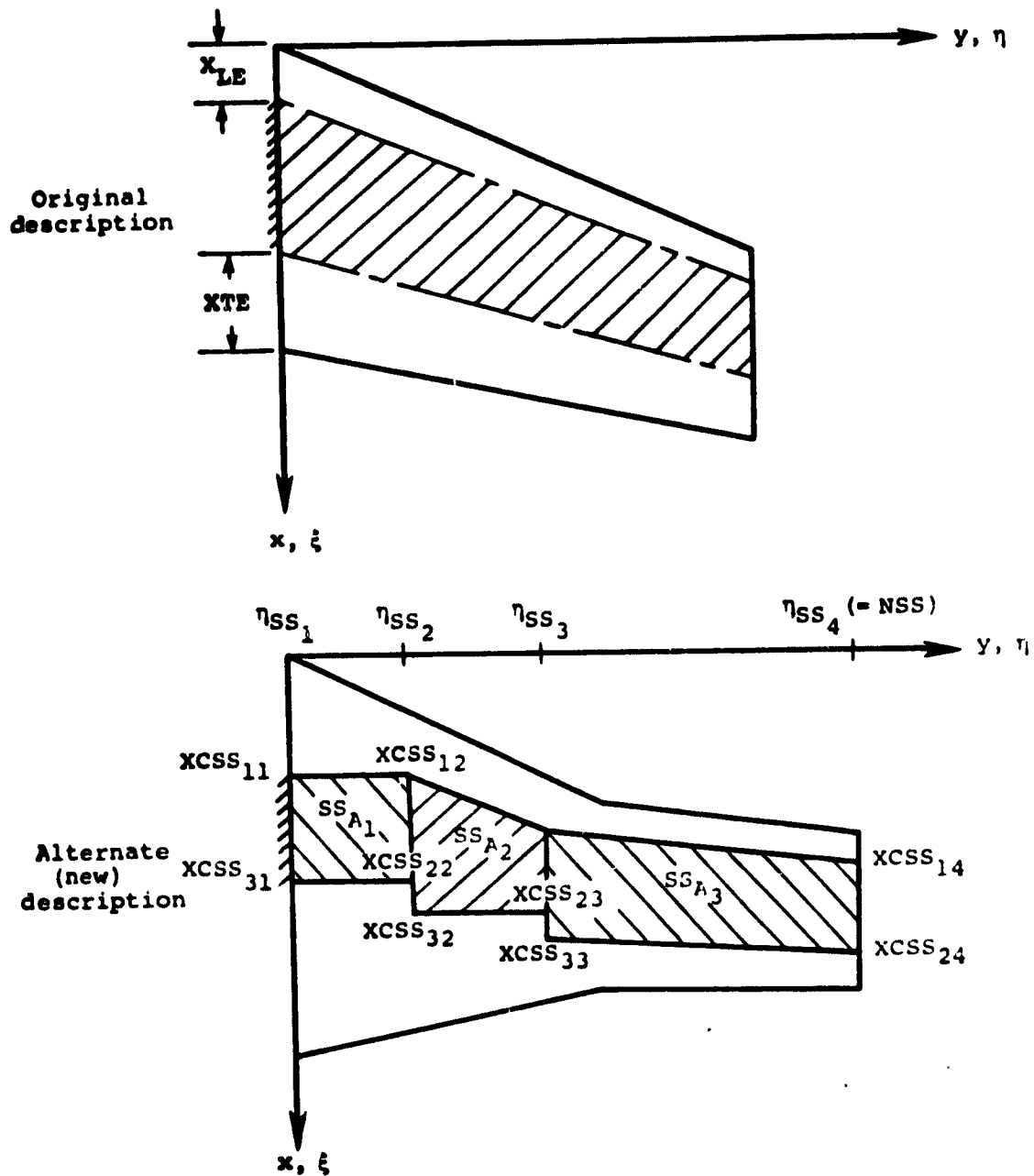


Figure 2.- Structural planform descriptions.

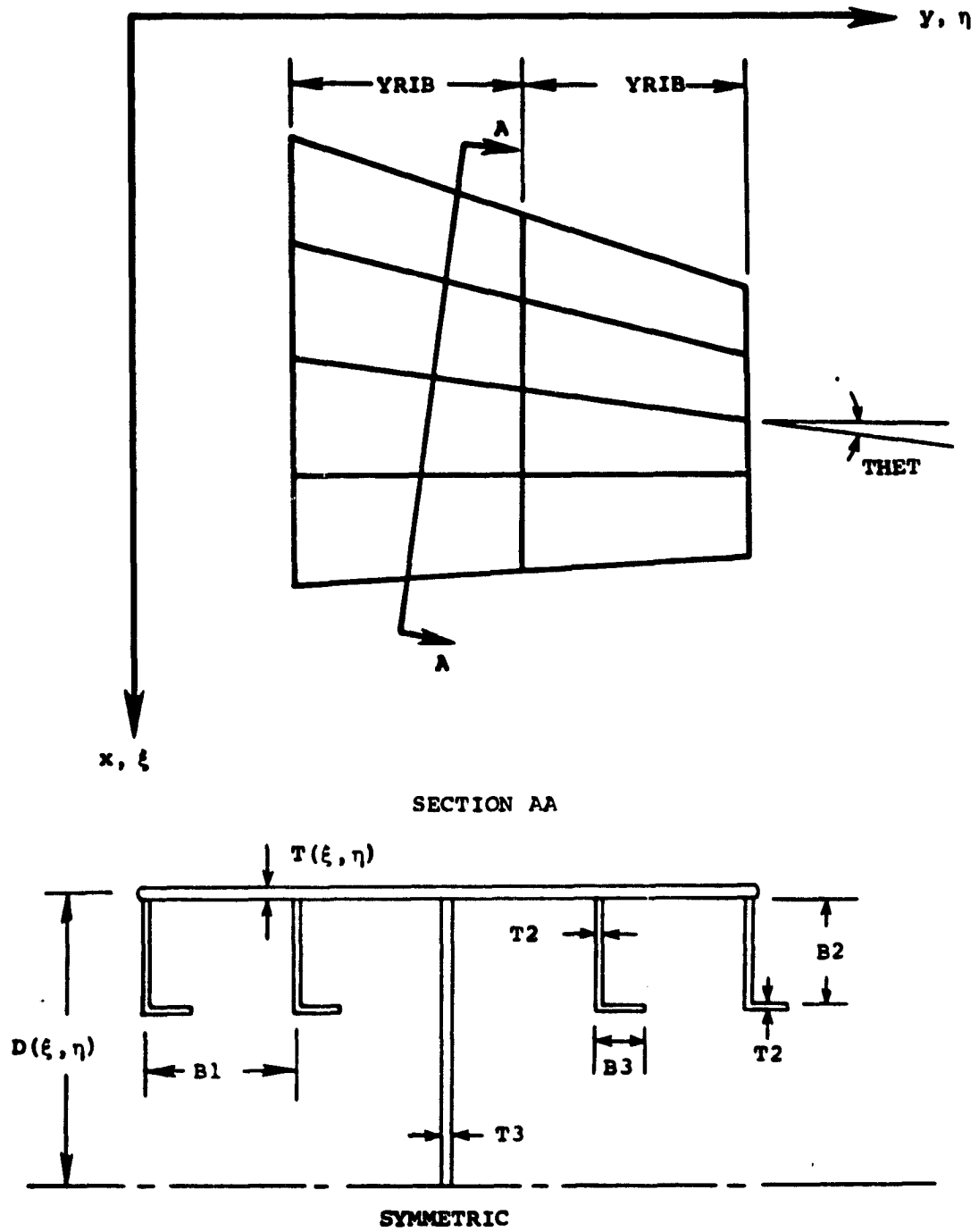


Figure 3.- Geometric description of wing-stiffened cover sheet model.

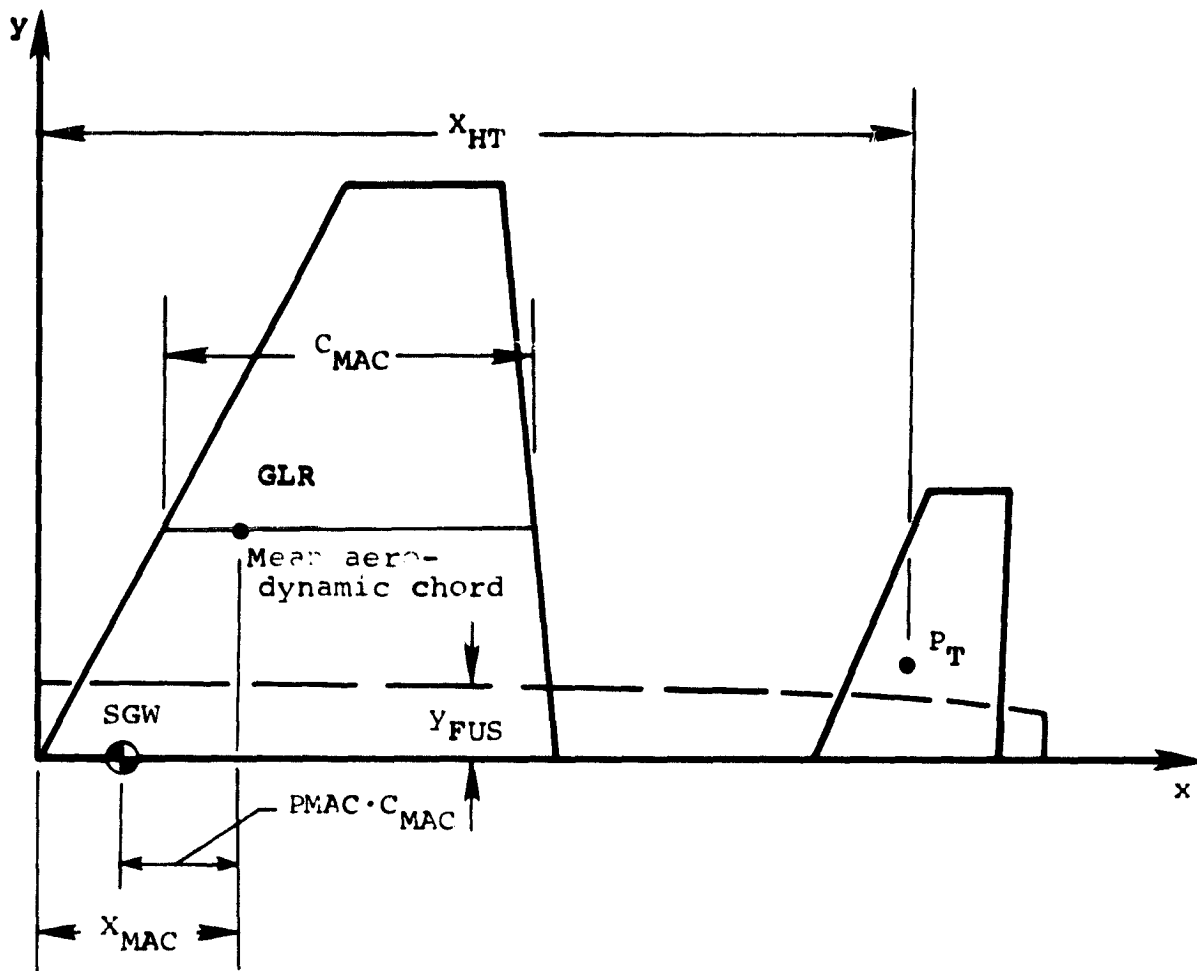


Figure 4.- Relative location of loads for trim flight.

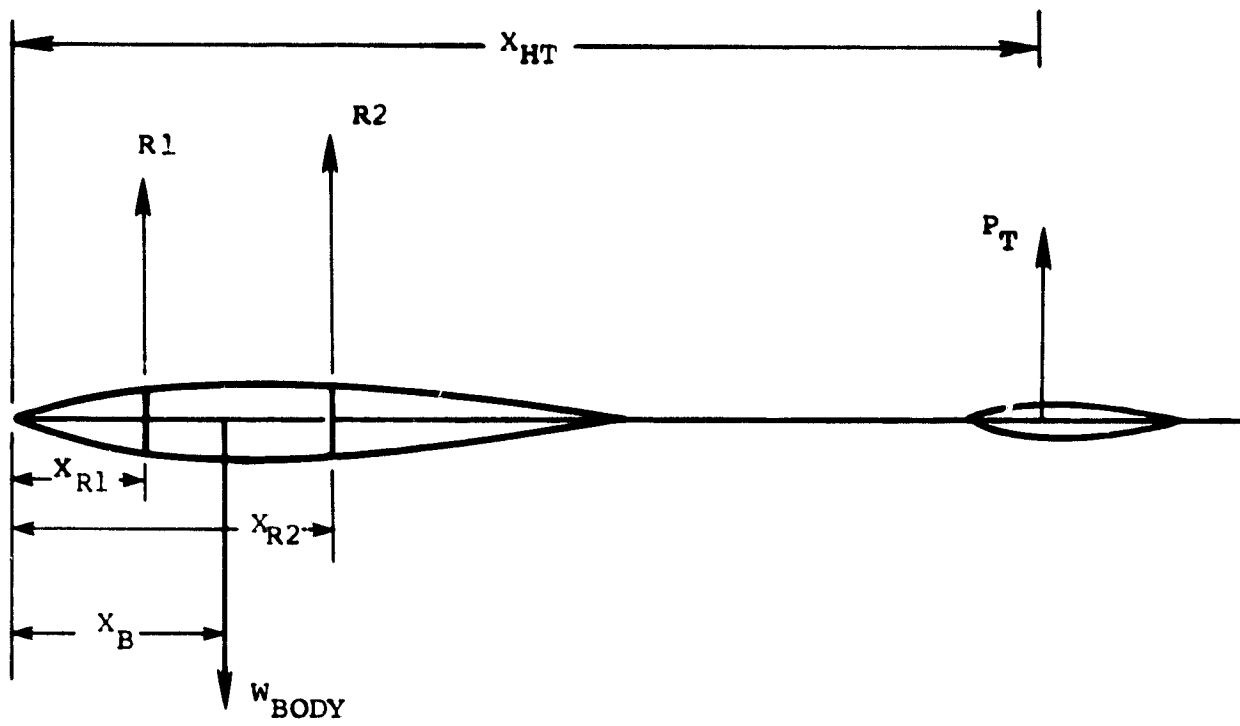


Figure 5.- Equivalent reactions at wing-fuselage junction.

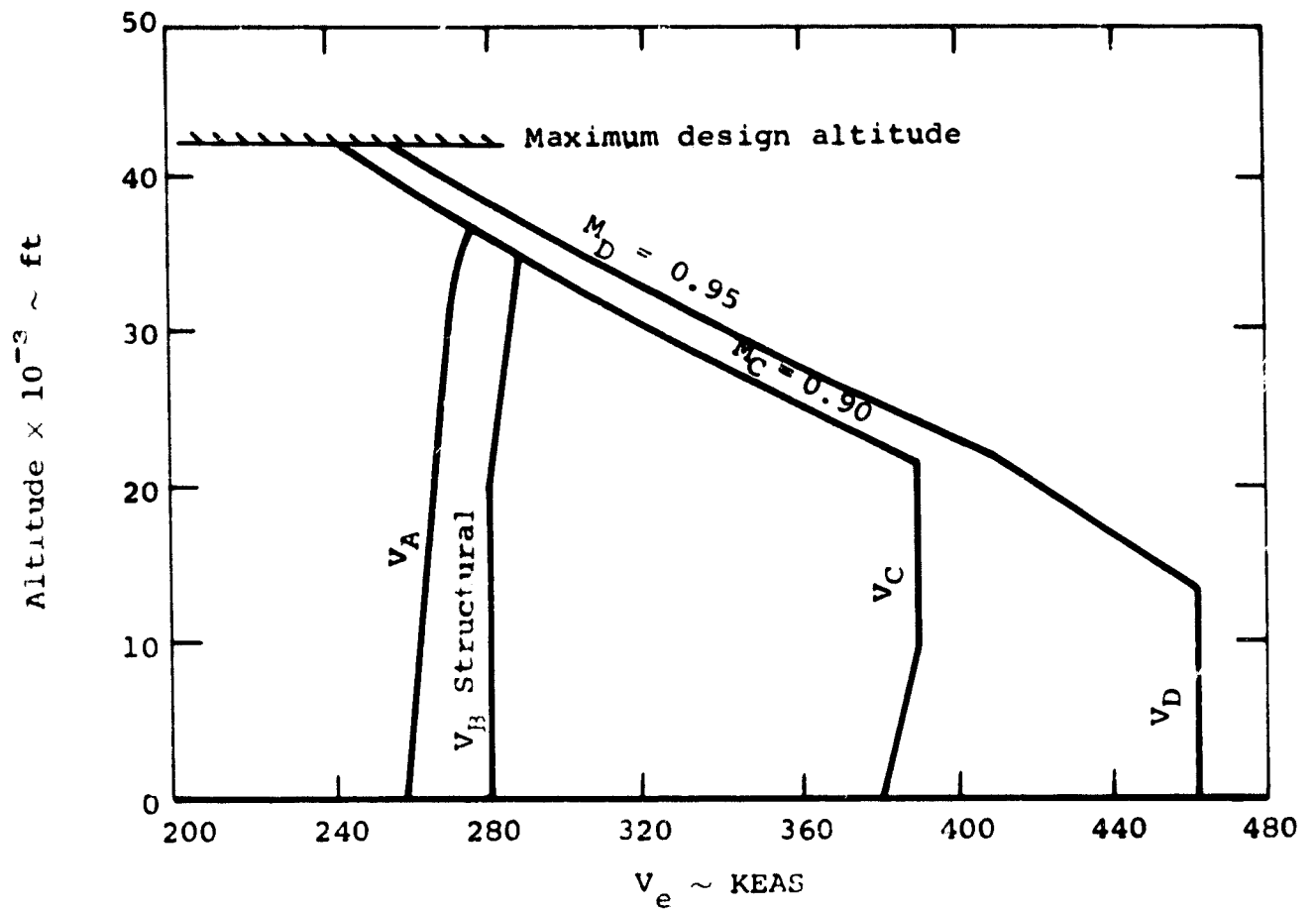


Figure 7.- Typical design speed versus altitude envelope.

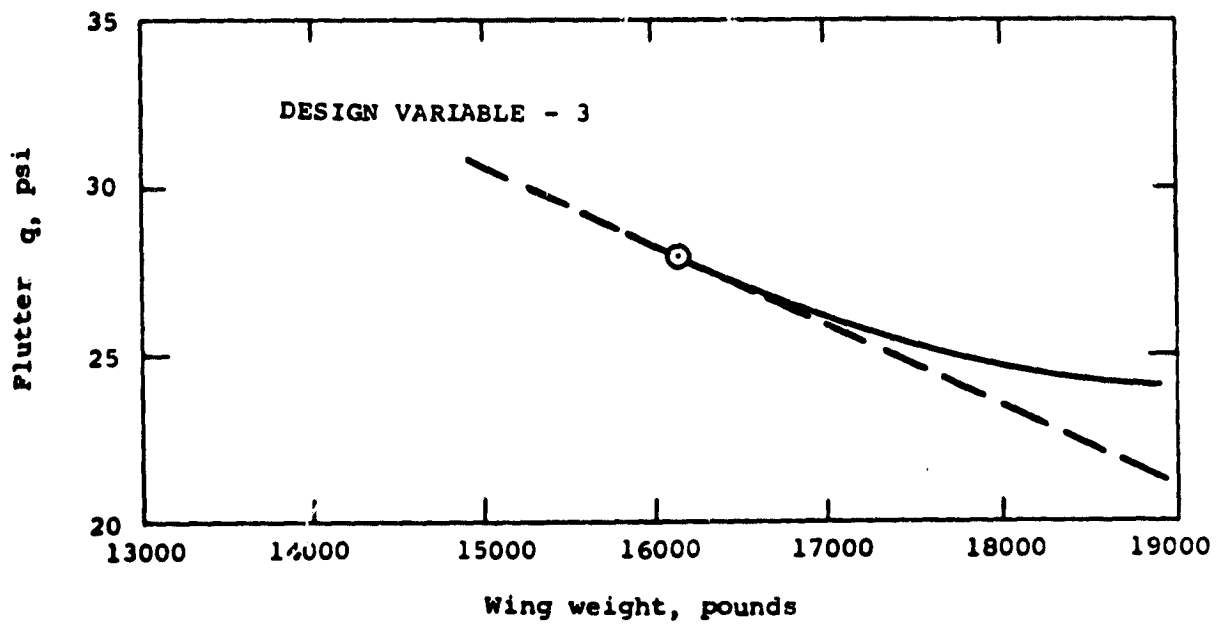
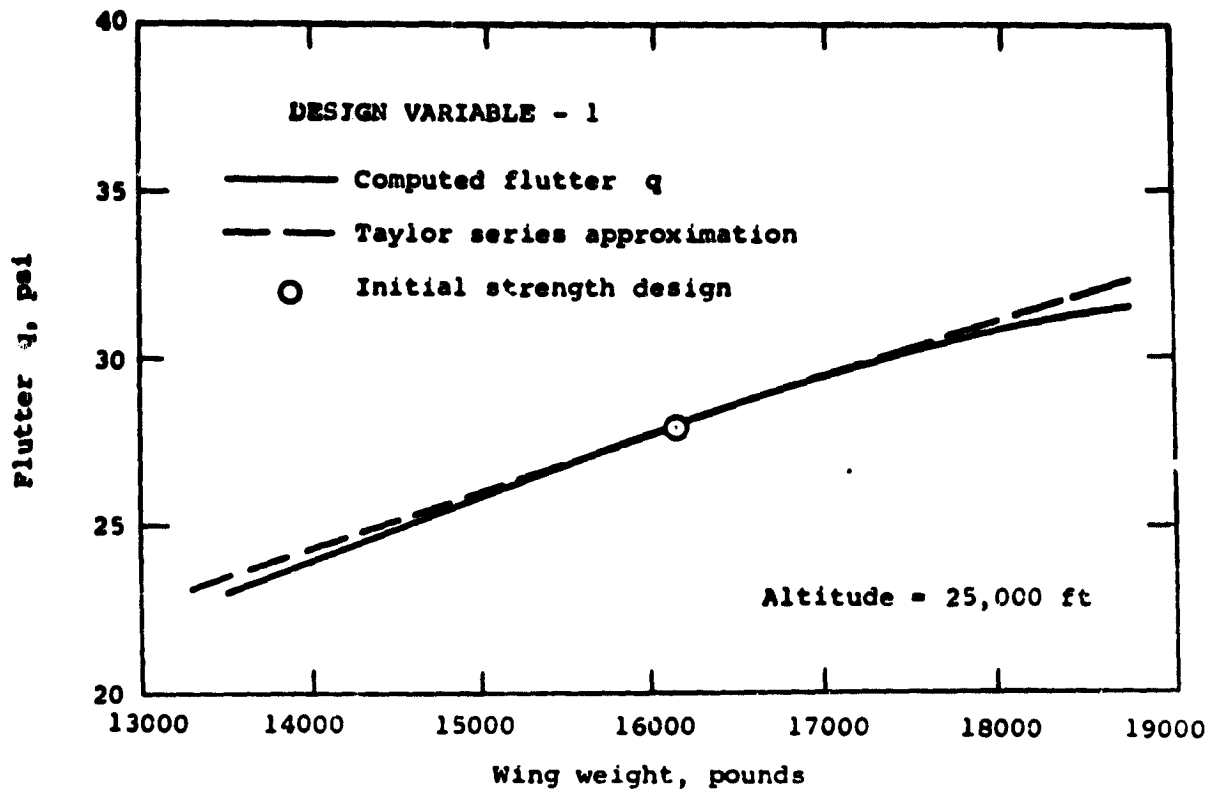


Figure 8.- Geometric description of wing-stiffened cover sheet model.

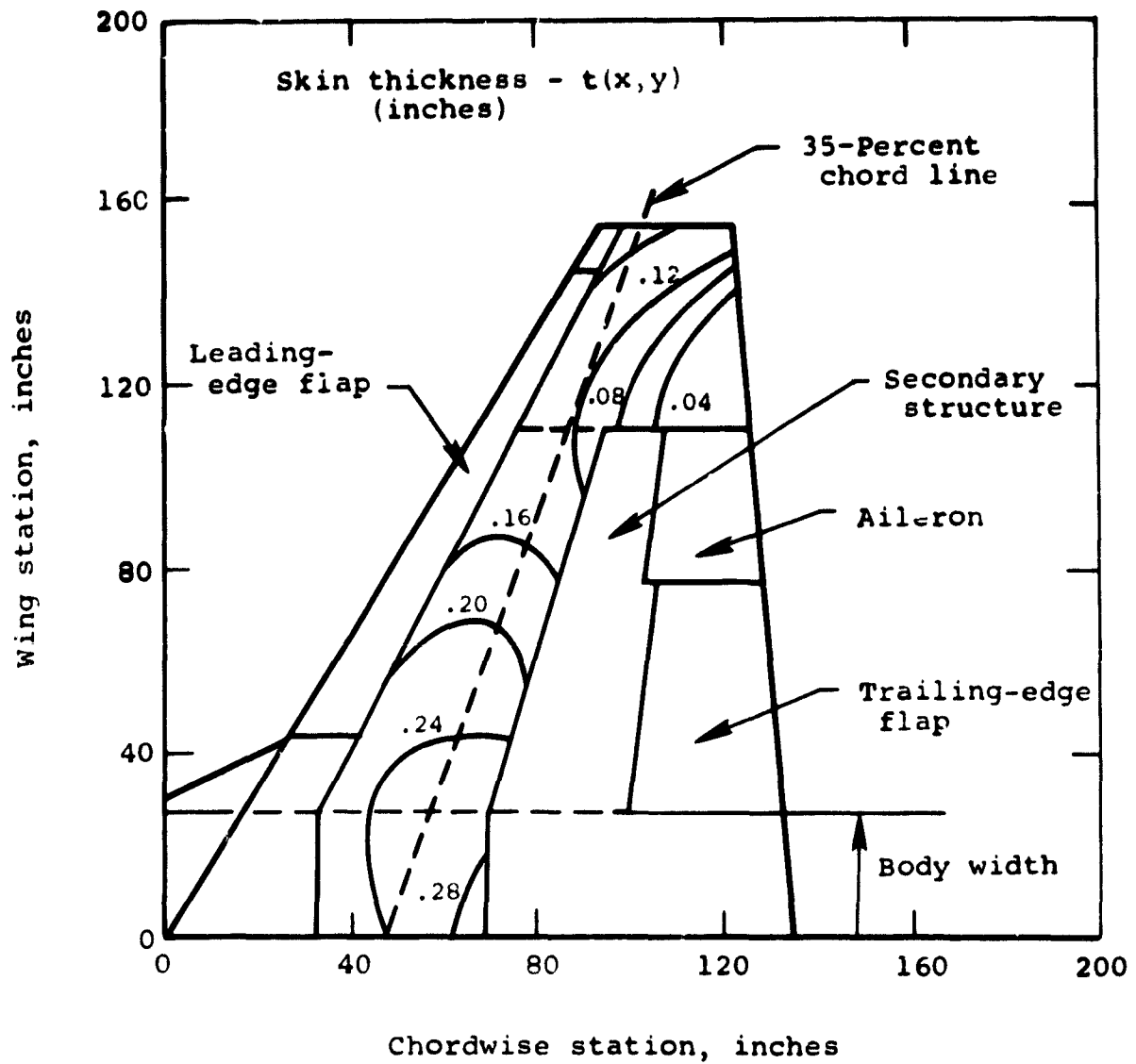


Figure 9.- F-5A/B planform layout and surface fit of skin thickness, $t(x,y)$.

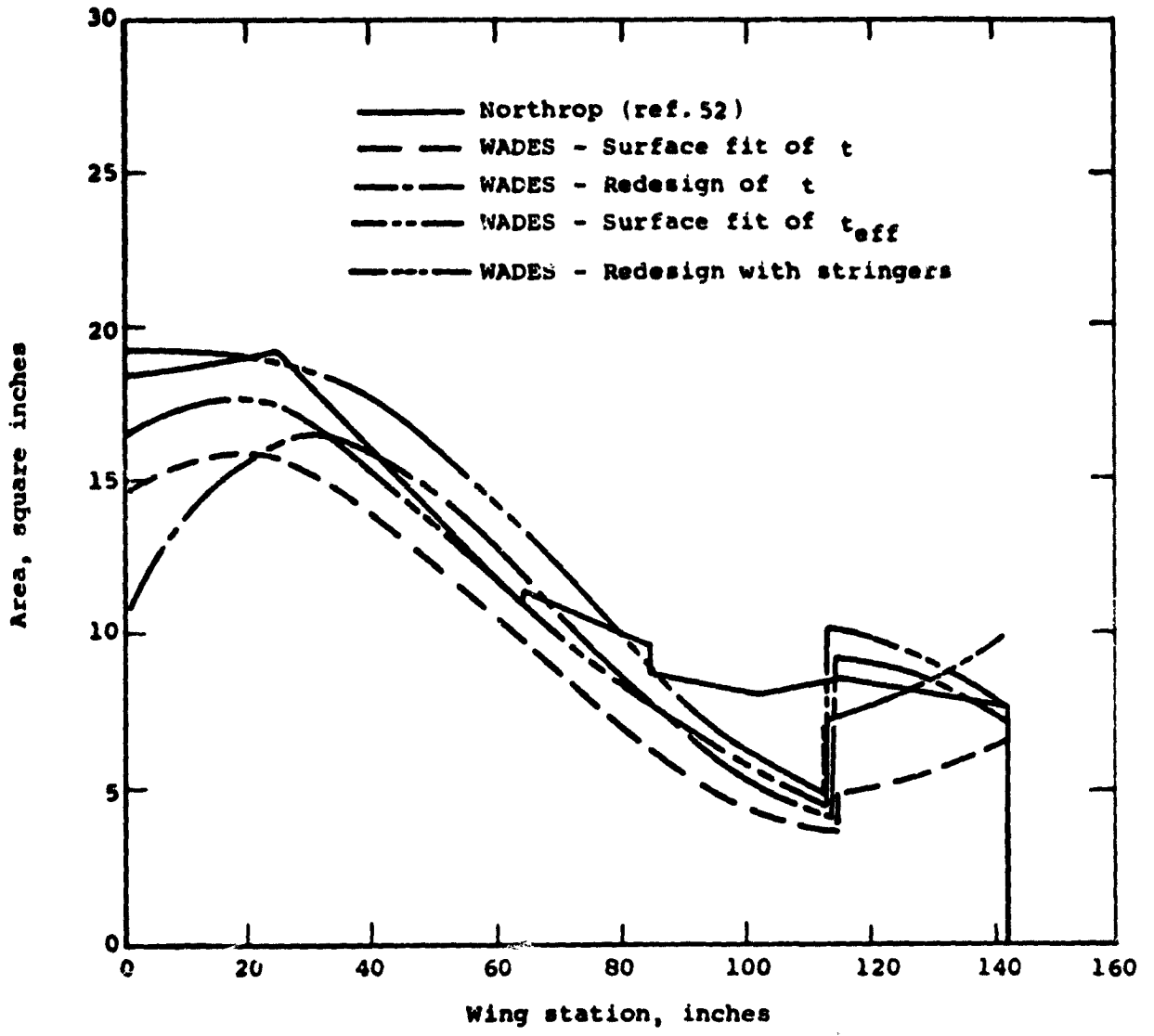


Figure 10.- F-5A/B Cross-sectional area of structural material versus span.

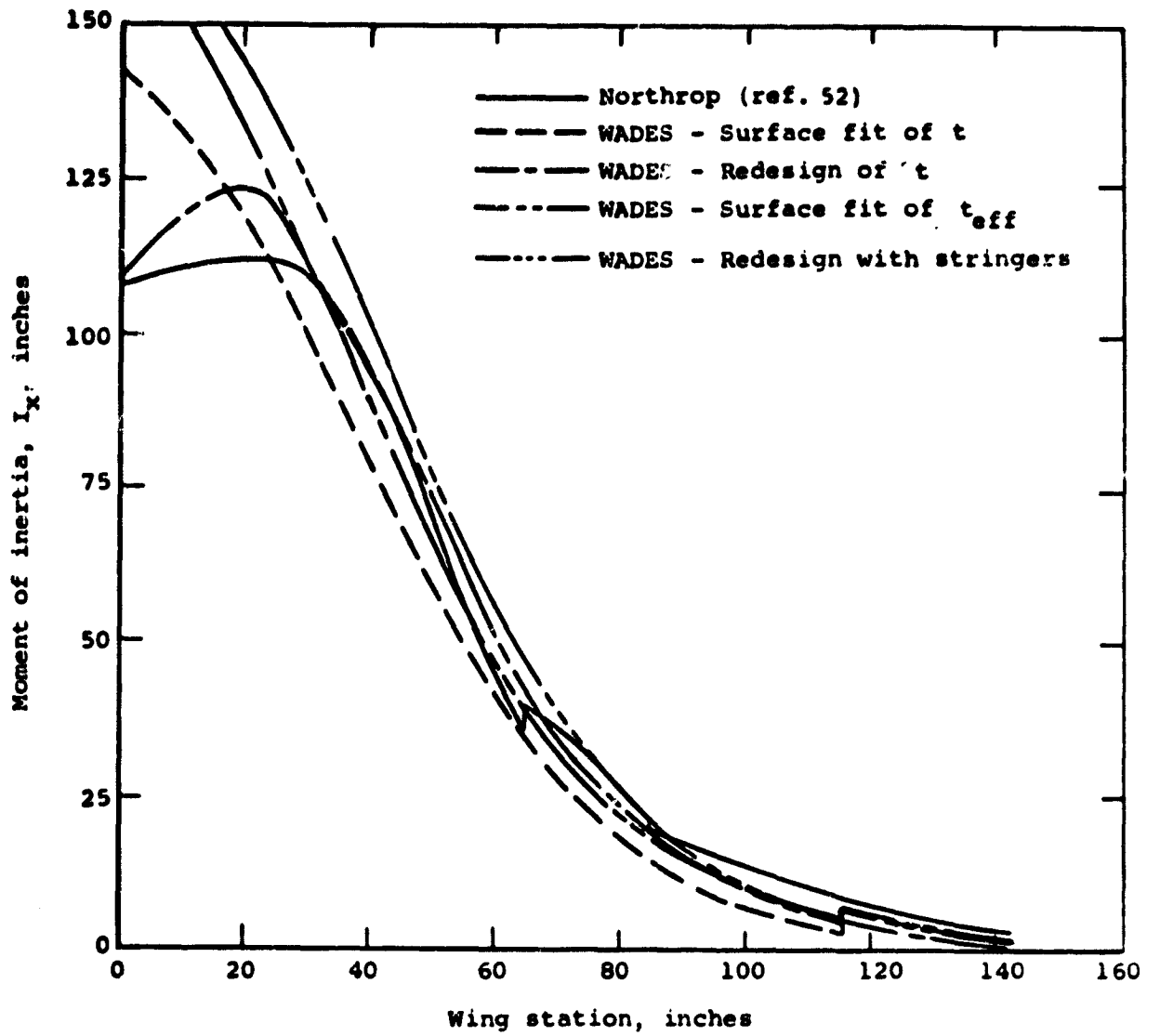


Figure 11.- F-5A/B Moment of inertia, I_x , of structural material versus span.

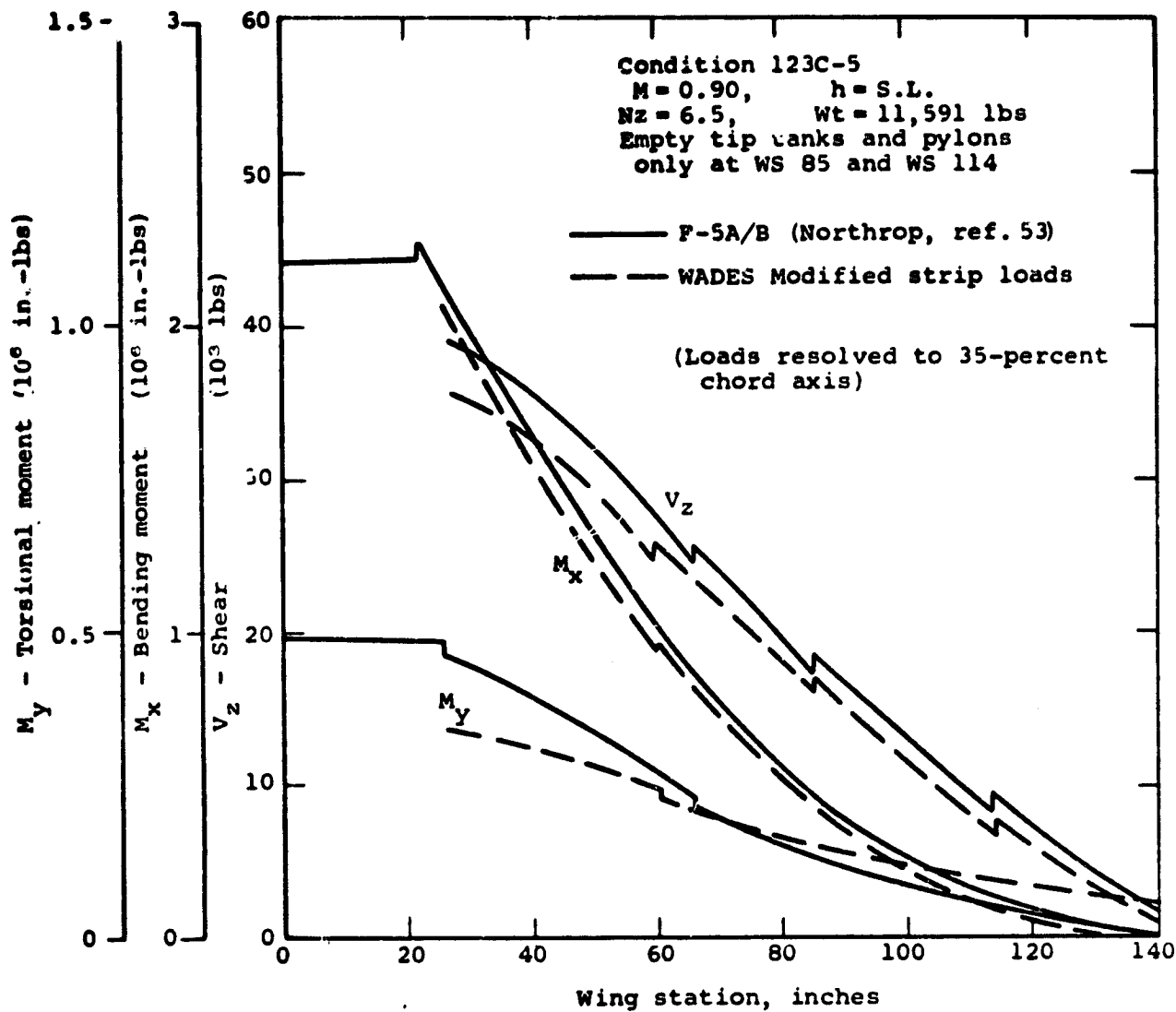


Figure 12.- F-5 Limit spanwise wing loads, flight condition 123C-5.

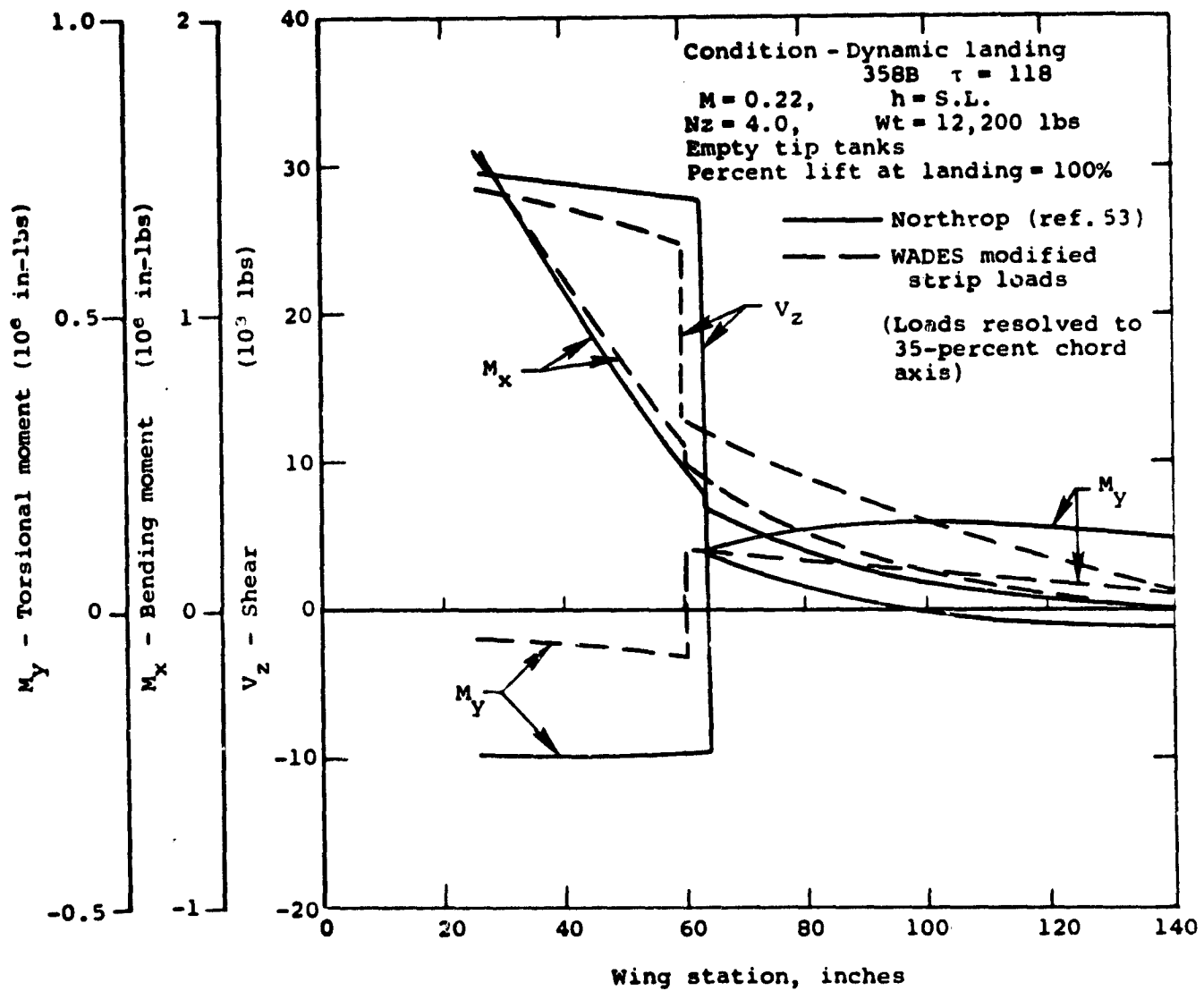


Figure 13.- F-5 Limit spanwise wing loads, flight condition-dynamic 358B landing, $\tau = 118$.

*** BODY GROUP ***

** FUSELAGE DESIGN CHECK CASE - C141

BULKHEADS AND FRAMES

734.00	337.5
958.00	948.9
1641.00	38.6
1728.00	41.3
351.00	137.1
998.00	1629.4
1058.00	193.1
1314.47	379.0
272.00	61.2
43.00	405.6
1398.00	108.9

MINOR FRAMES

1709.4

JOINTS, SPLICES AND FASTENERS

553.6

COVERING - UPPER BETWEEN LONGERONS
 - SIDE BETWEEN LONGERONS
 - LOWER BETWEEN LONGERONS

902.8
 2205.9
 802.1

COVERING LONGITUDINAL STIFFENERS - UPPER BETW. LONG.
 - SIDE BETW. LONG.
 - LOWER BETW. LONG.

513.9
 1141.7
 504.1

LONGERONS - UPPER
 - LOWER

373.5
 235.1

ENGINE DRAG

0.0

LONGITUDINAL PARTITIONS - (STRUCTURAL)

1124.0

FLOORING AND SUPPORTS - (BASIC STRUCTURE)

3421.1

FITTINGS

181.3

TOTAL - BASIC STRUCTURE

17909.0

Figure 14.- AN-9102-D Detailed weight statement -
 body group, C141.

*** BODY GROUP ***
 SECONDARY STRUCTURE

♦♦ FUSELAGE DESIGN CHECK CASE - C141		♦♦
ENCLOSURES (EXCLUDING TURRET ENCLOSURES)		
CANOPY - PILOT	0.0	
WINDSHIELD (EXCLUDING BULLET PROTECTION)	298.6	
WINDOWS AND PORTS INCL. FRAMES	212.5	
WINDOWS AND PORTS - CABIN	6.3	
FLOORING AND SUPPORTS (SECONDARY STRUCTURE)	404.4	
STAIRWAYS AND LADDERS (FIXED)	32.5	
NOSE RADOME	95.3	
SPEED BRAKES - STRUCTURE AND SUPPORTS	0.0	
TOTAL SECONDARY STRUCTURE		1049.6

Figure 14.- Continued.

*** BODY GROUP ***
 SECONDARY STRUCTURE
 (DOORS, PANELS AND MISCELLANEOUS)

•• FUSELAGE DESIGN CHECK CASE - C141

	AREA-SQ. FT.	
DOORS AND FRAMES		
• MAIN GEAR	163.0	863.9
• NOSE GEAR	32.9	164.5
• AFT CARGO	398.3	1039.1
• AFT RAMP	108.5	1071.4
• PRESSURE	65.7	327.1
• BOMB	0.0	0.0
• GUN		0.0
• AMMO		0.0
• ESCAPE	24.2	471.9
• ESCAPE	18.5	185.0
• PARATROOP	42.4	466.4
• ENTRANCE	12.2	122.0
• ACCESS		113.3
PANELS (NON STRUCTURAL)		
• SPOILER DEFLECTOR		22.0
• MAIN GEAR POD	700.0	1181.4
WALKWAYS, STEPS, GRIPS		168.2
ANTI-BNIO PROTECTION		58.9
FAIRING AND FILLETS		0.0
EXTERIOR FINISH		0.0
INTERIOR FINISH		248.5
TOTAL SECONDARY STRUCTURE (DOORS, PANELS, MISC.)		6503.4
TOTAL • BASIC STRUCTURE		17909.0
TOTAL SECONDARY STRUCTURE		1049.6
TOTAL • BODY GROUP		25462.0

Figure 14.- Continued.

*** BODY GROUP ***

** FUSELAGE DESIGN CHECK CASE = C141 **

BALANCE DATA

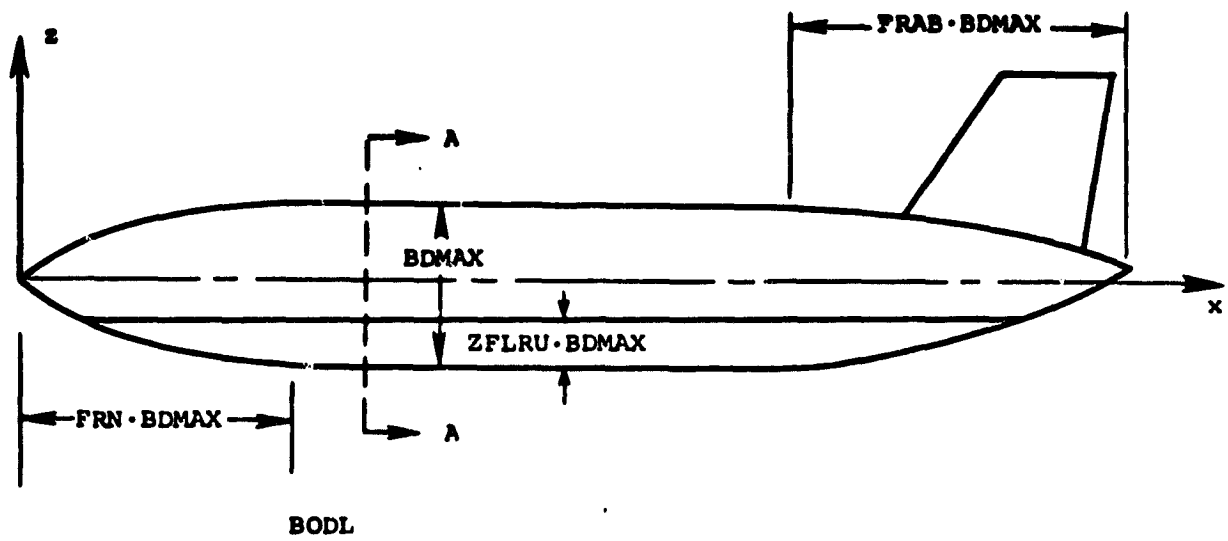
	WEIGHT	HORIZ. ARM
BULKHEADS AND FRAMES	6240.60	938.12
JOINTS, SPLICES AND FASTENERS	553.58	960.63
MINOR FRAMES	1709.40	952.49
COVERING - UPPER	902.84	991.54
SIDE	2205.89	967.43
LOWER	802.11	824.67
LONGERONS AND LONGITUDINAL STIFFENERS	513.93	1002.14
	1141.65	969.60
	504.11	867.22
	373.48	900.56
	235.07	1396.16
ENGINE DRAG	0.00	0.00
LONGITUDINAL PARTITIONS	1124.05	952.94
FLOORING AND SUPPORTS	3421.06	872.00
FITTINGS	181.26	0.00
TOTAL BASIC STRUCTURE	17909.02	927.33
SECONDARY STRUCTURE		
(1)	0.00	0.00
(2)	0.00	0.00
(3)	298.64	309.40
(4)	212.49	309.40
(5)	6.30	1020.00
(6)	404.43	385.30
(7)	32.45	442.60
(8)	95.27	319.00
(9)	0.00	0.00
(10)	0.00	0.00
(11)	0.00	0.00
(12)	0.00	0.00
TOTAL SECONDARY STRUCTURE	1049.58	347.91

Figure 14.- Continued.

*** BODY GROUP ***

DOORS, PANELS AND MISCELLANEOUS		
(13)	863.90	968.60
(14)	164.50	353.80
(15)	1039.07	1560.80
(16)	0.00	0.00
(17)	0.00	0.00
(18)	0.00	0.00
(19)	1071.36	1356.80
(20)	0.00	0.00
(21)	327.07	1411.00
(22)	0.00	0.00
(23)	0.00	0.00
(24)	0.00	0.00
(25)	471.90	810.90
(26)	185.01	842.50
(27)	466.40	1218.00
(28)	22.00	1200.00
(29)	122.00	468.00
(30)	113.27	850.00
(31)	0.00	0.00
(32)	0.00	0.00
(33)	0.00	0.00
(34)	0.00	0.00
(35)	0.00	0.00
(36)	1181.40	971.80
(37)	0.00	0.00
(38)	0.00	0.00
(39)	168.20	872.00
(40)	58.87	872.00
(41)	0.00	0.00
(42)	248.50	882.40
TOTAL SECONDARY STRUCTURE (DOORS, PANELS, MISC.)	6503.44	1119.96
TOTAL = BODY GROUP	25462.04	952.65

Figure 14.- Concluded.



SECTION AA

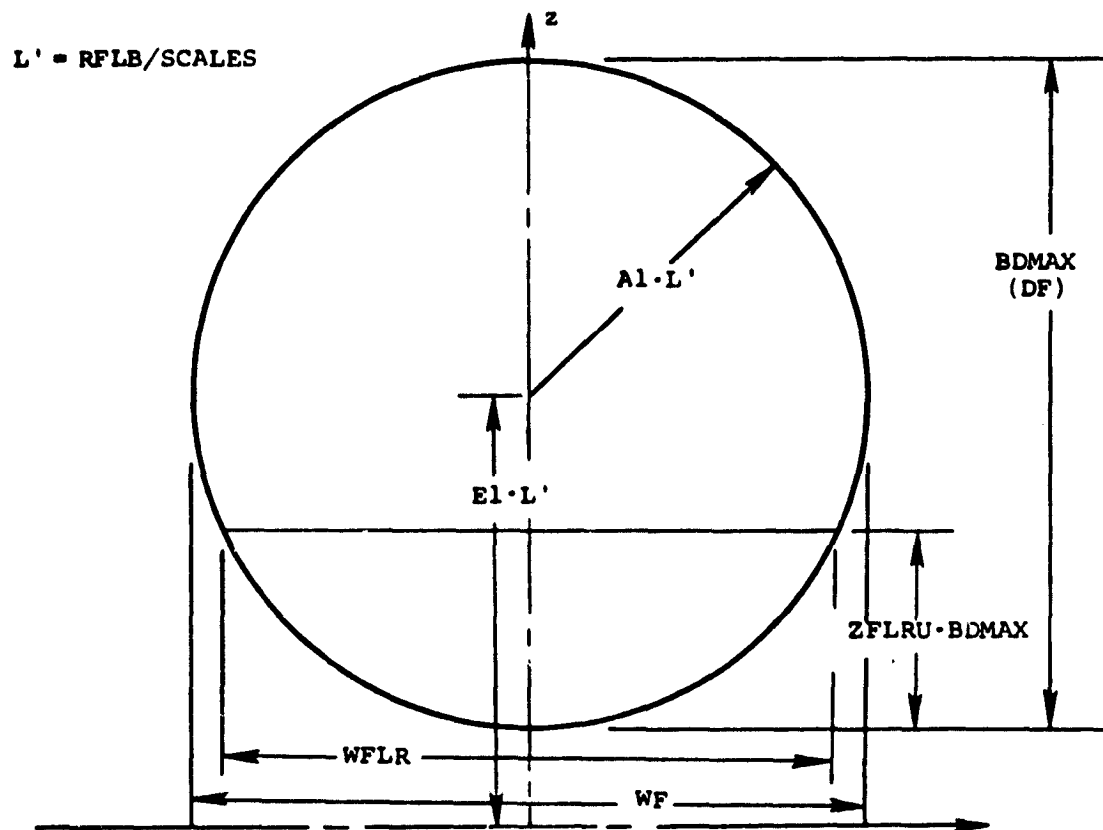


Figure 15.- Sears-Haack body with circular section.

$$L' = RFLB/SCALEB$$

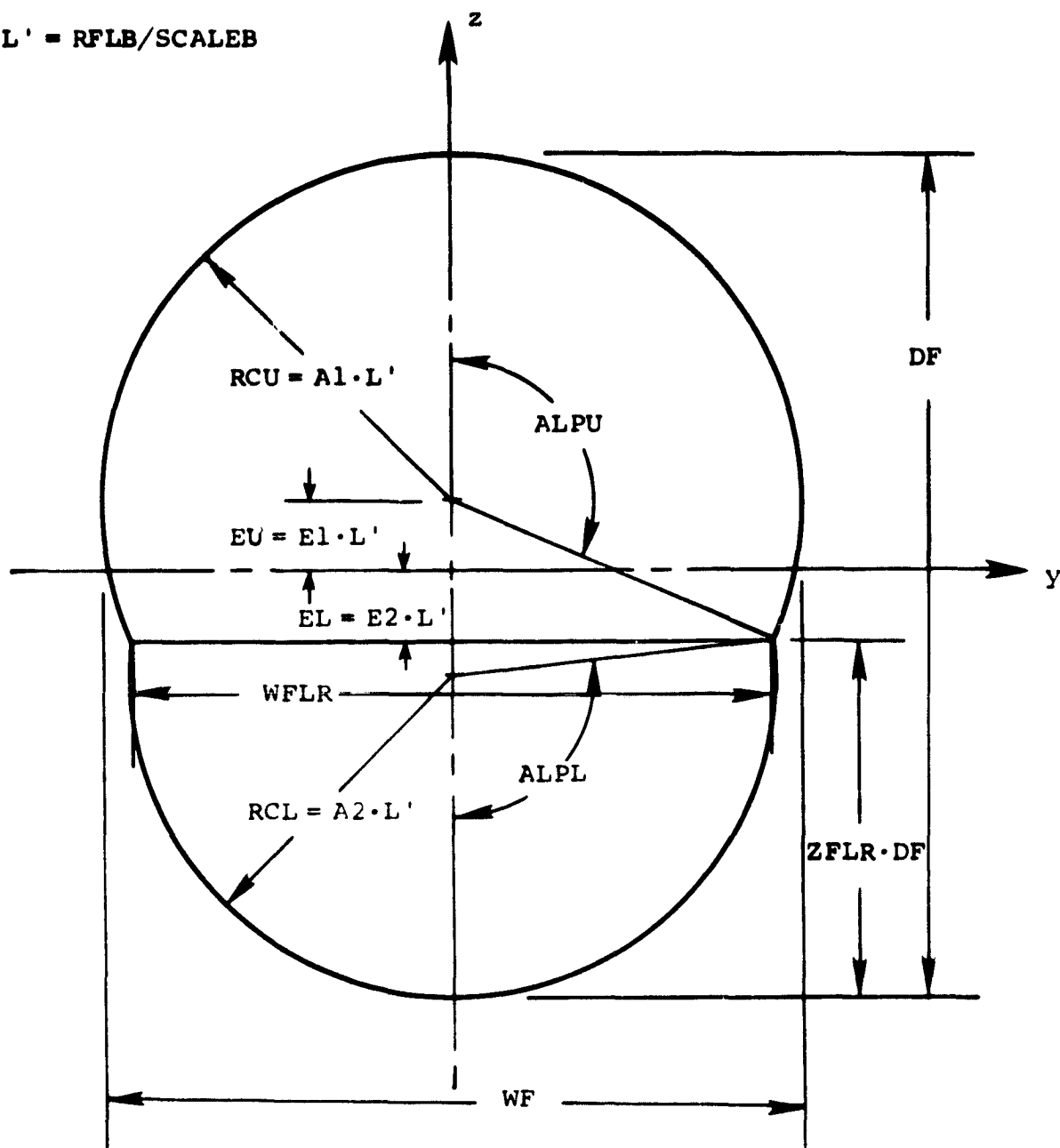


Figure 16.- Double-lobe cross section geometry.

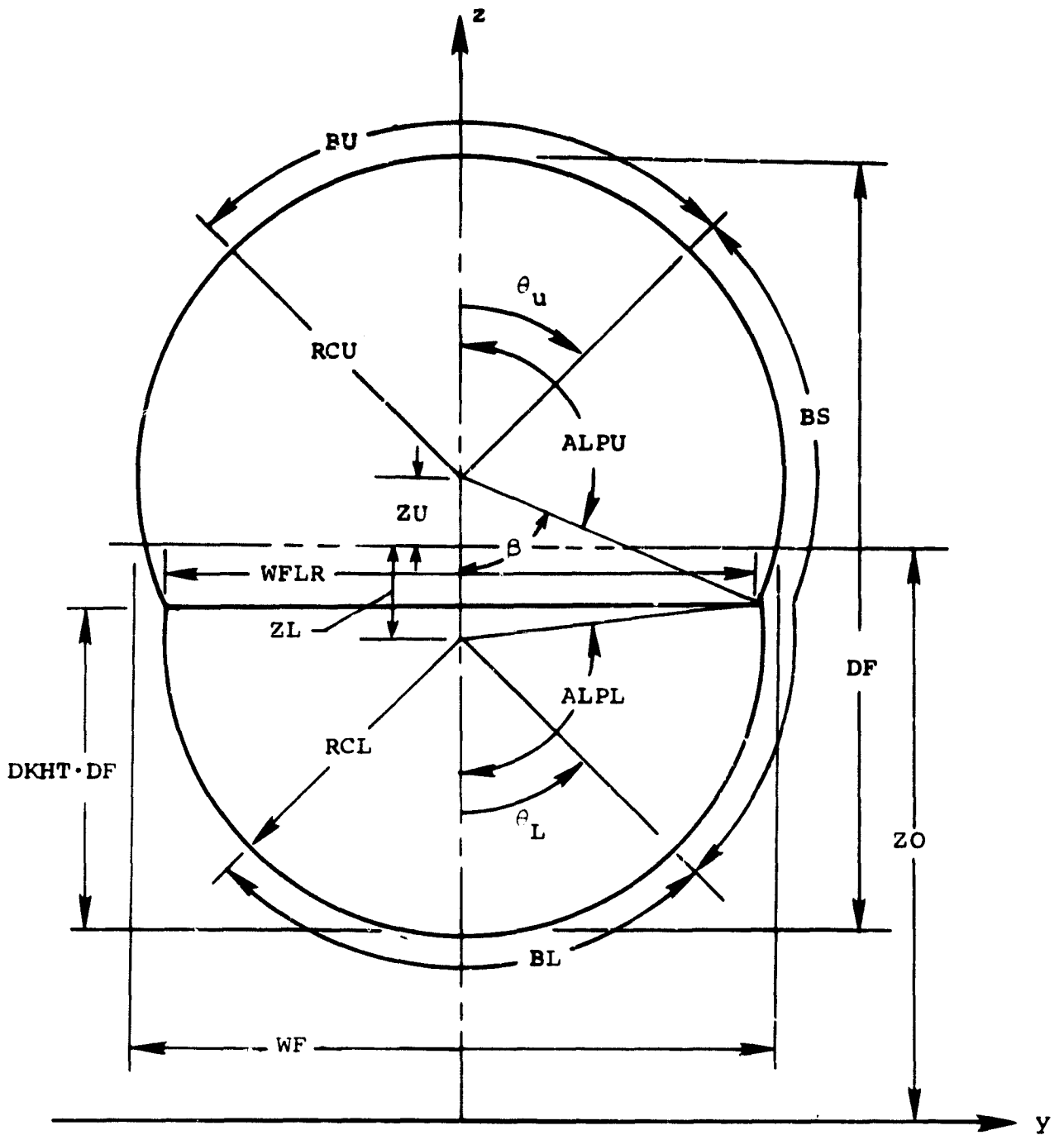
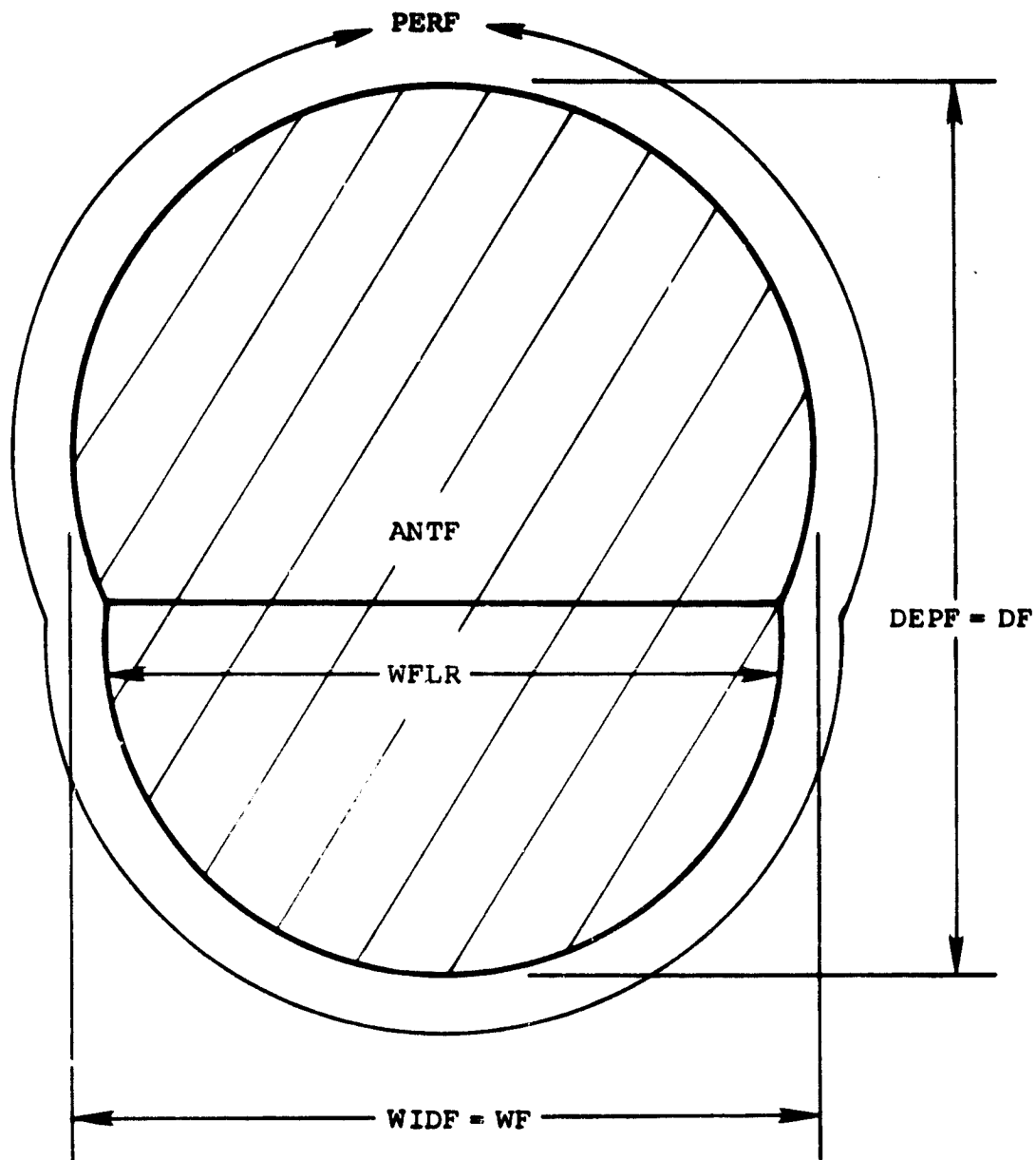


Figure 17.- Double-lobe structural sectors.



WIDF = WF
 DEPF = DF
 PERF = PER

PRDF = 0.
 ANTF = ARCS

Figure 18.- Double-lobe closed torque box.

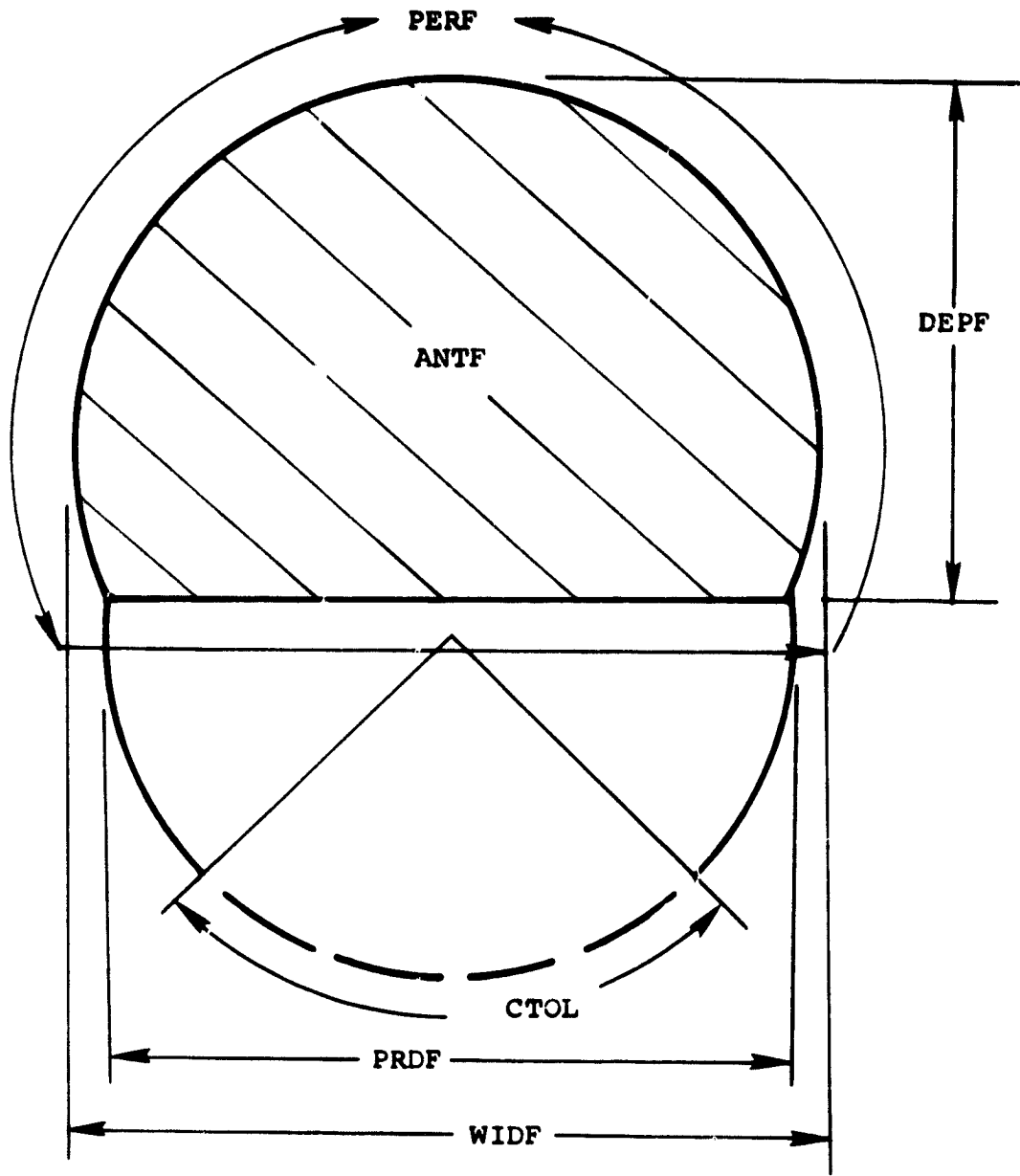


Figure 19.- Double-lobe torque box with lower cutout.

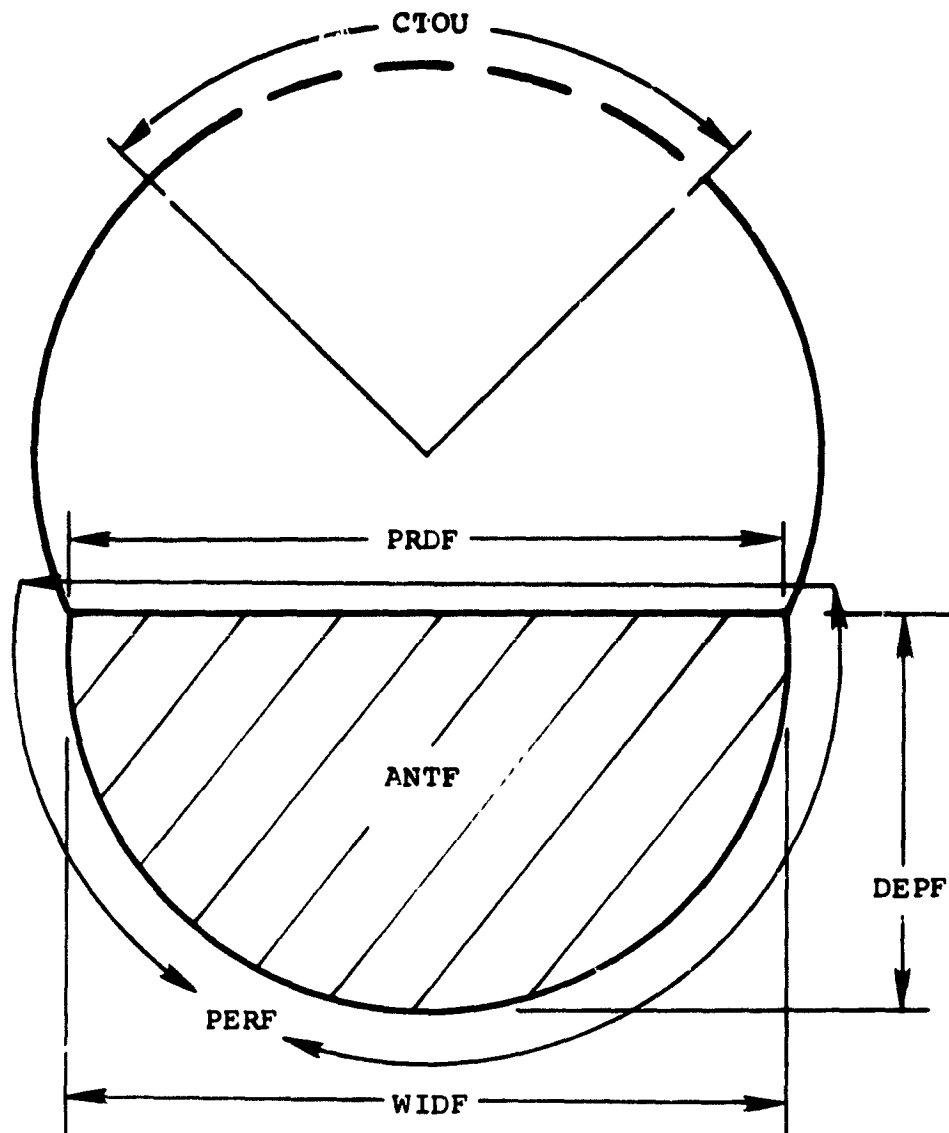


Figure 20.-- Double-lobe torque box with upper cutout.

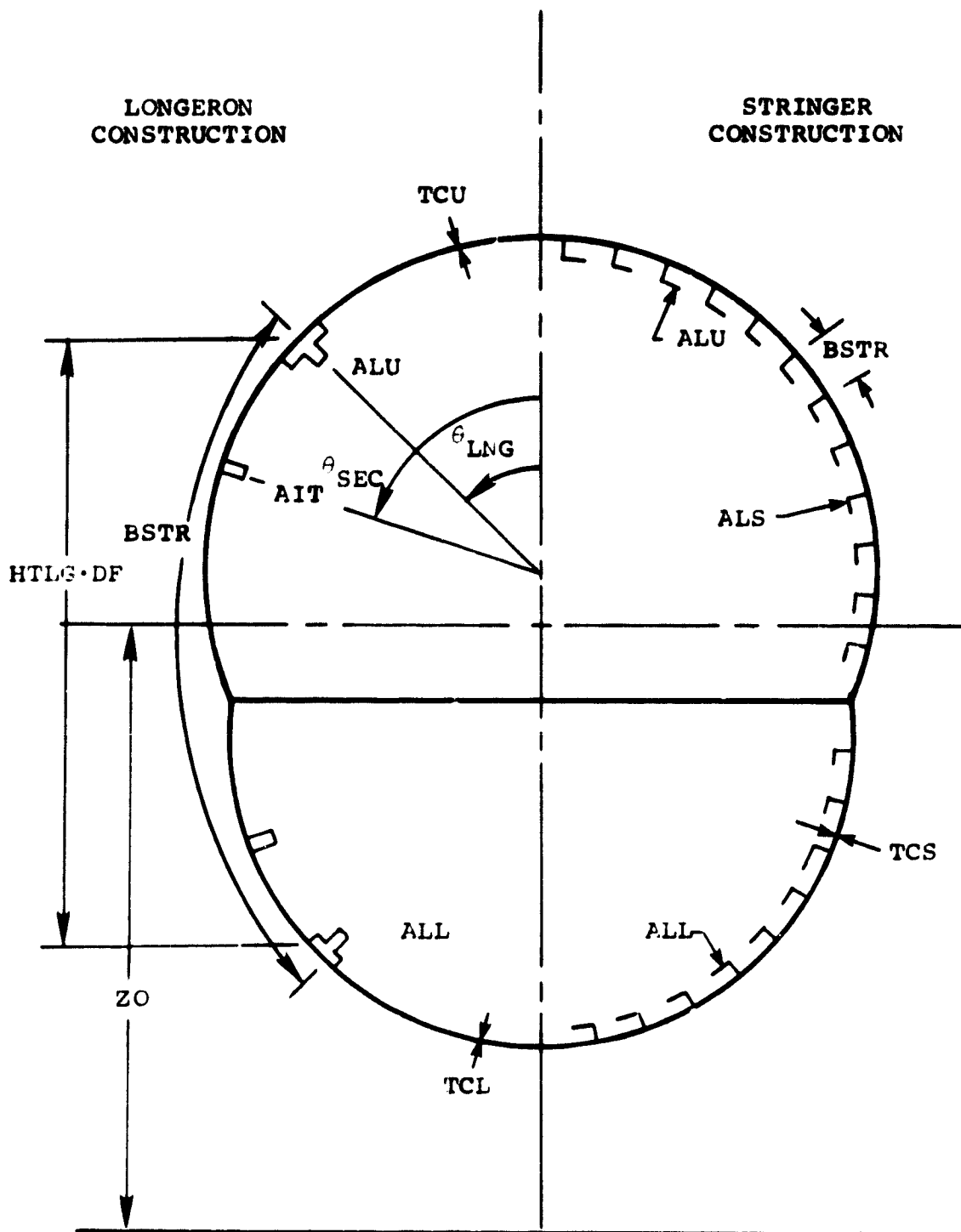


Figure 21.- Longeron and Stringer structural geometry.

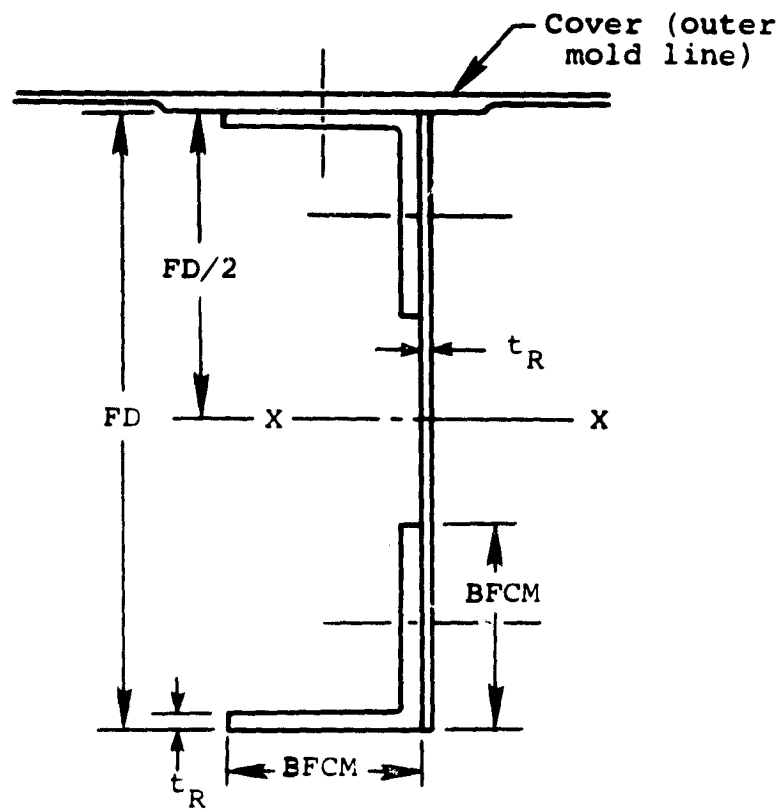


Figure 22.- Geometric model used in analysis of minor frames.

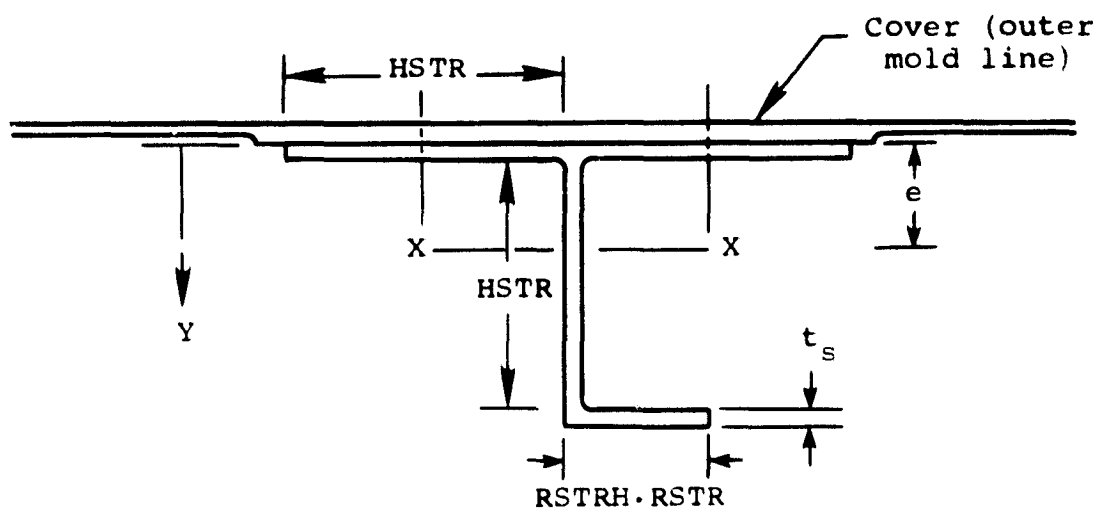


Figure 23.- Geometric model used in analysis of longitudinal members.